

Distribution Agreement

In presenting this thesis or dissertation as a partial fulfillment of the requirements for an advanced degree from Emory University, I hereby grant to Emory University and its agents the non-exclusive license to archive, make accessible, and display my thesis or dissertation in whole or in part in all forms of media, now or hereafter known, including display on the world wide web. I understand that I may select some access restrictions as part of the online submission of this thesis or dissertation. I retain all ownership rights to the copyright of the thesis or dissertation. I also retain the right to use in future works (such as articles or books) all or part of this thesis or dissertation.

Signature:

Adam S. Raymond

Date

Novel Tissue-Intrinsic Functions of SED1/MFG-E8 in the Epididymis

By

Adam S. Raymond
Doctor of Philosophy

Graduate Division of Biological and Biomedical Sciences
Biochemistry, Cell, and Developmental Biology

Barry D. Shur, Ph.D.
Advisor

Otto Froehlich, Ph.D.
Committee Member

William G. Kelly, Ph.D.
Committee Member

Andrew Kowalczyk, Ph.D.
Committee Member

Grace K. Pavlath, Ph.D.
Committee Member

Accepted:

Lisa A. Tedesco, Ph.D. Dean of the Graduate School

_____ Date

Novel Tissue-Intrinsic Functions for SED1/MFG-E8 in the Epididymis

By

Adam S. Raymond
B.S., University of Notre Dame, 2000

Advisor: Barry D. Shur, Ph.D.

An Abstract of
A dissertation submitted to the Faculty of the Graduate School of Emory University
in partial fulfillment of the requirements for the degree of Doctor of Philosophy in

Graduate Division of Biological and Biomedical Sciences
Biochemistry, Cell, and Developmental Biology

2009

Novel Tissue-Intrinsic Functions of SED1/MFG-E8 in the Epididymis

By Adam S. Raymond

SED1 is a bimeric cell adhesion molecule secreted by the initial segment of the epididymis where it binds sperm and facilitates adhesion to the egg coat. Herein, SED1-null animals are shown to harbor an unexpected increase in epididymal pathologies suggesting a previously unidentified tissue-intrinsic role for SED1 in the epididymis. Although the SED1-null epididymis develops and differentiates normally, >40% of SED1-null epididymides contain spermatic granulomas. Immunocytochemistry reveals that in addition to its apical secretion, SED1 is localized in basolateral domains of cells of the initial segment. In vitro assays show that SED1 supports epididymal cell adhesion via RGD binding to α_v integrins and epididymal cells from SED1-null males show reduced adhesion. These results suggest that SED1 facilitates epididymal cell adhesion that may be protective against spermatic granulomas, however the bulk of SED1 is expressed in the proximal epididymis while sperm granulomas most often manifest in the distal segments. In other models, disruption of fluid regulatory processes in proximal regions is accompanied by long-range effects including spermatic granulomas in the distal epididymis. In this regard, the SED1-null epididymis fails to properly acidify the luminal fluid, and the SED1-null epithelium exhibits histological hallmarks of disrupted luminal dynamics. Collectively, these data suggest that SED1 contributes to the regulation of epididymal fluid; however, a variety of proteins known to effect fluid transport and pH regulation are expressed normally. Since SED1 is secreted in exosomes that participate in fluid homeostasis, it is feasible that the loss of SED1 leads to defective exosome contents, a possibility that will be explored in future studies.

Novel Tissue-Intrinsic Functions for SED1/MFG-E8 in the Epididymis

By

Adam S. Raymond
B.S., University of Notre Dame, 2000

Advisor: Barry D. Shur, Ph.D.

A dissertation submitted to the Faculty of the Graduate School of Emory University
in partial fulfillment of the requirements for the degree of Doctor of Philosophy in

Graduate Division of Biological and Biomedical Sciences
Biochemistry, Cell, and Developmental Biology

2009

Acknowledgements

First and foremost, I would like to recognize my advisor, Dr. Barry Shur. Dr. Shur is responsible not only for guiding and funding my project, but also teaching me the tangible skills that have allowed me to execute it. Under his guidance I have learned how to “think” about science. I have developed a critical and discerning eye for interpreting scientific data and become a proficient writer and presenter. But most importantly, I am thankful for Dr. Shur’s friendship; for his interest and concern for my well-being and that of my family; and his support of my personal and professional growth outside the laboratory. He is true mentor in every sense.

I also would like to acknowledge a number of people who have contributed to my professional development. While I was a technician in his lab, Dr. Scott Devine took the time to counsel me as a student of science. He inspired my interest in basic research and pushed me to excellence, and I will be forever grateful for the opportunities he provided me. Dr. Cory Acuff offered me a glimpse of science beyond the bench. Under his guidance I discovered and developed talents that were under-utilized in bench research and gained the confidence to change career paths following the completion of my degree. I am also grateful for the members of the Shur Lab, past and present, who have all been friends and teachers to me. In particular I would like to recognize Dr. Michael Ensslin for his identification of the SED1-null epididymal phenotype and his constant support of my efforts on this project; and Rob Lyng for his friendship, without which I may never have reached graduation. I would like to acknowledge my committee for their input, and the faculty of the Department of Cell Biology, in particular Drs. Art English, Victor Faundez, Criss Hartzell, and Robert McKeon for their generosity with advice, reagents, and equipment.

Last but not least I would like to recognize my family, especially my wife Jaime Raymond and mother Beth Stalzer for their encouragement. Graduate school is a shared experience and Jaime has been unwavering in her support of my goals. And just 11 weeks ago we were blessed to welcome daughter Hope Cecile Raymond to our family. Already she has inspired me to work harder and do better in all of my life’s pursuits.

Table of Contents

Chapter 1: Introduction	1
1.1 Introduction to the bimotif adhesion protein SED1	2
1.1.1 Abstract	2
1.1.2 SED1 is a mosaic protein	3
1.1.3 SED1 contributes to phagocytic removal of apoptotic cells in many tissues and organs	9
1.1.4 SED1 facilitates a number of intercellular interactions	16
1.1.5 Concluding thoughts: SED1 as a therapeutic agent	27
1.2 Introduction to the male epididymis	29
1.2.1 Summary	29
1.2.2 Epididymal organization and anatomy	30
1.2.3 Epididymal function: protein secretion	31
1.2.4 Epididymal function: fluid reabsorption and pH modification	32
1.3 Focus of Dissertation	33
Chapter 2: Materials and Methods	35
2.1 Mice and recombinant SED1	36
2.2 Tissue preparation for histology	36
2.3 Epithelial morphometrics	37
2.4 Detection of endogenous β -galactosidase activity	37
2.5 Immunocytochemistry	38
2.5.1 In vivo	38
2.5.2 In vitro	38
2.6 Immunoblotting	39
2.6.1 MFG-E8 and α_v (Chapter 4)	39
2.6.2 All other immunoblots (Chapter 5)	40
2.7 Preparation and culture of primary cells	40
2.8 Cell adhesion assays	41
2.9 BrdU proliferation assays	42

2.10	Determination of luminal pH ex vivo	43
2.11	Intracellular vesicle quantification	43
2.12	Preparation of epididymosomes	44
Chapter 3: The SED1-null Contains an Unexpected Epididymal Phenotype		45
3.1	Introduction and experimental rationale	46
3.2	Results	47
3.2.1	SED1 localizes to numerous domains in principal, clear, and basal cells of the epididymis	47
3.2.2	SED1-null epididymides exhibit a loss in tubule integrity and an increase in spermatoc granulomas	51
3.2.3	Reproductive pathologies associated with the loss of SED1 are restricted to the epididymis	54
3.2.4	The SED1-null epididymis undergoes normal development and differentiation	57
3.3	Discussion	61
Chapter 4: A Novel Role for SED1 in Maintaining the Integrity of the Epididymal Epithelium		65
4.1	Introduction and experimental rationale	66
4.2	Results	68
4.2.1	SED1 is expressed in basal and basolateral domains of epididymal epithelia in vivo	68
4.2.2	SED1 is deposited basally by polarized epithelial cells in vitro	72
4.2.3	rSED1 increases the initial adhesion of primary epididymal epithelial cells	76
4.2.4	Epithelial cell adhesion to rSED1 is RGD-dependent	76
4.2.5	Epididymal epithelial cells express α_V integrins	81
4.2.6	α_V integrins are required for epididymal epithelial cell adhesion to SED1	84
4.2.7	SED1-null epithelial cells show reduced adhesion in vitro	89
4.3	Discussion	92

Chapter 5: Loss of SED1 Results in Altered Luminal Physiology in the Epididymis	100
5.1 Introduction and experimental rationale	101
5.2 Results	102
5.2.1 Loss of SED1 results in an increase in luminal pH	102
5.2.2 SED1-null epididymides exhibit morphological correlates of defective fluid regulation	105
5.2.3 Many proteins that regulate the composition of the luminal fluid are expressed and localized normally in the SED1-null epididymis	111
5.2.4 SED1 is associated with mouse epididymosomes	114
5.3 Discussion	132
Chapter 6: Conclusions and Future Directions	137
6.1 Conclusions	138
6.1.1 Overview	138
6.1.2 Maintenance of the epididymal epithelium	139
6.1.3 SED1 function in regulation of luminal fluid of the epididymis	139
6.1.4 Conclusions	140
6.2 Future directions	141
6.3 Use of SED1 in reproductive interventions	142
Chapter 7: References	146

List of Tables and Figures

Figure 1-1:	Structural motifs of SED1 and Del1, two proteins independently isolated that facilitate cell-matrix adhesions.	4
Figure 1-2:	Molecular models of SED1 C1 and C2 domains based upon the crystallographic analysis of the C2 domain of Factor V and VIII.	6
Figure 1-3:	SED1 is associated with microvesicles such as epididymosomes and exosomes.	23
Figure 3-1:	SED1 localizes to numerous cellular domains in epididymal epithelial cells in vivo.	49
Figure 3-2:	Epididymides from SED1-null males show epithelial breakdown.	52
Figure 3-3:	Testes and efferent ducts in the SED1-null male are morphologically normal.	55
Figure 3-4:	The SED1-null epididymis develops and differentiates normally.	59
Figure 4-1:	SED1 localizes to both apical and basolateral domains of epididymal epithelial cells in vivo.	69
Figure 4-2:	Polarized primary epididymal epithelial cells secrete SED1 both apically and basally.	73
Figure 4-3:	Exogenous SED1 supports epididymal epithelial cell adhesion in a dose-dependent manner.	77
Figure 4-4:	The addition of RGD peptides is sufficient to block the initial adhesion of epididymal epithelial cells to SED1.	79
Figure 4-5:	The α_v integrin subunit is expressed in epididymal epithelial cells and localizes to focal plaques in cells adherent to SED1.	82
Figure 4-6:	A small molecule inhibitor of $\alpha_v\beta_{3/5}$ integrin heterodimers (L-954) selectively blocks epididymal cell adhesion to SED1.	80
Figure 4-7:	Function-blocking antibodies against α_v integrin block epididymal cell adhesion to SED1.	85

Figure 4-8:	Loss of SED1 leads to deficient cellular adhesion in vitro.	90
Figure 4-9:	Working model of SED1-dependent epididymal epithelial cell adhesion.	96
Figure 5-1:	The SED1-null epididymis fails to acidify the luminal fluid.	103
Figure 5-2:	The SED1-null epididymis exhibits characteristics consistent with an elevated pH and hypo-osmotic luminal fluid.	106
Figure 5-3:	The SED1-null epididymis possesses characteristics consistent with compensatory endocytosis.	109
Figure 5-4:	SED1-null narrow and prominent cells exhibit altered morphology.	112
Table 5-1:	Proteins known to effect regulation of luminal composition and their reported expression and localization in the epididymis.	115
Table 5-2:	Proteins known to effect regulation of luminal composition and their observed expression and localization in the epididymis.	116
Figure 5-5:	Many proteins that regulate the composition of the luminal fluid are expressed and localized normally in the SED1-null epididymis.	117
Figure 5-6:	SED1 is associated with 30-60 nm epididymosomes.	130
Figure 6-1:	SED1-positive epididymosomes can be purified and analyzed by mass spectroscopy.	143

Chapter 1: Introduction

Some written material and figures in Chapter 1 have been published previously or will be published in the future (Raymond et al., 2009a; Raymond et al., 2009b; Raymond and Shur, 2009; Shur et al., 2004).

Chapter 1: Introduction

1.1 Introduction to the bimotif adhesion protein SED1

1.1.1 Abstract

MFG-E8 was initially identified as a principal component of the Milk Fat Globule, a membrane-encased collection of proteins and triglycerides that bud from the apical surface of mammary epithelia during lactation. It has since been independently identified in many species and by many investigators and given a variety of names, including p47, lactadherin, rAGS, PAS6/7, and BA-46. The acronym SED1 was proposed to bring cohesion to this nomenclature based upon it being a Secreted protein that contains two distinct functional domains: an N-terminal domain with two EGF-repeats, the second of which has an integrin-binding RGD motif, and a C-terminal domain with two Discoidin/F5/8C domains that bind to anionic phospholipids and/or extracellular matrices. SED1 is now known to participate in a wide variety of cellular interactions, including phagocytosis of apoptotic lymphocytes and other apoptotic cells, adhesion between sperm and the egg coat, repair of intestinal mucosa, mammary gland branching morphogenesis, angiogenesis, among others. This article will explore the various roles proposed for SED1, as well as its provocative therapeutic potential.

1.1.2 SED1 is a mosaic protein

In most species examined thus far, SED1 occurs as a ~53 kDa secreted glycoprotein that possesses a cleavable signal peptide, followed by two N-terminal epidermal growth factor (EGF)-like repeats and two C-terminal Discoidin/F5/8C domains (referred to as F5/8C domains) (Andersen et al., 1997; Couto et al., 1996; Ensslin et al., 1998; Larocca et al., 1991; Ogura et al., 1996; Stubbs et al., 1990) (Fig. 1-1). The second EGF domain also contains an arginine-glycine-aspartic acid (RGD) integrin-binding motif that engages $\alpha_v\beta_{3/5}$ integrin heterodimers to facilitate cell adhesion as well as induce integrin-mediated signal transduction (Andersen et al., 1997; Andersen et al., 2000; Ensslin and Shur, 2007; Raymond and Shur, 2009; Taylor et al., 1997). Since the EGF domains are highly homologous to those that mediate binding between *Drosophila* Notch-1 and its ligand, Delta, it has been suggested that the EGF repeats may pair with one another to form SED1 multimers, similar to the ability of EGF repeats to multimerize other types of cell adhesion molecules (Balzar et al., 2001).

The C-terminal F5/8C domains have sequence homology to the animal lectin discoidin and the C2 domain of blood coagulation Factor V and Factor VIII (Ogura et al., 1996; Stubbs et al., 1990). Each F5/8C domain is composed of an eight-strand anti-parallel β -barrel, from which two or three hypervariable loops extend from the base (Lin et al., 2007; Shao et al., 2008; Shur et al., 2004) (Fig.1-2). The exposed amino acid residues that compose these hairpin loops dictate the protein's binding specificity. In some instances, such as in the discoidin protein from *Dictyostelium* and the chitobiase

Figure 1-1: Structural motifs of SED1 and Del1, two proteins independently isolated that facilitate cell-matrix adhesions. Both proteins contain Notch-like EGF repeats, the second of which possess an RGD integrin-binding motif, as well as two discoidin/F5/8 C domains that are able to bind phospholipid bilayers and/or extracellular glycosides via 2-3 hairpin loops projecting from the central barrel core. Both SED1 and Del1 are believed to facilitate cell-matrix adhesion via RGD-dependent binding to cell surface $\alpha_v\beta_3$ integrin receptors, whereas the discoidin/F5/8C domain is also thought to bind to cell membranes via intercalation into the lipid bilayer. Alternatively, the discoidin/F5/8C domains may coordinate binding to extracellular glycoside substrates, similar to that seen in the sugar-binding discoidin domains. Del1 contains a third EGF repeat not found within SED1. [Reprinted from (Shur et al., 2004)].

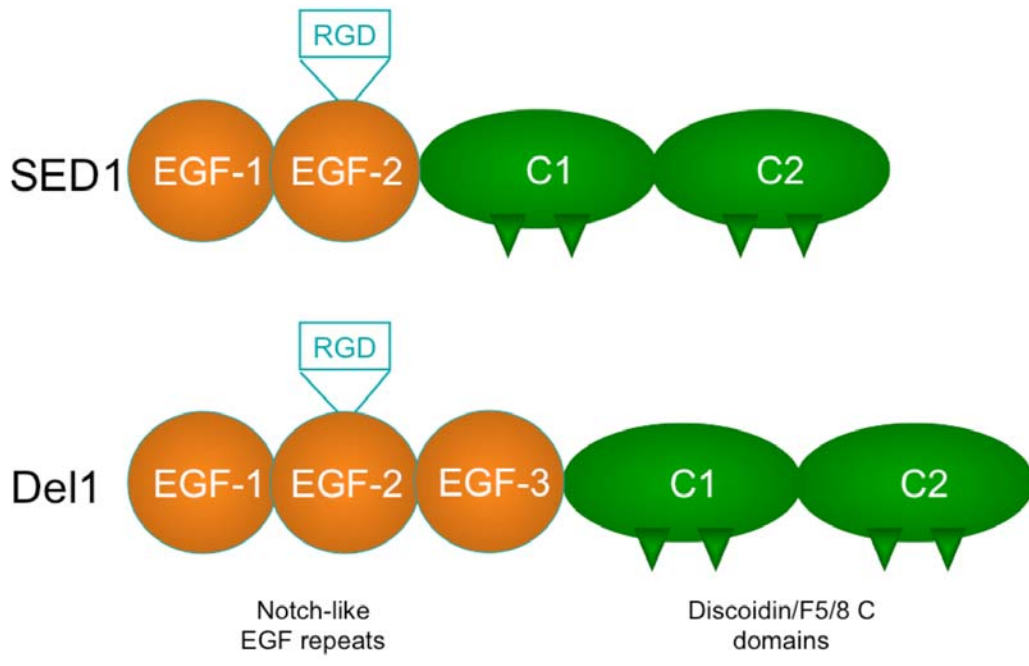
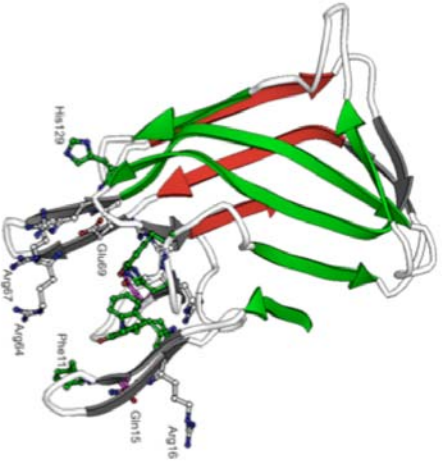
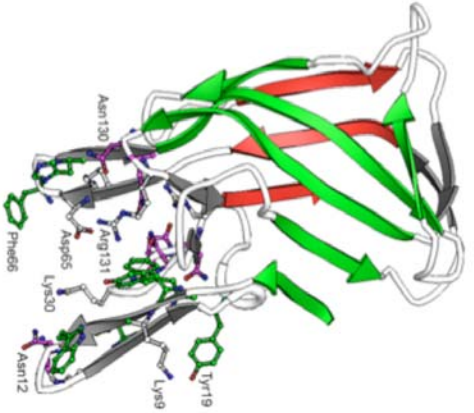


Figure 1-2: Molecular models of SED1 C1 and C2 domains based upon the crystallographic analysis of the C2 domain of Factor V and VIII. The discoidin/F5/8 C domain core is composed of an eight-stranded β sheet, five of which appear in the front (green arrows) and three in the rear of the barrel (red arrows). Each C domain projects two large hairpin loops (or spikes), as well as a smaller, irregular intermediate loop. The C1 and C2 domains of SED1 are more similar to the Complement C2 domain than to the Complement C1 domain, in that they both possess the β -hairpin loops required for association with lipid bilayers. However, the homologous loops in C1 and C2 display distinctly different amino acid side chains that may dictate unique binding specificities. The aromatic residues are shown in green, charged residues in white, and uncharged polar residues in magenta. Sequence alignments of the SED1 C1 and C2 domains with Factor V and VIII C2 domains are pictured, with identical residues in red and conserved residues in green. The relative positions of the hairpin loops, or spikes, is indicated as determined by crystallographic analysis (Fuentes-Prior et al., 2002). [Reprinted from (Shur et al., 2004)].



SED1 C1



SED1 C2

```

SED1-C1  QISKLVYVWVGF-NGIDLRGGEELIARIVRGTIIVAMRNSVYDSEIPVITDGNLLPKRURISGVWVPGGASRAGAAVYIKRFRVAVSINGRPFETQD--EISGDKRIFLDRVANNSELRVAMRIPTEIAAOI
FY-C2    QITASERKRSNH--GDVYEFPRARLNKGEIRNANMOIKANNNOQMLHILLIKITAIITDQCGESISEVYIKSVTIRHSEGVNPFPELIS-SMVKIIEENRKHQIKAFRNP3IISPTI
FYIII-C2 QITNSGVYFNMF--NINSSIKKALHLSGERSHNRQVYRFRNEMDGVDFQITRFRVYVITDQVRESHLSSEYVKEFLDSSQSHQVTLFTQ--NINAVVFOQNDSTFVNSLDQ3LITRVL

SED1-C2  QNSASSEVYTR----NEAAGVYHLDGRIQDQCKTRMAPAGSRANRHLQVVDLGTQDQITGIIPOGARDDGHIQVYVPSVVAHSDQGVQVVEE--QSSKVFQGLANNSIKWIEKPRMA
FY-C2    QITASSEPKSIR-N-----GDVYEFPRARLNKGEIRNANMOIKANNNOQMLHILLIKITAIITDQCGESISEVYIKSVTIRHSEGVNPFPELIS-SMVKIIEENRKHQIKAFRNP3IISPTI
FYIII-C2 QITASGVYFNMF--NF----ATNS3SKRHLFDQGRSHNARPEVYRPHMLQVDFQITRFRVYVITDQVRESHLSSEYVKEFLDSSQSHQVTLFTQ--NINAVVFOQNDSTFVNSLDQ3LITRVL
    
```

spike 1

spike 2

spike 3

enzyme from *Arthrobacter*, these loops mediate binding to carbohydrate moieties on the surface of cells and in the extracellular matrix, whereas coagulation Factor V, Factor VIII, and the second C-terminal domain of SED1 bind to anionic phospholipids of cellular membranes (Andersen et al., 1997; Andersen et al., 2000; Fuentes-Prior et al., 2002; Macedo-Ribeiro et al., 1999; Pratt et al., 1999; Reitherman et al., 1975; Shi et al., 2004; Shi et al., 2008). Crystallographic analysis suggests that hydrophobic residues of the F5/8C2 hairpin loops insert into the lipid bilayer, whereas basic residues at the base of the loop “dock” with the phospholipid headgroups (Macedo-Ribeiro et al., 1999; Pratt et al., 1999; Shur et al., 2004). While both F5/8C domains of SED1 maintain a similar overall structure to the C2 domains of the blood coagulation factors, the second F5/8C domain of SED1 contains an amino acid substitution that results in considerably higher affinity for phosphatidylserine membranes than does the C2 domains of Factors V and VIII (Shao et al., 2008).

In mouse and rat, SED1 also occurs as a ~66 kDa splice variant that includes an *O*-glycosylated, 37 amino acid (56 amino acid in rat) proline/threonine-rich sequence inserted between the second EGF domain and the first discoidin domain (Burgess et al., 2006; Oshima et al., 1999). Expression of the two splice variants shows spatial and temporal specificity. For example, the 53 kDa variant is expressed in many tissues including the mammary glands of virgin female mice, whereas the 66 kDa variant shows limited tissue distribution and predominates during the late stages of pregnancy and during lactation (Oshima et al., 1999). Nevertheless, the function of the proline/threonine rich insertion is unknown. It may increase the binding efficiency of SED1 to

phospholipids (Hanayama et al, 2002; Oshima et al, 1999) and/or increase the efficiency of secretion (Oshima et al, 1999). In this regard, it is interesting that when the two isoforms are expressed in epidermal keratinocytes, the long form is secreted into the culture supernatant, whereas the short form remains associated with the cell surface (Watanabe et al, 2005).

1.1.3 SED1 contributes to phagocytic removal of apoptotic cells in many tissues and organs

Macrophage removal of apoptotic lymphocytes

Given the known phospholipid binding specificity for the C-terminal F5/8C domains, it is not surprising that SED1 has been identified as a key regulator of apoptotic cell removal in numerous systems (Fens et al., 2008; Hanayama et al., 2002; Leonardi-Essmann et al., 2005). The first and best-studied example pertains to macrophage recognition of apoptotic lymphocytes in germinal centers. Upon activation, phagocytes secrete SED1 as they encounter apoptotic cells. The C-terminal domains mediate attachment to phosphatidylserine and phosphatidylethanolamine residues exposed on the surface of the apoptotic lymphocyte, whereas the RGD motif binds to α_v integrins expressed on the advancing phagocyte (Hanayama et al., 2002; Leonardi-Essmann et al., 2005). As expected, activated peritoneal macrophages harvested from SED1-null animals have a reduced capacity to engulf apoptotic cells compared to wildtype (Hanayama et al., 2004). Surprisingly though, these macrophages can still bind apoptotic cells suggesting that SED1 is required for the process of engulfment rather than simply

functioning as a molecular bridge between cellular debris and the phagocyte (Hanayama et al., 2004). Mutation of the RGD motif to RGE has no effect on the protein's binding to apoptotic cells, which is mediated by the C-terminal domain; but rather blocks phagocyte engulfment, further implicating integrin binding in this processes (Asano et al., 2004). Additionally, adult SED1-null animals display characteristics of autoimmunity, including an enlarged spleen, a marked increase in serum antibodies against double-stranded DNA and nuclear proteins, and glomerulonephritis, a condition caused by the deposition of circulating antibodies in the kidney (Hanayama et al., 2004). These pathologies are phenocopied in wildtype mice injected with RGE-mutant SED1, which serves as a dominant-negative inhibiting phagocytic engulfment of self-antigens (Asano et al., 2004). Analogously, the human homolog of SED1 (hMFG-E8) was also found to bind phosphatidylserine and engage $\alpha_v\beta_3$ integrins (Yamaguchi et al., 2008). As expected, low levels of hMFG-E8 were found to enhance phagocytosis, however, at high concentrations, engulfment was inhibited in a dose-dependent fashion (Yamaguchi et al., 2008). These surprising results are of interest in light of the fact that some human patients suffering from the chronic autoimmune condition systemic lupus erythematosus have elevated serum levels of hMFG-E8 (Yamaguchi et al., 2008).

An interesting corollary has been suggested for microglial cells that assume a phagocytic role in the clearance of apoptotic neurons. Fractalkine is a chemokine expressed by non-hematopoietic cells, such as endothelia, neurons, and glial cells, that when released from the cell surface by the TACE protease, elicits a gradient-dependent chemoattraction of macrophages and other immune cells (Leonardi-Essmann et al.,

2005). Gene chip analysis of microglia transcripts following exposure to fractalkine revealed significant up-regulation of SED1 (Leonardi-Essmann et al., 2005). This raises the interesting hypothesis that fractalkine serves as both a chemoattractant leading microglia to damaged neurons, as well as a priming factor, inducing the production of SED1 that will subsequently mediate engulfment of the apoptotic cell (Leonardi-Essmann et al., 2005).

Clearance of mammary epithelial cells during involution

SED1 performs a similar function during the clearance of apoptotic cells resulting from involution of the lactating mammary gland. Involution is triggered when the suckling stimulus by the pups is lost, and can be divided into two phases. A reversible phase occurs during the first 48 hours when apoptotic cells are shed into the alveolar lumen, where they are cleared by “nonprofessional” phagocytes, such as neighboring epithelial cells. In the second phase, which can last 8 days, the extracellular matrix and basement membrane are digested by proteases, leading to a destruction of the lobular-alveolar architecture. Apoptotic epithelial cells are removed by phagocytes that migrate into the involuting gland, and adipocytes concurrently reappear to reorganize the mammary gland to the pre-pregnant stage (Fadok, 1999; Monks et al., 2002; Monks et al., 2005).

During the first two days of involution, SED1-deficient mice show an increased level of apoptotic cells in the alveolar lumen, but the frequency of apoptotic cells in the alveolar epithelium is similar to control animals. This suggests that SED1-null cells have

impaired phagocytosis. Consistent with this, primary mammary epithelial cells from SED1 mutants have significantly lower phagocytic potential when compared to controls. At later stages of involution, the proportion of apoptotic cells is similar to controls compensatory pathways. Multiple cycles of pregnancies, involution and inflammation result in a dramatic dilatation of the mammary gland ductal network indicating an important role for SED1 in maintaining normal mammary gland function. In later stages of involution, the residual milk fat globules and apoptotic cells, both of which have high phosphatidylserine content, are removed by macrophages that express high levels of SED1. In the absence of SED1, the apoptotic cells are not cleared efficiently and membranous material accumulates within the gland during involution, leading to enlarged ducts.

Diurnal clearance of photoreceptor outer segments

The phototransduction machinery of the retinal photoreceptors lies adjacent to the retinal pigmented epithelium (RPE), which expresses components that stabilize retinal adhesion as well as remove fragments of the photoreceptor outer segments (POS) that are shed daily from the photoreceptors (Burgess et al., 2006). Previous studies indicated a requirement for $\alpha_v\beta_5$ integrin in both retinal adhesion and RPE-mediated phagocytosis of POS fragments (Nandrot et al., 2006; Nandrot et al., 2004). Since SED1 is a known ligand for $\alpha_v\beta_5$ integrins, and is localized to RPE, it raised the obvious possibility that SED1 could be the “link” between the integrin receptor on RPE and shed POS fragments (Burgess et al., 2006).

The adhesion of the RPE to the neural retina is slightly (~20%), but significantly decreased in SED1-deficient mice, coincident with the peak period of retinal adhesion (Nandrot et al., 2007). Adhesion at non-peak times is unaffected in SED1-deficient mice (Nandrot et al., 2007). Since the loss of $\alpha_v\beta_5$ leads to a much greater loss of RPE-neural retina adhesion, the authors conclude that SED1 does not likely play a major role in retinal adhesion, as does $\alpha_v\beta_5$ (Nandrot et al., 2007). However, the mice used in these studies are not traditional SED1 knockout mice, but rather, express SED1 that is engineered to remain membrane-bound and not secreted, as is the wildtype protein (Atabai et al., 2005). Consequently, the membrane-associated SED1 may still be able to partially mediate intercellular adhesion via integrin binding (Nandrot et al., 2007). Nevertheless, the lack of secreted SED1 leads to a dramatic reduction in phagocytosis of outer segment markers (Nandrot et al., 2007). Furthermore, RPE isolated from SED1-deficient mice show reduced (~50%) binding of POS, relative to RPE from control mice (Nandrot et al., 2007). Finally, exogenous SED1 can rescue the reduced binding of mutant RPE, as well as promote binding of POS to RPE cell lines (Nandrot et al., 2007). These results support the notion that SED1 is critical for the circadian removal of shed POS by the RPE (Nandrot et al., 2007). It should be noted that other investigators were unable to confirm these studies using siRNA constructs to knockdown SED1 mRNA in cultured RPE cells, as opposed to the use of genetically-engineered mice (Burgess et al., 2006).

Clearance of apoptotic cell debris in atherosclerotic vessels

Recent data suggests that the opsonizing characteristics of SED1 may also function in removal of pathogenic plaques. Atherosclerotic plaques accumulate cell debris, including apoptotic cells, which leads to plaque progression and disease. Phagocytic clearance of this apoptotic cell debris is critical for homeostatic maintenance and activation of anti-inflammatory pathways. Not surprisingly, SED1 is expressed in normal endothelial cells, smooth muscle and plaque-associated macrophages. To explore SED1 function in the clearance of the atherosclerotic debris, *ladler* *-/-* mice, which are susceptible to atherosclerosis, were irradiated and reconstituted with either wildtype or *Mfge8*-deficient bone marrow (Ait-Oufella et al., 2007). After 8 weeks on an atherogenic diet, the mice reconstituted with wildtype bone marrow developed early lesions of atherosclerosis that were devoid of apoptotic cells (Ait-Oufella et al., 2007). However, in mice reconstituted with *Mfge8*-null marrow, the frequency of apoptotic cells in lesions was markedly elevated, resulting in a 70% increase in lesion size (Ait-Oufella et al., 2007). Interestingly, this phenotype is similar to that seen in $\alpha_v\beta_5$ deficiency, which participates in SED1-mediated clearance of apoptotic cells (Weng et al., 2003). Furthermore, the accumulated apoptotic debris is associated with decreased anti-inflammatory interleukins (IL-10) in the spleen, and increased IFN- γ in both spleen and atherosclerotic arteries (Ait-Oufella et al., 2007). These and other results suggest to the authors that SED1 expression in bone marrow-derived cells is critical for maintenance of the normal systemic immune response (Ait-Oufella et al., 2007).

Clearance of A β amyloid plaques in Alzheimer's disease

A recent study reported that cultured astrocytes express SED1, which can be found in their released exosomes (Boddaert et al., 2007). Similarly, SED1 expression is readily seen in astrocytes in cadaveric brains, but its expression is greatly decreased in the vicinity of A β plaques in brains from Alzheimer's disease (AD) patients. mRNA levels are also reduced by 35% in AD brains as compared to healthy controls (Boddaert et al., 2007). Consistent with a possible casual relationship between SED1 expression and the clearance of A β plaques, the authors reported a direct interaction between recombinant SED1 and the A β 1-42 peptide; substitution of the RGD motif with RGE inhibited interaction with the A β peptide (Boddaert et al., 2007). More directly, FITC-conjugated A β peptide was taken up by murine macrophages and microglial cells (Boddaert et al., 2007). Similar results were seen using blood-derived human macrophages, which were inhibited by incubation with anti-SED1 antibodies (Boddaert et al., 2007). Finally, peritoneal macrophages from SED1-null mice had a severely reduced ability to phagocytose A β 1-42 peptide (Boddaert et al., 2007). Collectively, these data suggest that similar to resolution of atherosclerotic plaques, SED1 serves a role in preventing the accumulation of A β amyloid.

1.1.4 SED1 facilitates a number of intercellular interactions

SED1 mediates sperm-egg binding

SED1 was independently identified as a component of porcine sperm that has binding affinity for glycoproteins of the egg coat (Ensslin et al., 1998). Sperm membranes were solubilized and applied to affinity columns containing immobilized zona pellucida (i.e., egg coat) glycoproteins (Ensslin et al., 1998). Sequencing of the predominant eluted protein resulted in identification of porcine SED1, originally named p47 (Ensslin et al., 1998). The ability of SED1 to function as a sperm receptor for the egg coat was confirmed by analysis of SED1-null male mice, which are sub-fertile in vivo and whose sperm are unable to bind eggs in vitro (Ensslin and Shur, 2003).

Sperm acquire SED1 during two phases of their development. The first evidence of SED1 immunoreactivity occurs in the Golgi complex of spermatogenic cells, where it is presumably secreted onto the sperm surface (Ensslin and Shur, 2003). However, the majority of sperm-associated SED1 is derived from secretions of the initial segment of the epididymis, where it binds to the anterior dorsal aspect of the sperm plasma membrane, the area known to be responsible for mediating initial adhesion to the egg coat (Ensslin and Shur, 2003).

Studies with truncated proteins devoid of specific functional domains indicate that the gamete binding activity of SED1 lies in the C-terminal F5/8C discoidin domains (Ensslin and Shur, 2003). The function of the EGF domains in this circumstance remains uncertain, but it is thought that integrin binding does not participate in sperm-egg adhesion in mice (Ensslin and Shur, 2003). One model for SED1 function during sperm-

egg adhesion suggests that the two different F5/8C domains have preferential binding affinities: the C2 domain binding exposed phosphatidylserine residues on the sperm membrane, and the C1 domain binding the egg's zona pellucida, analogous to the C1 domain of Del1, a SED1 homolog that binds to the extracellular matrix (Ensslin and Shur, 2003; Hidai et al., 2007; Shur et al., 2004). In this way, SED1 could serve as a molecular bridge linking the two gametes. Since two EGF repeats are capable of mediating multimerization of other cell adhesion molecules, it is possible that SED1 functions as a dimer or multimer brought about by EGF-dependent multimerization (Ensslin and Shur, 2003; Shur et al., 2004). More recent studies suggest that sulfation of SED1 may also be important for its activity in sperm-egg binding. TPST-2 is a Golgi-localized sulfotransferase that mediates protein-tyrosine sulfation in the male reproductive tract (Hoffhines et al., 2008). *Tpst-2* knockout mice are infertile, and their sperm exhibit reduced motility and fertilizing capability (Hoffhines et al., 2008). SED1 has been identified as substrate for TPST-2, and *Tpst-2* knockout mice produce non-sulfated SED1, which suggests this post-translation modification is critical for its function in fertilization (Hoffhines et al., 2008).

Maintenance and repair of the intestinal epithelium

The epithelial lining of the gut undergoes continuous turnover, with stem cells located deep within the crypts being induced to differentiate into absorptive enterocytes and secretory cells as they migrate out of the crypt onto the villus surface (Bu et al., 2007). Not surprisingly, SED1 is expressed in murine macrophages of the intestinal

lamina propria, which led investigators to examine its potential role in repair and maintenance of the intestinal epithelium (Bu et al., 2007). Unlike what is reported for other systems, the addition of exogenous SED1 accelerates the rate of migration of IEC-18 cells, an enterocyte cell line, in a PKC-dependent manner (Bu et al., 2007). The exogenous SED1 binds to the posterior region of the migrating cells, possibly to a patch of exposed phosphatidylserine (Bu et al., 2007). In vivo, SED1 is found on crypt cells following injury, consistent with a potential role in epithelial repair (Bu et al., 2007). More directly, anti-SED1 antibodies arrest the migration of BrdU-labeled cells out of intestine crypts, and a similar reduction in crypt cell migration is seen in SED1-null mice (Bu et al., 2007). As shown by others (Miksa et al., 2006; 2007), SED1 expression is dramatically reduced following sepsis, which is also associated with reduced enterocyte migration from the crypts to the villus (Bu et al., 2007). Remarkably, administration of SED1 to septic mice restores crypt cell migration (Bu et al., 2007). How SED1 promotes migration of intestinal epithelial cells is unclear, but may involve a relocalization of Arp2/3 and dissolution of actin-based stress fibers, along with the establishment of a new lamellipodia (Bu et al., 2007).

SED1 facilitates mammary gland branching morphogenesis

In addition to its role in the clearance of apoptotic cells during mammary gland involution, SED1 also participates during development of the mammary gland. SED1-null females show greatly diminished mammary glands, reflecting a severe reduction in the frequency of branching from both epithelial ducts and from terminal end buds, which

are thin and poorly developed (Ensslin and Shur, 2007). During normal development, the expanding epithelial tree develops from reciprocal inductive interactions between the two cell types that constitute the double-layered epithelial tube: luminal epithelial cells and myoepithelial cells. SED1 is expressed by the epithelial cells where it binds to $\alpha_v\beta_{3/5}$ integrin receptors on myoepithelial cells, leading to MAPK activation and subsequent cell proliferation and duct outgrowth (Ensslin and Shur, 2007). The absence of SED1 leads to a near total loss of MAPK activation in myoepithelial cells, with a concomitant reduction in cell proliferation and branching throughout the epithelial tree (Ensslin and Shur, 2007).

SED1 and its homolog Del1 promote vascularization

Del1 (Development endothelial locus-1) is a structural and functional homolog of SED1 that contains a signal sequence followed by three EGF-like, and two C-terminal F5/8C/discoidin-like domains. Identified via an enhancer-trap event in a transgenic mouse, Del1 is secreted onto the extracellular matrix by endothelial cells during embryonic vasculogenesis (Hidai et al., 1998). In vitro studies suggest that Del1 serves autocrine and paracrine roles by supporting the migration and proliferation of both endothelial cells and vascular smooth muscle cells (Penta et al., 1999; Rezaee et al., 2002). In this regard, the addition of Del1 to chick chorioallantoic membrane assays results in a potent pro-angiogenic response suggesting a role in vascularization (Penta et al., 1999). This is consistent with the ability of Del1 to increase vascular branching in the intestinal mesentery of transgenic mice that over-express Del1 (Hidai et al., 2005)

Further molecular characterization indicates that Del1 serves as a ligand for $\alpha_v\beta_5$

integrins, inducing aggregation of focal adhesion proteins and initiating intracellular signaling cascades including MAPK phosphorylation (Hidai et al., 1998; Penta et al., 1999; Rezaee et al., 2002). Del1 is therefore thought to facilitate vascular wall development and vascular remodeling by directing endothelial angiogenesis, and migration and proliferation of vascular smooth muscle cells, in-part through activation of anti-apoptotic pathways (Penta et al., 1999; Rezaee et al., 2002). Furthermore, endothelial derived Del1 has been reported to inhibit leukocyte adhesion to the endothelium, suggestive of an anti-inflammatory function for Del1 (Choi et al., 2008)

These findings are supported by the observation that endogenous Del1 is upregulated in ischemic hind limbs (Zhong et al., 2003). Therapeutic delivery of Del1 to the ischemic tissue, either through protein-soaked implants or gene transfer, enhances disease recovery by increasing vessel formation, capillary density, vascular flow, and muscle function (Ho et al., 2004; Zhong et al., 2003). Exogenous Del1 appears to first engage $\alpha_v\beta_5$ integrins leading to upregulation of the Hox D3 transcription factor and subsequent increased expression $\alpha_v\beta_3$ integrins (Zhong et al., 2003). Activation of $\alpha_v\beta_3$ integrins through binding to Del1 or other ligands is then thought to enhance vascular recovery by triggering an increase in endothelial cell proliferation (Zhong et al., 2003).

In an analogous manner, SED1 may facilitate neovascularization in adult tissue through similar mechanisms. Unlike Del1, SED1 is expressed in the vasculature of healthy adult tissues including the aorta and hindlimb muscles (Silvestre et al., 2005). Ectopic expression of VEGF is pro-angiogenic in in vitro assays, and increases capillary densities and angiography scores in an ischemia recovery model in mice (Silvestre et al.,

2005). Importantly, ischemic muscle of SED1-deficient mice is unaffected by VEGF over-expression, while over-expression of SED1 in wildtype muscle induces recovery independent of VEGF (Silvestre et al., 2005). These data suggest SED1 is a required, downstream effector of pro-angiogenic VEGF signaling (Silvestre et al., 2005). Further investigation into this pathway indicates that SED1 serves as a ligand for $\alpha_v\beta_3$ and/or $\alpha_v\beta_5$ integrins that in turn elevates AKT phosphorylation, a known mediator of endothelial cell survival and proliferation (Silvestre et al., 2005).

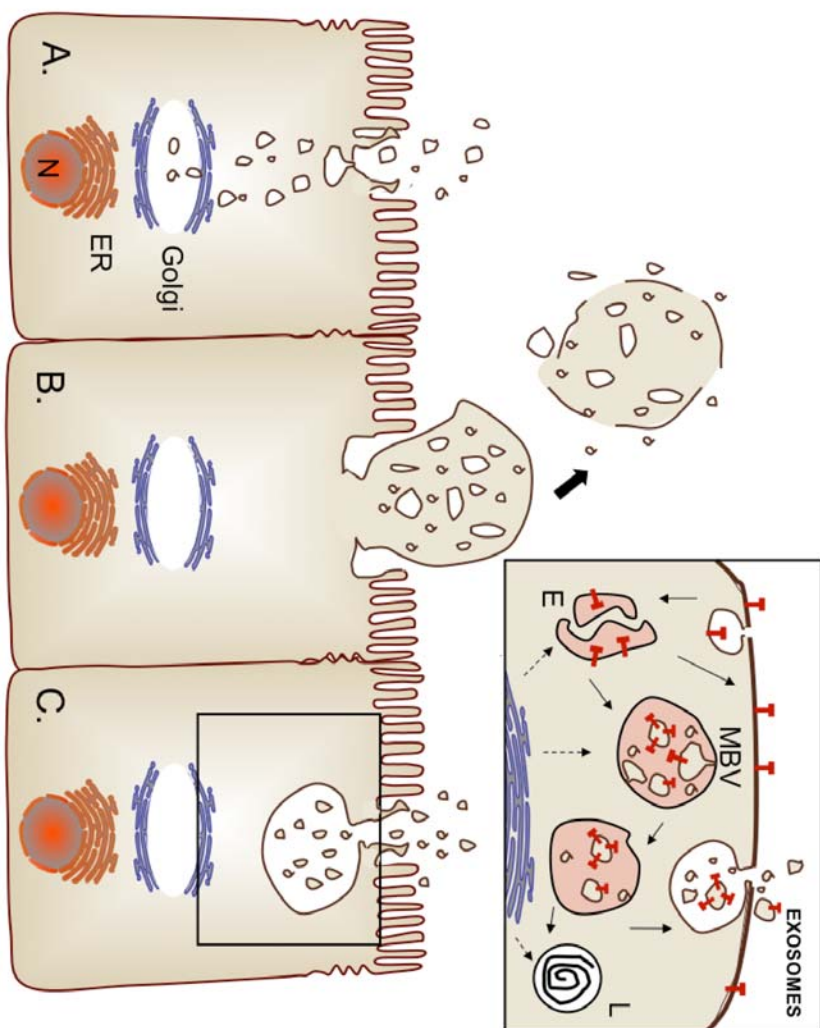
While these data support the substantial potential for Del1 and SED1 in therapeutic neovascularization, other studies indicate circumstances where inhibition of these proteins may also be desirable. Del1 was found to be misexpressed in naturally occurring adult, human tumor tissues (Aoka et al., 2002). In a disease model developed to investigate this phenomenon, multiple tumor cell lines transfected with Del1 exhibit increased capillary density and growth, and reduced apoptosis during tumor formation in nude and syngeneic mice (Aoka et al., 2002). Additional molecular studies indicate that Del1 expression in tumor cells is activated by tumor-derived growth factors, including VEGF, and support a role for Del1 in pathological angiogenesis (Aoki et al., 2005). Furthermore, SED1 is found in murine tumor cell lines and is up-regulated in angiogenic islets and tumors of an in vivo model for pancreatic carcinogenesis (Neutzner et al., 2007). Interestingly, SED1-deficient mice exhibit only a modest reduction in tumor frequency and survival, and although vascular permeability and proliferation of the tumors are somewhat reduced, other pro-angiogenic signals, including FGF2 and Del1, are elevated suggesting tumorigenesis circumvented the requirement for SED1 (Neutzner

et al., 2007). These data indicate that SED1 and Del1 may serve similar roles in embryonic (Del1) and adult (SED1) vascular modeling, and point to each being a candidate for endovascular enhancement as well as a target for anti-angiogenic/tumorigenic therapies.

Facilitating exosome-function in dendritic cells

An interesting feature of SED1 secretion in all cell types thus far examined is that it is found associated with exosomes - small membrane-bound vesicles released from the cell upon fusion of multivesicular bodies with the plasma membrane (Denzer et al., 2000) (Fig. 1-3). In this regard, SED1 is found as a predominant component of the mammary fat globule released into milk, as well as exosome-like vesicles called epididymosomes in the epididymis (Gatti et al., 2005). Early studies of SED1's association with exosomes suggest it may be important for the formation and/or secretion of exosome vesicles. In this regard, COS-7 cells transfected with full-length SED1 localize the protein to punctate aggregates on the cellular membrane, as well as the surface of secreted exosome-like microvesicles (Oshima et al., 2002). Transfection with SED1 also increases exosome secretion three-four fold (Oshima et al., 2002). Moreover, expression of mutant constructs with either C-terminal domain deleted abolishes both cell-surface and exosome localizations of the protein, and the C2 domain in particular was found to be indispensable for SED1-dependent increases in exosome secretion (Oshima et al., 2002).

Figure 1-3: SED1 is associated with microvesicles such as epididymosomes and exosomes. A) SED1 may be secreted as a soluble protein through classical mechanisms, however SED1's association with microvesicles suggests it is also secreted through non-classical pathways including B) apocrine shedding (epididymosomes) and C) multivesicular body fusion with the apical plasma membrane (exosomes).



However, the significance of SED1 association with exosomes remains obscure. It is presently unclear if SED1 association with exosomes simply reflects its means of transport to the cell surface, or rather, has additional functional significance. In this regard, epididymosomes are thought to influence sperm maturation by bringing critical proteins in contact with the sperm plasma membrane, where they can transfer from vesicles to the plasma membrane in a zinc and pH-dependent mechanism (Sullivan et al., 2005). However, most insight into the function of exosome-associated SED1 has come from studies of dendritic cells.

Dendritic cells (DC) are professional antigen presenting cells that contribute to tolerance and immunity by accumulating antigens from their microenvironment. Circulating (immature), DC are highly phagocytic, engulfing antigens and processing them into peptides that are presented on the cell surface in association with Major Histocompatibility Complexes (MHC). Under homeostatic conditions immature DC help to preserve tolerance, however, when an antigen of pathologic origin is detected, DC initiate a maturation process. The cell migrates to the lymph node, presenting antigen/MHC and various other co-stimulatory molecules to T cells. Although both immature and mature dendritic cells secrete exosomes, the components and activity of these vesicles are distinct, suggesting they have different functions depending on the cell's maturation state. In fact, exosomes secreted by mature DC are 50- to 100- times more effective at inducing a T cell immune response than are exosomes from immature DC (Segura et al., 2005). Alternatively, exosomes from immature DC, which are known to carry antigen/MHC complexes, are thought to amplify the immune response by

providing both immature and mature DC with additional unique antigens for presentation to T cells (Segura et al., 2005).

Not surprisingly, the discovery that SED1 is highly expressed by immature DC, but significantly reduced in mature DC, has led to several investigations into its function (Miyasaka et al., 2004; They et al., 1999; Veron et al., 2005). Given the well-documented adhesive nature of SED1, investigators initially proposed that exosome-associated protein could facilitate docking or uptake of secreted exosomes to target effector cells (Miyasaka et al., 2004; Morelli et al., 2004; They et al., 1999; Veron et al., 2005). However, exosomes isolated from SED1-deficient mice are nearly as efficient in transferring antigen/MHC complexes to recipient DC as vesicles isolated from wildtype mice, indicating this is probably not the case (Veron et al., 2005). Furthermore, SED1 is not required for mature DC-mediated T cell activation (Segura et al., 2005).

Alternatively, DC are known to phagocytose a wide range of materials including pathogens, dying cells, and in some cases live cells; therefore, a second hypothesis suggests that SED1 secreted by immature DC may facilitate engulfment through mechanisms similar to its well-characterized role in macrophage clearance of apoptotic cells (Akakura et al., 2004). One study indicates that SED1 binds to $\alpha_v\beta_5$ integrins on immature DC via its RGD motif, initiating a signal transduction cascade through DOCK180 and Rac1 that potentiates phagocytosis (Akakura et al., 2004). Conversely, SED1 and DOCK180 are both down-regulated in mature DC, cells that exhibit reduced phagocytosis relative to their immature counterparts (Akakura et al., 2004). Importantly, the nature of SED1 secretion either soluble or in association with

exosomes, was not specifically addressed in this study, and therefore the role of exosomes in this pathway remains somewhat unclear.

1.1.5 Concluding thoughts: SED1 as a therapeutic agent

The various roles established for SED1 immediately suggest a number of potential therapeutic opportunities. Oncological studies indicate that SED1 is expressed and often up-regulated on the surface of breast carcinoma cells, and antibodies against the protein have met with some success in cancer diagnosis and therapy (Larocca et al., 1991). More recently, investigators have been successful in priming cytotoxic T cells to target SED1-positive breast cancers (Liu et al., 2005). In this case, adeno-associated virus-based gene loading was used to delivery SED1 to dendritic cells, which in turn presented the protein to cytotoxic T cells in the form of antigen/MHC under co-stimulatory conditions (Liu et al., 2005). Alternatively, fusion of the C-terminal domains of SED1 to a tumor antigen has been found sufficient to target the otherwise soluble antigen to secreted exosome-like vesicles (Zeelenberg et al., 2008). In this investigation, a vesicle-associated tumor antigen induced a stronger T cell-mediated immune response than did the same antigen secreted as a soluble protein. As a result, tumors secreting vesicle-associated antigens were slower growing, and a DNA-vaccine therapy featuring an antigen-SED1 fusion construct had a protective effect, limiting tumor size in a mouse tumor progression model (Zeelenberg et al., 2008).

As mentioned above, the clear involvement of SED1, and its homolog Del1, in angiogenesis raises a number of intriguing possibilities regarding their potential clinical

use. Investigators have already applied these observations to enhance recovery of ischemia in a rodent model. Finding that inappropriate activation of this pathway initiates angiogenesis in developing tumors also suggests that SED1 antagonists could be used to arrest tumor growth. How the SED1 antagonists will be targeted to the appropriate site is unclear, but workers have suggested that RGD-bearing chemotherapeutic agents could be targeted to the SED1-dependent phagocytic activity of endothelial cells in angiogenic tumors (Fens et al., 2008).

A number of studies also indicate that SED1 expression is dramatically reduced during sepsis, and in at least one instance, exogenous administration SED1 was able to reverse some of the cellular defects associated with sepsis (Bu et al., 2007; Miksa et al., 2007; Miksa et al., 2006). The decrease in SED1 expression during sepsis is also associated with a decrease in clearance of apoptotic cells, an effect that can be partially rescued by the administration of SED1-containing exosomes collected from immature DC. Exosome administration also leads to increased survival of septic animals (Miksa et al., 2006). In this regard, administration of the cytokine, fractalkine, to septic animals, induces SED1 expression and enhances clearance of apoptotic cells (Miksa et al., 2007).

A few other therapeutic applications of SED1 are less well-defined, but nonetheless bear mentioning. One of the first reported functions for SED1 in breast milk is to prevent rotavirus infection in breast-fed infants, and the protein has also been found to block enterotoxigenic *E. coli* attachment to the intestinal villi of piglets (Kvistgaard et al., 2004; Newburg et al., 1998; Shahriar et al., 2006). Together, these data raise the possibility of supplementing formula with SED1 to boost immunity for formula-fed

children. SED1 has also been utilized similarly to annexin V as a reagent for identifying apoptotic cells, and recent membrane-binding studies reveal that the affinity of SED1 for phosphatidylserine-containing membranes is more than 100-fold greater than that of Factor VIII C2 (Shao et al., 2008; Shi and Gilbert, 2003; Venegas and Zhou, 2007). In fact, SED1 directly competes for the phospholipid binding sites of Factor V and Factor VIII, therefore inhibiting prothrombinase and Xase complexes that are activated during the coagulation cascade (Shi et al., 2008). These data suggest SED1, perhaps even the C2 domain alone, could serve as potent anti-coagulant, or alternatively, a targeting molecule directing a therapeutic-of-interest to phosphatidylserine-rich membranes (Shao et al., 2008).

These are just a few of the rich possibilities that present themselves, reflecting the many distinct types of cellular interactions mediated by SED1. Although all of these potential uses raise many more questions than they answer, it is clear that this unusual multi-domain protein offers much potential for research and therapeutics.

1.2 Introduction to the male epididymis

1.2.1 Summary

The epididymis is part of the male excurrent duct and its proper function is critical for male reproductive health. Upon leaving the testis, sperm pass through the efferent ducts and into the epididymis where they are modified by epididymal secretions that are required for the acquisition of motility and fertilizing ability (Orgebin-Crist, 1969).

Furthermore, the efferent ducts and epididymis are responsible for absorbing up to 75% of the testicular fluid and reducing the pH by 0.5 units to compact and inactivate the sperm for storage in the distal segment (Levine and Marsh, 1971). As the molecular nature of these functions are better understood, the epididymis has received increased attention as a target of post-meiotic male contraceptive technologies, while remaining an excellent model for investigating complex questions in tubule development, differentiation, and maintenance.

1.2.2 Epididymal organization and anatomy

The epididymis consists of a single highly convoluted tubule of pseudostratified epithelium wrapped in smooth muscle and packaged in a fibrous capsule that resides immediately adjacent to the testis (Setchell et al., 1994). The mouse epididymis can be separated into three anatomical segments based on function, cell morphology, and gene/protein expression (Abou-Haèila and Fain-Maurel, 1984; Flickinger, 1981). The region proximal to the testis is composed of the “initial segment” and caput, which collectively are responsible for fluid reabsorption and protein secretion (Abou-Haèila and Fain-Maurel, 1984). Subsequently, the sperm transit through the corpus segment into the distal cauda epididymis where mature sperm are stored (Setchell et al., 1994).

The epididymal epithelium is composed predominately of principal cells, protein secretory cells responsible for modifying the luminal contents and the surface of the sperm membrane (Robaire and Hinton, 2002; Setchell et al., 1994). Principal cells change dramatically from a tall columnar morphology in the initial segment to low

cuboidal cells in the cauda (Abe et al., 1983; Abou-Haèila and Fain-Maurel, 1984). Interspersed among the principal cells are clear cells, a specialized epithelial cell type distinct from principal cells in both protein expression and function (Robaire and Hinton, 2002; Setchell et al., 1994). Present throughout the caput, corpus and cauda, clear cells express VATPase proton transporters that contribute to reduction in luminal pH from 7.3 to 6.8, which maintains sperm in a quiescent state during storage (Breton et al., 1996; Hinton and Palladino, 1995; Levine and Marsh, 1971).

1.2.3 Epididymal function: protein secretion

During epididymal transit, sperm undergo a gradual maturation process that includes addition of epididymal proteins, reduction in testicular fluid volume by as much as 75% to compact the sperm for storage, and a reduction in luminal fluid pH by 0.5 units to maintain sperm in a metabolically-quiescent state (Levine and Marsh, 1971). Epididymal function can be divided into several key events unique to each anatomical region (Flickinger, 1981; Glover and Nicander, 1971; Pavlok, 1974). The tall columnar cells of the initial segment secrete factors into the luminal fluid that bathe the sperm, while adding various membrane-associated proteins to the sperm surface (Hinton and Palladino, 1995). Modification of the sperm surface with epididymally-secreted proteins such as SED1, is known to be critical for imparting the sperm with the ability to become motile and fertilize eggs (Ensslin and Shur, 2003; Robaire and Hinton, 2002).

Secretion of proteins in the initial segment occurs through traditional secretory pathways as well as non-classical mechanisms such as apocrine shedding, a process that

involves the formation and detachment of membrane-bound protrusions known as apical blebs (Flickinger, 1981; Hermo and Jacks, 2002). As these projections are shed into the lumen, the plasma membrane fragments, releasing its cache of soluble and membrane-associated proteins. The membrane-associated components are packaged into small (50-800 nm) vesicles called epididymosomes, which encounter and/or exchange lipid and protein components with sperm (Hermo and Jacks, 2002; Rejraji et al., 2006).

1.2.4 Epididymal function: fluid reabsorption and pH modification

The principal cells that populate the initial segment and caput also express a host of acid/base transporters and enzymes that facilitate water absorption and acidification of the luminal fluid (Badran and Hermo, 2002; Bagnis et al., 2001; Breton et al., 1999; Chew et al., 2000; Cyr et al., 1996; Hermo et al., 2005; Isnard-Bagnis et al., 2003; Jensen et al., 1999a; Jensen et al., 1999b; Kaunisto et al., 1995; Levy and Robaire, 1999a; Pushkin et al., 2000; Wagenfeld et al., 2002; Yeung et al., 2004b). Apical sodium/hydrogen exchangers reabsorb sodium that drives water absorption through aquaporin channels and leaky tight junctions (Levine and Marsh, 1971; Robaire and Hinton, 2002). In exchange for sodium, protons are secreted, that in conjunction with luminal carbonic anhydrase, react with bicarbonate to generate carbon dioxide and water (Pastor-Soler et al., 2005). The carbon dioxide diffuses into cells along its concentration gradient where intracellular carbonic anhydrase directs the reverse reaction back to protons and bicarbonate. Basolateral sodium/bicarbonate transporters complete the cycle by secreting sodium and bicarbonate into the interstitial fluid.

The maturation process is continued in the corpus, and completed and sustained in the cauda epididymis where sperm are stored until ejaculation (Setchell et al., 1994). In the cauda, however, pH is not regulated by principal cells, but rather by clear cells that secrete protons through membrane-associated VATPase complexes localized at the luminal plasma membrane (Breton et al., 1996; Brown et al., 1992). Localization of VATPase is tightly tethered to luminal pH, cycling between the apical membrane and late endosomes under acidic conditions, but remaining static at the membrane when bicarbonate levels are high (Pastor-Soler et al., 2003). High bicarbonate levels and alkaline pH are known activators of sperm, and therefore the acidic, low bicarbonate environment of the cauda is thought to maintain the concentrated sperm in a quiescent state during storage (Acott and Carr, 1984; Carr et al., 1985; Hinton and Palladino, 1995; Pastor-Soler et al., 2005).

1.3 Focus of Dissertation

As described in the Introduction, our lab has recently identified SED1 as a sperm-associated protein critical for sperm binding to the egg coat during fertilization. SED1 is secreted by the initial segment of the epididymis where it coats the anterior surface of sperm during sperm maturation. Development of the SED1-null mouse resulted in male-specific subfertility *in vivo*, and SED1-null sperm are deficient in binding eggs *in vitro*. Unexpectedly, this study revealed that SED1-null male mice also exhibit swollen epididymides compared to their wildtype counterparts. This observation suggests an unappreciated tissue-intrinsic role for SED1 in the epididymis.

The epididymis serves indispensable roles in sperm maturation and storage and a functional epididymis is necessary for male fertility. In addition to serving as an excellent model of tubule development, differentiation, and maintenance; the epididymis offers a novel avenue for treating male infertility as well as a viable target for post-meiotic male contraception. Therefore, I investigated the function of SED1 in the epididymis to uncover the basis for the unexpected swelling found in the SED1-null male. This dissertation provides a detailed analysis of pathologies and histological abnormalities associated with the SED1-null epididymis. An *in vitro* system is introduced and used to explore underlying SED1-dependent molecular mechanisms, and models for tissue-intrinsic functions for SED1 in the epididymis are considered.

Chapter 2: Materials and Methods

Some written material in Chapter 2 has been published previously or will be published in the future (Raymond et al., 2009a; Raymond and Shur, 2009).

The SED1-null mouse was developed by Michael A. Ensslin.

All assays described in Chapter 2 were developed or modified by Adam S. Raymond with the exception of section 2.6.2 [All other immunoblots (Chapter 5)] that was developed by Adam S. Raymond and Brooke Elder.

Chapter 2: Materials and Methods

2.1 Mice and recombinant SED1

All experiments were conducted using wildtype and SED1-null congenic C57/B6 males, with exception of following: ZO-1 and SED1 immunocytochemistry in primary cells (in vitro); Syntaxin-3 staining and endogenous β -galactosidase detection in vivo were carried out with tissue isolated from the original B6/129 mosaic line; and all adhesion assays were conducted with commercially available CD1 males (Charles Rivers). rSED1 refers to purified recombinant protein prepared as described (Ensslin and Shur, 2003) or purchased commercially (R&D System 2805-CF).

2.2 Tissue preparation for histology

Paraffin-embedded tissue was prepared in either of two ways: 1) whole animal perfusion using 4% paraformaldehyde followed by post-dissection submersion fixation in the same, or 2) dissection and overnight submersion fixation in Bouins fixative (Sigma HT10-1-32). Tissue was dehydrated, infiltrated with paraffin, and 5 or 10 μ m sections were prepared using a Microm microtome. Alternatively, frozen 7 or 10 μ m cryosections were fixed with 2% paraformaldehyde prior to staining. Sections of wildtype and SED1-null tissue were stained with hematoxylin and eosin or processed for immunocytochemistry. Tissue for electron microscopy was freshly dissected and submersion-fixed in 2% glutaraldehyde buffered with cacodylate. Fixed tissue was

stained with osmium and processed for semi-thin and thin sections by the Emory University School of Medicine Electron Microscopy Core.

2.3 Epithelial morphometrics

Paraffin-embedded sections were immunostained with anti-AQP-9 and counterstained with hemotoxylin to define basic cell structure and AQP-9 reactive stereocilia. The initial segment region was identified by morphology and proximity to the efferent ducts, and measurements were conducted using IPLab image analysis software calibrated with an optical micrometer. Cell heights of principal cells were measured parallel to cell-cell borders from the basement membrane to the apical membrane, and stereocilia were measured along the same trajectory from the apical membrane to the distal end of the cilia. Only tubules perpendicular to the plane of section (seen as circular, doughnut-like tubule cross-sections) were measured. All data points from each single epididymide were averaged and constitute one experiment. Graphed data represents six independent experiments from each genotype.

2.4 Detection of endogenous β -galactosidase activity

Fresh frozen sections (7 μ m) were prepared and fixed in 50/50 acetone/chloroform for 10 min. Sections were incubated with 1mg/ml x-gal diluted in staining buffer (5 mM $K_3Fe(CN)_6$, 5 mM $K_3Fe(CN)_6 \cdot 3H_2O$, 2 mM $MgCl_2 \cdot 6H_2O$ in PBS) at 37 °C for 24 hours (dark). Slides were washed with PBS, counterstained with hematoxylin, and embedded with aquatex for viewing at light-level.

2.5 Immunocytochemistry

2.5.1 In vivo

Paraffin-embedded or fresh-frozen sections were subjected to antigen retrieval using 10 mM sodium citrate buffer, blocked with 2% BSA and 1% normal goat serum, and processed for indirect light-level or fluorescent immunolocalization. Analysis included use of commercially available antibodies MFG-E8, LAMP-1, E-cadherin, NHE3, NHE2, NBC1, EAAC1, AE2, AQP-9, VATPase, Cx43, ZO-1, CAII, CAIV, EAAC1, and Syntaxin-3; as well as reagents obtained from other investigators including rabbit anti-SED1 polyclonal antibody [1:100; (Ensslin and Shur, 2003)], and CLC-3/5 antibody (Isnard-Bagnis et al., 2003). Signal was detected by one of two methods: 1) fluorescence using appropriate secondary antibodies conjugated with a fluorescent tag excitable at 595, or 488 nm, or 2) light level using an appropriate HRP-conjugated secondary exposed to DAB. Some staining included a biotin-avidin signal-amplification step.

2.5.2 In vitro

For immunodetection of SED1, polarized cultures were fixed with histology-grade methanol (Sigma M-1775) at -20°C for 10 minutes, blocked with 5% chicken serum, and stained with rabbit anti-SED1 polyclonal antibody (1:100). Bound antibody was detected with biotinylated anti-rabbit IgG (1:500; Zymed 65-6140) and avidin conjugated with Fluorescein (Vector). Isolated cells stained for α_v (1:200; Chemicon AB1930, rabbit polyclonal), ZO-1 (1:100; Zymed 61-73000, rabbit polyclonal), pan

cytokeratin (1:500; Sigma C-2562, mouse monoclonal), or desmin (1:100; Sigma D-1033, mouse monoclonal) were fixed with 4% paraformaldehyde containing 0.5% Triton in PBS. SED1 and α_v were detected using biotinylated anti-rabbit IgG (Vector BA-1000) and streptavidin conjugated with Alexa Fluor 488 (1:500; Molecular Probes S11223). ZO-1 was detected with anti-rabbit IgG conjugated with FITC (1:500, Sigma F-0382). Cytokeratin and desmin were detected with anti-mouse IgG Rhodamine RedX (1:500, Molecular Probes). Some cells were counterstained with DAPI (Sigma 9542) or propidium iodide (Molecular Probes P1304MP).

2.6 Immunoblotting

2.6.1 SED1 and α_v (Chapter 4)

Epididymides were subdissected into initial segment, caput, and cauda segments. Like segments were pooled from 2 animals/genotype and tissue was homogenized in 20 mM Tris pH 7.5. Material was centrifuged at 12,000 x g for 5 minutes at 4°C, and the insoluble pellet was resuspended in cold RIPA buffer and sonicated. Single cells (isolated as described above) from a pool of 3 animals/genotype were lysed in RIPA buffer. Fifty micrograms of protein/sample was resolved by 10% SDS-PAGE under non-reducing conditions and transferred to PDVF. The blot was blocked with blotto and incubated with primary antibody (non-immune serum 1:1,000; rabbit anti- α_v polyclonal, 1:1,000; hamster anti-MFG-E8 monoclonal, 1:1,000; or anti- β -tubulin mouse monoclonal, 1:10,000). Signal was detected using secondary antibodies conjugated with HRP (anti-rabbit, 1:50,000, Santa Cruz sc-2004; anti-hamster, 1:25,000, Santa Cruz sc-

2445; or anti-mouse 1:50,000, Santa Cruz sc-2005). Between probes, the blot was stripped for 20 minutes with stripping buffer (200 mM glycine, 0.4% SDS, pH 2.5).

2.6.2 All other immunoblots (Chapter 5)

Both epididymides from a single animal were subdissected and pooled by anatomical region to constitute one sample. Tissue was solubilized in 20 mM Tris, RIPA buffer, or Cooper Buffer, as indicated in Results. Protein concentrations were determined by Bradford assay, and equal protein loads were diluted in reducing or non-reducing sample buffer and resolved by 10% SDS-PAGE. Following transfer to PDVF, blots were blocked, probed, stripped, and reprobed as described using antibodies listed above (immunocytochemistry).

2.7 Preparation and culture of primary cells

Primary cell isolation and culturing was modified from (Carballada and Saling, 1997). Briefly, initial segment tissue was dissected into RPMI 1640 media and single cells were generated by mechanical dissociation followed by serial digestions in 0.5X trypsin/EDTA (Invitrogen 15400) for 20 minutes and 2.4 U/ml dispase (Invitrogen 17105-041) supplemented with 51.6 U/ml Type I collagenase (Invitrogen 17100-017) for 30 minutes. The resulting slurry was passed through Nytex mesh (pore size ~ 0.035 mm²; ~16 pores/mm²) to remove undigested tissue, washed several times, and resuspended in RPMI 1640 media containing 5% fetal bovine serum (FBS) and supplemented with 100 ng/ml EGF (BD Bioscience 354001) and 200 nM testosterone

(Sigma T-5035). Cell aggregates were passed through a cell strainer (BD Falcon 352235) and cells were “pre-plated” at approximately 10^5 cells/60 mm tissue culture dish, pre-coated with 20 μ g fibronectin (Invitrogen F1141) at 32°C. Following 2 hours of pre-plating, non-adherent epithelial-enriched cells were aspirated, washed, and cultured on transwell filters (Costar 3470), glass chamberslides (Nalge Nunc 154526), or tissue culture plastic (Falcon 353004) using serum-free media or media containing 5% FBS supplemented with 100 ng/ml EGF and 200 nM testosterone at 32°C with 5% CO₂.

2.8 Cell adhesion assays

Ninety-six well assay plates (Falcon 353072) were pre-coated with 500 ng/well recombinant protein for 4 hours, and washed and blocked with 10 mg/ml BSA for 1 hour prior to adhesion assays. Cells were harvested as described above from CD1 mice, 5-8 weeks of age. Single cells were cultured on 60 mm tissue culture dishes pre-coated with 20 μ g of rMFG-E8/SED1 for 96 hours. Through this process, healthy cells recovered from the initial isolation protocol proliferated, while damaged and dead cells were removed by serial washes. Following the culture period, cells were removed with 0.1X trypsin and 5 mM EDTA in Hanks Buffer and allowed to recover from trypsinization in fresh media for 2 hours at 32°C. For adhesion assays, cells were resuspended in serum-free RPMI 1640 media containing 100 ng/ml EGF/200 nM testosterone and 10 mg/ml BSA with or without peptide or inhibitors. Peptide inhibitors (GRGDNP, Biomol P-700; GRADNP, BiomolP-701) were found to reduce the pH of the media, and consequently, media containing peptides was buffered at 32°C, 5% CO₂ for 30 minutes prior to the

addition of cells. For antibody blocking experiments featuring RMV-7 (rat anti-mouse α_V monoclonal, Chemicon CBL1346) and rat IgG control (Abcam RTK2071), cells were pre-incubated with antibody for 30 minutes at 4°C prior to plating. Fifteen thousand cells in 100 μ l of media were added to each assay well and cells were allowed to adhere for 30 minutes. Non-adherent cells were removed by vacuum aspiration and wells were washed twice with 100 μ l PBS. Adherent cells were fixed and detected with 0.1% crystal violet solution according to Current Protocols in Cell Biology (Humphries, 1998). Unless indicated otherwise, individual data points from multiple experiments were converted to a percentage of mock control and averaged.

2.9 BrdU proliferation assays

Single cells were isolated from the initial segment of wildtype and SED1-null epididymides as described above. Enriched epithelial cells were applied to either uncoated or rSED1/MFG-E8 (800 ng) coated glass chamber slides at a concentration of 2.5×10^5 cells/chamber in 0.5 ml of serum-free RPMI 1640 media containing 100 ng/ml EGF and 200 nM testosterone. Cells were allowed to adhere and proliferate; non-adherent, dead, and damaged cells were removed by washing with RPMI 1640 media. After 96 hours, media was spiked with 100 μ g/ml BrdU (Sigma 85881). After 5 hours, adherent cells were fixed with acid-alcohol (10% acetic acid, 70% ethanol v/v) and processed for BrdU detection with biotinylated anti-BrdU antibody according to manufacture's protocol (1:50, Genetek GTX29557). BrdU-positive cells were visualized with streptavidin conjugated with Alexa Fluor 594, and all nuclei were counterstained

with SYTO24 (1:5,000; Invitrogen S7559). Cells were counted using a 40X objective and BrdU-positive cells were expressed as a percentage of total cells counted and normalized to wildtype values on glass. To compare the proliferation kinetics between uncoated and rSED1/MFG-E8-coated surfaces, only epithelial islands containing greater than four nuclei and less than a single field at 40X were scored.

2.10 Determination of luminal pH

A protocol for measuring luminal fluid pH was modified from a previous report (Yeung et al., 2004b). Single pairs of age-matched wildtype and SED1-null mice were sacrificed by cervical dislocation, and epididymides were quickly removed and subdissected by anatomical region. Luminal contents were gently expressed onto Hydrion pH paper (Microfine, range 6.0-7.4; MF-1615). pH was determined by immediately comparing expressed luminal fluid to a series of buffered standards ranging from 6.8-7.4. Each epididymis was analyzed separately by two independent observers and data points from all measurements were averaged to generate a pH value for each experiment. Graphed data represents two independent experiments featuring a minimum of eight epididymides from each genotype.

2.11 Intracellular vesicle quantification

Tissue was fixed by whole animal cardiac perfusion using 2% glutaraldehyde buffered with cacodylate. Semi-thin sections were prepared by the Emory University School of Medicine Electron Microscopy Core, and stained with toluidine blue. Images

were taken of circular, caput III tubules identified in stained-sections by morphology and presence of multivesicular body-like structures. Vesicles were identified and counted based on the absence of stain. Average vesicle number was expressed as function of total adluminal membrane perimeter for all counted tubules, measured using IPLab image analysis software.

2.12 Preparation of epididymosomes

Epididymosomes were collected using a previously reported method with some modifications (Rejraji et al., 2006). Briefly, epididymides were removed, subdissected and pooled by anatomical region, and bathed in 250 ml of PBS with 1 mM EDTA, or previously defined “bud buffer” designed to mimic intracellular conditions (Clift-O'Grady et al., 1998). The external capsule and internal tubules were penetrated in multiple locations with a 27G ½ inch needle, and fluid contents were released through the poked holes and into the buffer by gentle massaging of the tissue. Sperm were removed by two serial centrifugations at 1000 x g for 5 min. Total protein of the remaining sperm-free luminal fluid was determined by Bradford assay. The whole membrane fraction was collected from total luminal fluid by ultracentrifugation at 200,000 x g for 1 hr; or one mg of total protein in 250 µl of “bud buffer” was resolved through 10-45% sucrose or 5-25% glycerol gradients prepared as described previously (Clift-O'Grady et al., 1998; Salazar et al., 2004). Fractions were collected by gravity, and proteins were separated by 10% SDS-PAGE, transferred to PDVF, and probed by western blotting.

Chapter 3: The SED1-null Contains an Unexpected Epididymal Phenotype

Some written material and figures in Chapter 3 have been published previously or will be published in the future (Raymond et al., 2009a; Raymond and Shur, 2009).

All data and figures in Chapter 3 are the work of Adam S. Raymond.

Chapter 3: The SED1-null Contains an Unexpected Epididymal Phenotype

3.1 Introduction and experimental rationale

The epididymis is a highly convoluted tubule connecting the testis with the vas deferens in which mammalian sperm acquire the ability to fertilize eggs. The most proximal portion of the epididymis, or initial segment, secretes numerous factors critical for sperm maturation and storage. One such factor is SED1, a bi-motif protein composed of two N-terminal EGF domains, the second of which contains an RGD motif, and two C-terminal F5/8C-discoidin domains. Previous studies have reported that SED1 is secreted into the epididymal lumen, where it coats sperm and later facilitates sperm-egg binding. Here, we report that although the upstream tissues of the testis and efferent ducts appear normal, SED1-null males harbor an unexpected epididymal phenotype consisting of spermatocytic granulomas and granuloma-associated pathologies. To investigate a possible tissue-intrinsic function for SED1, we first characterized SED1 expression throughout the epididymis. Furthermore the role of SED1 in epididymal development was investigated by examining various hallmarks of epididymal development and differentiation in mutant animals.

3.2 Results

3.2.1 SED1 localizes to numerous domains in principal, clear, and basal cells of the epididymis

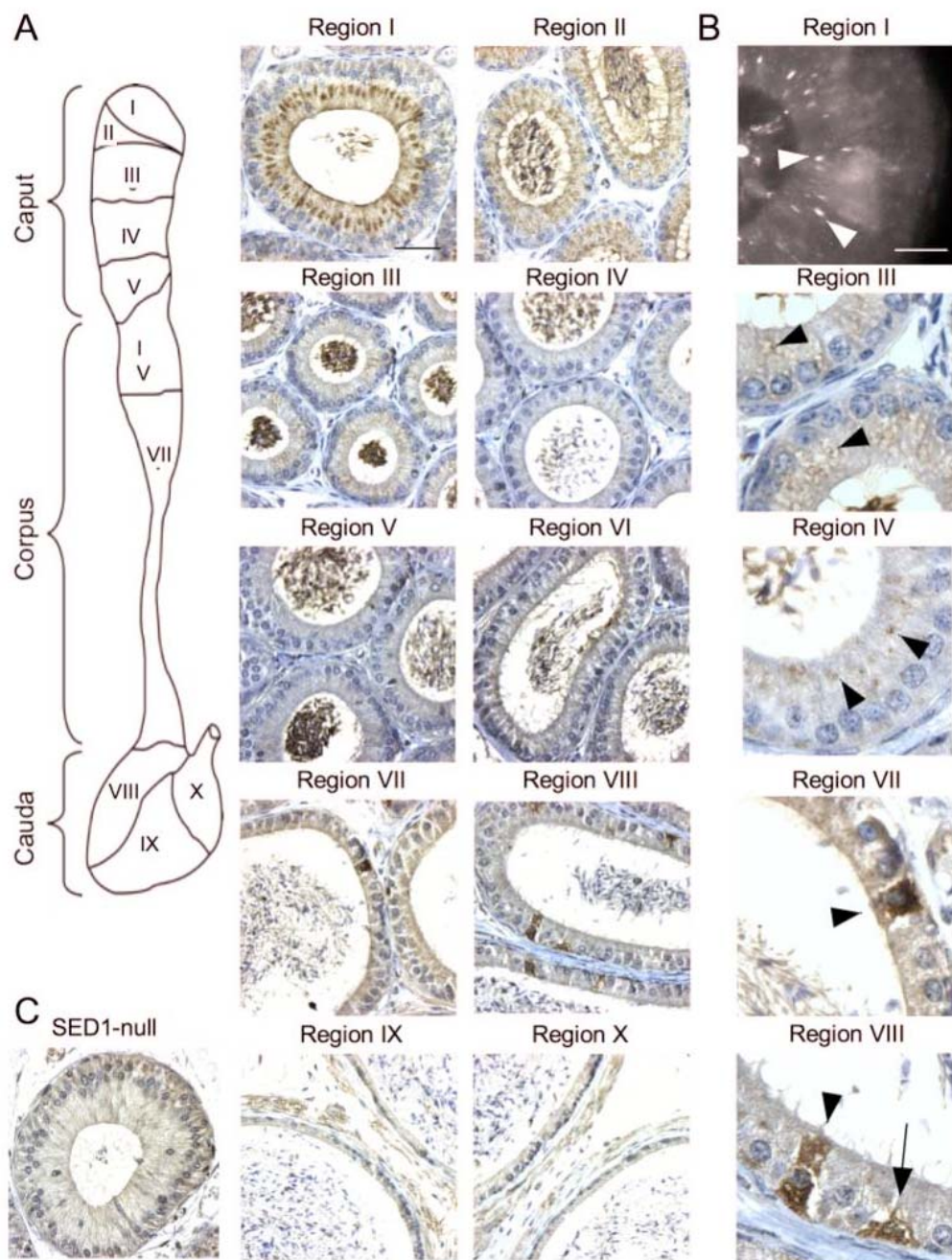
SED1 was originally identified as an exosome-associated secretion of the principal cells of the initial segment, where it is transferred to the sperm membrane as they progress through the epididymis. To more fully appreciate its potential functions, as well as serve as a guide for the interpretation of pathologies reported here, we undertook a more detailed analysis of SED1 localization throughout the epididymal epithelium. The three major anatomical segments of the epididymis are subdivided by fibrous septa into ten regions that exhibit subtle differences in cell morphology (Johnston et al., 2005). Therefore, this analysis required precisely oriented epididymal tissue sections to appreciate each of five caput, two corpus, and three cauda sub-regions that were not carefully considered in previous analyses.

As reported earlier, SED1 is highly expressed in the tall columnar principal cells of the initial segment, where it is concentrated in the Golgi region and punctate apical vesicles characteristic of the classical secretory pathway (Fig. 3-1) (Ensslin and Shur, 2003). Additionally, initial segment principal cells also exhibit linear SED1 plaques that align with basolateral cell-cell borders, the significance of which is pursued in more detail in Chapter 4. Caput II is characterized by a shortened epithelial cell height and an increase in the number of “prominent” clear cells (Abou-Haèila and Fain-Maurel, 1984).

SED1 localization is somewhat reduced in the principal cells of this region, however the protein is concentrated at the apical membrane and stereocilia remain strongly positive (Fig. 3-1). Clear cells are also immunoreactive in this region. In caput III, the tubule narrows and numerous multivesicular bodies fill the apical domain of the principal cells (Abou-Haèila and Fain-Maurel, 1984). Here, SED1 is absent from the Golgi region and the shortened stereocilia, however a subset of multivesicular bodies are strongly positive (Fig. 3-1). Some punctate vesicular staining returns in caput IV, but fades again in caput V, which is devoid of SED1 immunoreactivity at this resolution. SED1 expression remains low or absent from the proximal corpus epididymis, but returns strongly in a subset of clear cells and basal cells of the distal corpus and proximal cauda before disappearing in the most distal cauda region adjacent to the vas deferens (Fig 3-1). Clear cells are highly endocytic and these cells are not labeled when probed for SED1 by in situ hybridization, which suggests the protein is endocytosed by these cells (data not shown) (Robaire and Hinton, 2002). Furthermore, although the subcellular distribution of SED1 in basal cells is not evident at this resolution, the protein may contribute to the ability of these cells to regulate the adjacent luminal epithelial cells (Cheung et al., 2005). Additional investigation is required to determine the function of SED1 in these non-principal cell types.

Figure 3-1: SED1 localizes to numerous cellular domains in epididymal epithelial cells in vivo. (A) Diagram of the mouse epididymis* illustrates ten sub-regions: caput I (initial segment), caput II-V, corpus VI-VII, cauda VIII-X (adapted from Johnston et al., 2005). SED1 is highly expressed in the initial segment of the mouse epididymis, where it localizes to the para-Golgi region of principal epithelial cells in Bouins-fixed sections. Immunofluorescent localization in PFA-perfused tissue reveals basolateral plaques on principal cells (B, arrowheads). SED1 is also expressed throughout the proximal caput: in the apical membrane and microvilli in region II, multivesicular bodies in region III (B, arrowheads), and punctate apical granules in region IV (B, arrowheads). SED1 is also found in a subset of clear cells (B, arrowheads) and basal cells (B, arrow) in corpus VII and cauda VIII. (C) SED1-null tissue produces background immunoreactivity. bars = 75 μ m (A); 30 μ m (B)

* Diagram of the mouse epididymis modified from (Johnston et al., 2005).



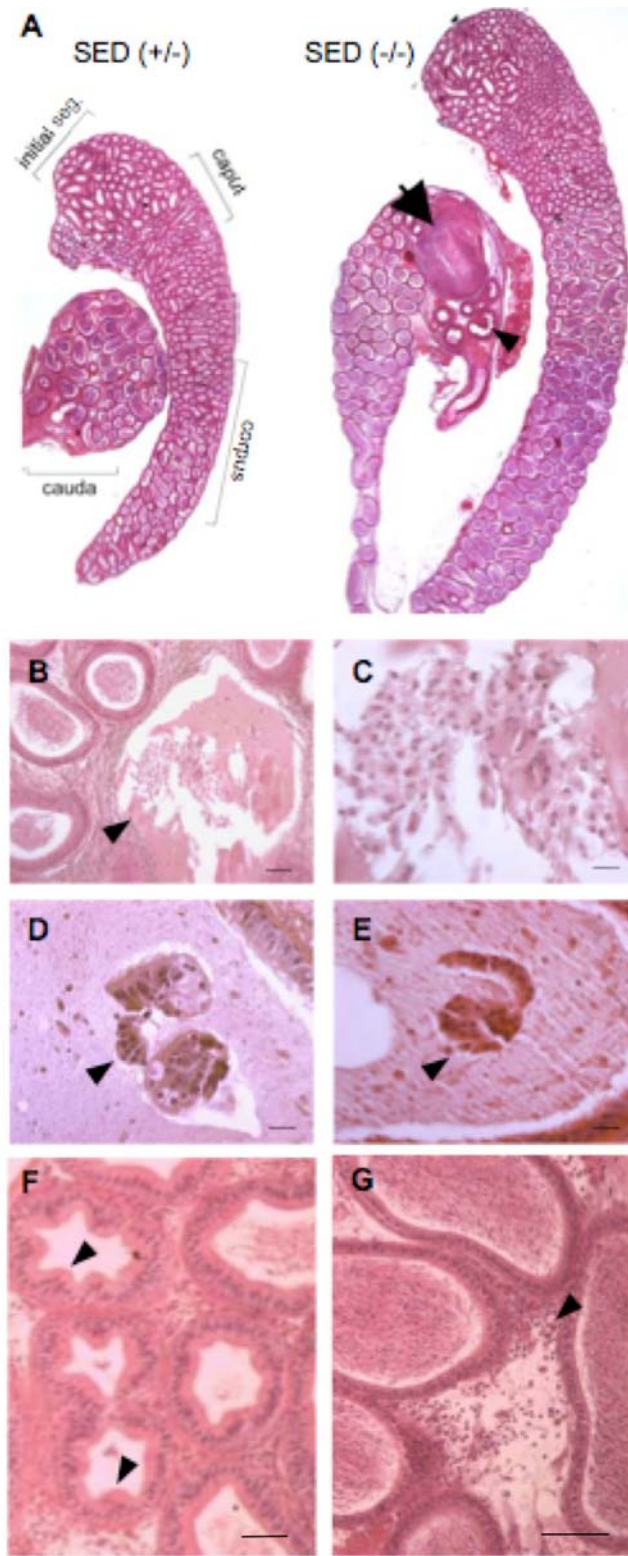
3.2.2 SED1-null epididymides exhibit a loss in tubule integrity and an increase in spermatic granulomas

Histological analysis of wildtype and SED1-null epididymides reveals a requirement for SED1 in maintaining the integrity of the epididymal tubule. SED1-null males have an increased incidence of spermatic granulomas, large lesions that occur when sperm-associated antigens breach the blood-epididymal barrier and invoke an autoimmune response (Flickinger et al., 1995). In a representative population of 106 SED1-null epididymides, 42 (40%) showed macroscopic abnormalities visible to the naked eye, occurring as early as seven weeks of age (Fig. 3-2A, arrow). Affected SED1-null epididymides often show complete occlusion of the tubule, evidenced by swelling of tubule cross-sections upstream of the lesion and the absence of sperm in downstream sections (Fig. 3-2A, arrowhead). Although 40% of the SED1-null males showed macroscopic lesions, the epididymal phenotype is more penetrant than this, since histological analysis of macroscopically-normal SED1-null epididymides revealed microscopic lesions similar to that seen in Fig. 3-2B. However, the full penetrance of the epididymal phenotype is unclear, as a comprehensive histological analysis of all epididymides was not undertaken in this study.

In addition to spermatic granulomas, SED1-null epididymides display an absence of an intact epithelia and the presence of shed, free-floating cells morphologically consistent with a detached tubule epithelium (Fig. 3-2C-E). Other hallmarks of epithelial breakdown are evident, including lymphocyte infiltration, vacuoles in the basal aspects of

Figure 3-2: Epididymides from SED1-null males show epithelial breakdown. (A)

Photomicrographs of paraffin-embedded epididymal tissue with the major functional regions identified. Sagittal sections from SED1 heterozygous (+/-) and null (-/-) littermates at 8 weeks of age stained with hematoxylin and eosin and imaged at identical magnification. The caudal segment of the SED1-null (-/-) epididymis contains a large spermatic granuloma (arrow) characterized by breakdown of the tubule and resulting in a bolus of sperm, fluid, and immune cells. Occlusion of the tubule results in severe tubule swelling upstream of the lesion (compare corpus regions) and an absence of sperm in downstream tubules (arrowhead). (B-E) Other SED1-null pathologies not directly associated with the lesion site include detached, free-floating cells within the lumen suggestive of shed epithelium (arrowheads, C,D,E) (C) is an enlargement of (B), hyperplasia (arrowheads, F), and infiltration of lymphocytes (arrowhead, G). bars = 50 μ m (B); 20 μ m (C-E); 50 μ m (F,G)



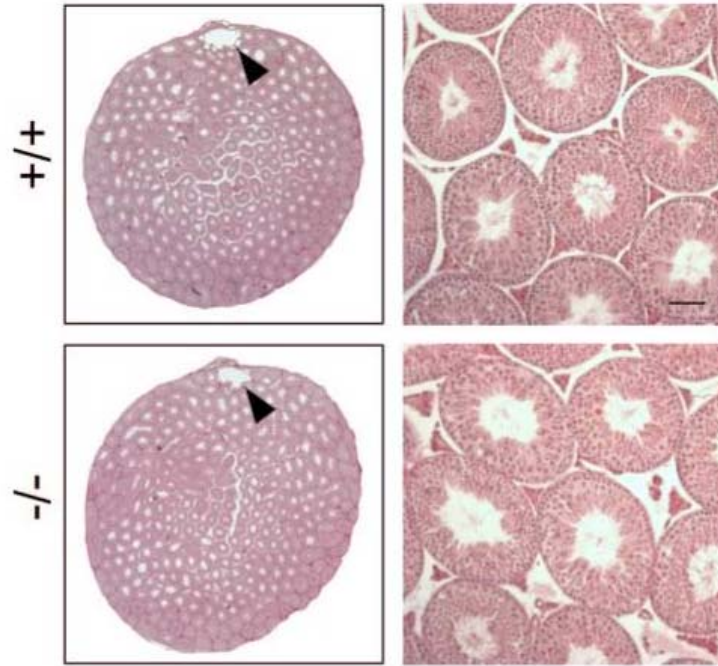
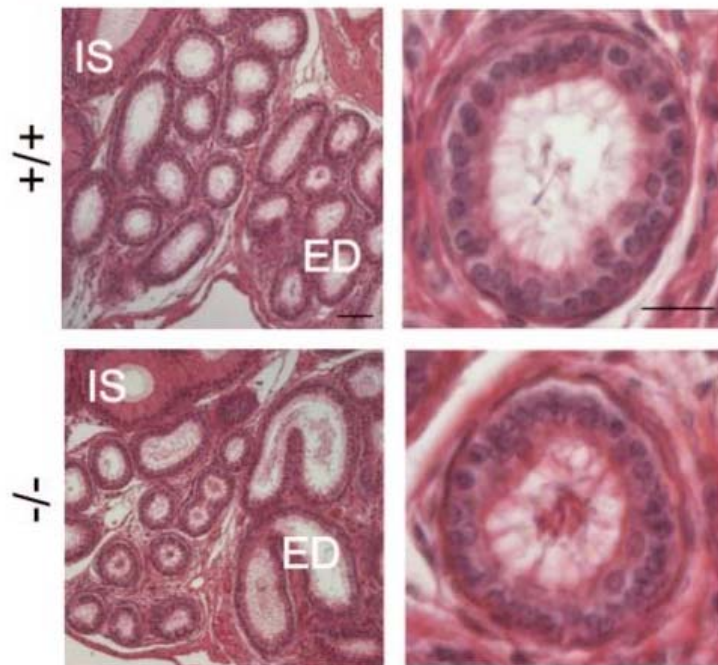
the epithelium, epithelial metaplasia, and lymphocyte infiltration, similar to that reported by others (Fig. 3-2F-G) (Flickinger et al., 1995; Hess et al., 2000).

3.2.3 Reproductive pathologies associated with the loss of SED1 are restricted to the epididymis

Since some spermatic granulomas are thought to be a secondary consequence of dysfunction in upstream regions of the reproductive tract, we investigated the possibility that epididymal granulomas in SED1-null males reflect abnormalities in the testis and/or the efferent ducts. Paraffin sections of testes and efferent ducts dissected from SED1-null males whose epididymides contained sperm granulomas were stained with hematoxylin and eosin, and examined by light microscopy. Although SED1 is known to be expressed in the Golgi region of developing spermatocytes (Ensslin and Shur, 2003), SED1-null testes are intact and both the seminiferous tubules and spermatozoa appear morphologically normal (Fig. 3-3A). Both wildtype and SED1-null testes contain the expected cell types, including Leydig cells, Sertoli cells, spermatogonia, spermatocytes at various stages of differentiation, and sperm-filled lumens. Other structures, such as the rete testes (arrowheads Fig. 3-3A), are also easily identified in the SED1-null, and appear normal. These observations are in good agreement with previous findings suggesting that despite their reduced binding to the zona pellucida, the overall morphology, count, and velocity of SED1-null sperm are otherwise normal (Ensslin and Shur, 2003).

The efferent ducts are petite tubules that bridge the rete testes with the initial segment of the epididymis and begin the process of reducing the luminal fluid by more

Figure 3-3: Testes and efferent ducts in the SED1-null male are morphologically normal. Testes and efferent ducts were isolated from SED1-null males containing epididymal granulomas, sections were prepared and stained with hematoxylin and eosin. Testes and efferent ducts of SED1-nulls are intact and without visible pathologies. A) The rete testis (arrowheads) appears normal and the seminiferous tubules contain the expected cell types, including Leydig cells, and Sertoli cells, and all spermatogenic stages. B) The efferent ducts (ED), which lie immediately upstream of the initial segment (IS), are also morphologically normal, containing a polarized ciliated epithelium, similar to wildtype. bars = 50 μm (A); 50 μm (B,left), 20 μm (B, right)

A Testis**B Efferent ducts**

than half to compact the sperm for storage (Hinton and Palladino, 1995; Levine and Marsh, 1971). This process requires an estrogen-dependent signaling cascade that facilitates synthesis and localization of NHE3 sodium/hydrogen exchangers to the apical surface of efferent duct epithelial cells (Zhou et al., 2001). Disruption of this fluid reabsorption pathway, such as in estrogen receptor (ER) knockout mice, results in severely altered efferent duct morphology and function, and a coincident increase in the appearance of spermatic granulomas in the cauda epididymis (Hess et al., 2000). We therefore considered the possibility that the efferent ducts of the SED1-null males may also be compromised. Immunostaining indicates that SED1 is not expressed in wildtype efferent ducts (data not shown). Furthermore, the efferent ducts of SED1-null males containing epididymal granulomas are morphologically normal (Fig 3-3B). Together, these data suggest that the cause of epididymal spermatic granulomas detected in SED1-null males is intrinsic to the epididymis.

3.2.4 The SED1-null epididymis undergoes normal development and differentiation

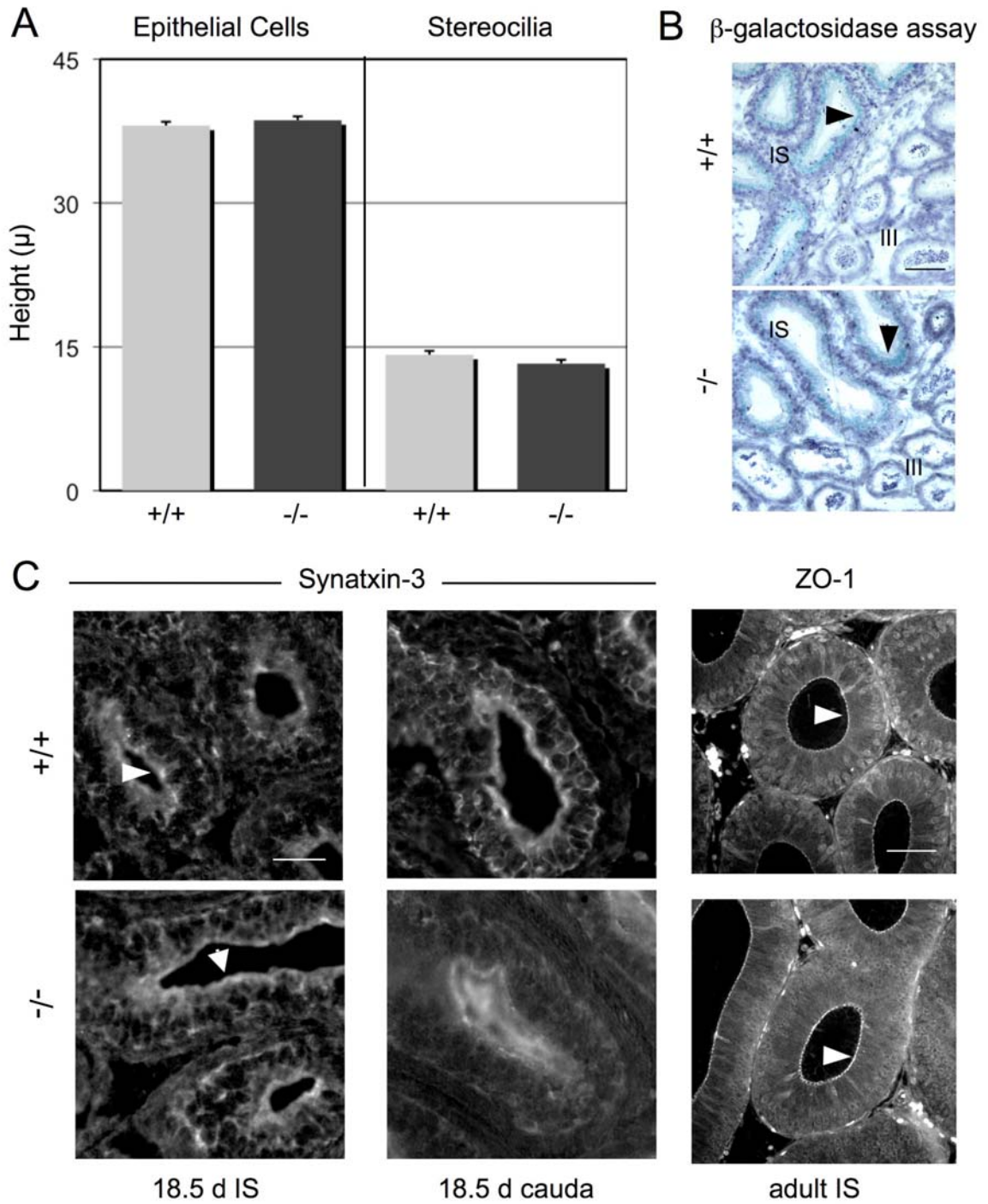
We next considered the possibility that epididymal pathologies in the SED1-null may be the secondary consequence of defective epididymal development and/or differentiation. To investigate this possibility, we first examined the overall constitution of SED1-null epididymides by light microscopy. Utilizing precisely oriented SED1-null epididymal tissue, all ten above-described epididymal regions are present in SED1-null epididymides (data not shown). Of particular interest is the initial segment, which expresses SED1 in numerous prominent localizations. Morphologically, the epithelium

of the initial segment consists of tall columnar principal cells featuring lengthy stereocilia that project into the lumen and provide an expanded apical membrane surface to which channels and transporters are localized (Badran and Hermo, 2002). In the ER knockout, both epithelial cell height and microvilli length are reduced in the dysfunctional epithelium of the efferent duct (Hess et al., 2000). Therefore, we determined the epithelial cell height and stereocilia length for tubules in initial segments of six different wildtype and knockout epididymides. The resulting average epithelial height is 38.1 ± 4.4 μm in wildtype and a statistically similar 38.6 ± 5.2 μm in SED1-nulls (Fig 3-4A). Stereocilia are also similar: 14.2 ± 3.8 μm and 13.3 ± 2.9 μm in wildtype and SED1-null, respectively; however, the small (7%) decrease in stereocilia height seen in SED1-null cells borders on statistical significance ($p=0.049$). These data suggest the SED1-null initial segment and caput regions are properly patterned and morphologically differentiated.

Next, we examined the functional differentiation of the tissue. The caput epididymis exhibits a high level of β -galactosidase activity, which is at a maximum in the initial segment and absent from caput III. Detection of endogenous β -galactosidase activity has been used previously to distinguish between epididymal regions that are morphologically abnormal, and those that are improperly differentiated (Avram and Cooper, 2004). Therefore, wildtype and SED1-null tissue sections were incubated with buffered x-gal to identify endogenous β -galactosidase activity. A similar gradient of x-gal reactivity is found in the initial segment and caput of both genotypes, indicating that the knockout epithelium is functionally differentiated (Fig. 3-4B).

Figure 3-4: The SED1-null epididymis develops and differentiates normally. A)

Sections of initial segment were immunolabeled with anti-AQP9 antibody and counterstained with hematoxylin to identify stereocilia and cell borders. Cell height and stereocilia length were quantified in 105 wildtype and 101 SED1-null cells using image analysis software; wildtype (+/+) and SED1-null (-/-) show similar cell heights and stereocilia lengths (n=6). B) Frozen sections were prepared and stained with buffered x-gal to detect endogenous β -galactosidase activity. Region I of wildtype (+/+) and SED1-null (-/-) epididymides exhibit comparable levels of endogenous β -galactosidase activity, suggesting the mutant is functionally differentiated. C) Epididymal sections were immunostained with Syntaxin-3 and ZO-1 at the indicated stages of development. Both proteins are properly localized to the appropriate apical domains (arrowheads) in wildtype (+/+) and SED1-null (-/-) epithelial cells, suggesting the mutant epithelium is properly polarized and forms a blood-epididymal barrier. bars = 100 μ m (B); 25 μ m (C, Syntaxin), 50 μ m (C, ZO-1)



Although these data suggest that the SED1-null epididymis is patterned properly, we further investigated other hallmarks of epididymal development, including establishment of the blood-epididymal barrier and aspects of apical secretion. Epididymal tissue was harvested from wildtype and SED1-null animals at 9.5 days, 18.5 days, 1 month, and 3 months of development, and immunostained with cellular markers including the tight junction component ZO-1, adherens junction protein E-cadherin, and the t-snare Syntaxin-3 (Cyr et al., 1999; Levy and Robaire, 1999b). At all stages examined, wildtype and knockout tissue exhibit similar ZO-1 (Fig. 3-4C) and E-cadherin (data not shown) localizations, suggesting that SED1-null epididymides properly organize protein components into functional junctions. Furthermore, similar to wildtype, SED1-null tissue properly localizes Syntaxin-3 to the apical membrane of epithelial cells suggesting these cells are polarized and secretory (Fig 3-4C). Together these data indicate that the SED1-null epididymis is properly patterned and differentiated, and that the appearance of normal junctional components suggests the emergence of spermatid granulomas is not the de facto result of a non-existent blood-epididymal barrier.

3.3 Discussion

We first sought to bring cohesion to previous reports of SED1 localization in the epididymis by investigating its localization in all ten epididymal sub-regions. Here we confirm that the protein is highly expressed by the initial segment of the epididymis, where it is found in secretory granules as well as basolateral arrays that align with cell-cell borders. SED1 is also expressed in some sub-regions of the caput, including the

apical membrane and stereocilia of caput II, multivesicular bodies of caput III, and punctate apical vesicles of caput IV. Caput V and corpus VI are not immunoreactive, while clear cells and basal cells are SED1-positive in corpus VII and cauda VIII, but not cauda IX or X. Clear cells are highly endocytic and the lack of in situ hybridization for SED1 suggests this immunolocalization reflects reabsorption of unbound protein from the lumen. However, gene array experiments by others report low levels of SED1 mRNA detectable in all three segments of the cauda, leaving unresolved the possibility that the protein is also synthesized in this region (Johnston et al., 2005). Nonetheless, as discussed in the next Chapter, most clear cells in these areas do not express LAMP-1, a hallmark of lysosomes, which suggests the protein is not destined for degradation in these cells, but rather plays some unknown function. Clear cells have a well-documented function in luminal pH regulation, and although the role of basal cells remains more ambiguous, these cells may contribute to regulation of the luminal epithelium (Cheung et al., 2005). At this time, the function of SED1 in clear cells and basal cells remains undefined, however in light of the critical roles that these cells play in the epididymis, SED1 function in these cells requires more attention.

We also describe an unexpected phenotype in the SED1-null epididymis consisting of an increase in spermatic granulomas and other pathologies characteristic of a breakdown in the integrity of the tubule epithelium (Flickinger et al., 1995; Hess et al., 2000). Although spermatic granulomas are occasionally evident in the caput and corpus segments of SED1-null epididymides, they are most often manifest in the cauda segment. This is similar to the ER-null epididymides where spermatic granulomas occur at similar

frequency and distribution to that seen in SED1-null males (Flickinger et al., 1995; Hess et al., 2000). Presumably, the preponderance of granulomas in the distal cauda, irrelevant of where the primary insult occurs, is a consequence of its short, cuboidal epithelium that may be particularly sensitive to disruptions in normal cell and/or fluid dynamics (Flickinger et al., 1995). Examination of the ER knockout reveals that disruption of fluid regulatory processes in the efferent ducts are accompanied by long-range effects in the distal segment of the epididymis, including spermatic granulomas (Hess et al., 2000; Zhou et al., 2001). We therefore felt it prudent to first identify the source of the malfunction in the SED1-null. Testes and efferent ducts were isolated from SED1-null animals containing epididymal lesions and prepared for histological analysis. SED1-null testes are indistinguishable from wildtype, featuring all expected cell-types and intact tubules in a variety of stages of spermatogenesis. The SED1-null also features well-formed rete testes and efferent ducts that are morphologically similar to wildtype, suggesting upstream tissues are unaffected in the absence of SED1. These data suggest that the cause of epididymal-associated pathologies is intrinsic to the epididymal tissue.

In the *c-ros* knockout, epididymides develop that are morphologically devoid of the initial segment (Sonnenberg-Riethmacher et al., 1996). Similarly, epithelial cell and microvilli heights are reduced in the dysfunctional ER knockout efferent ducts (Hess et al., 2000). We therefore employed a series of histological, cell biological, and biochemical assays to examine epididymal development and differentiation in SED1-null animals. Unlike the *c-ros* knockout, the SED1-null epididymis is morphologically similar to wildtype, featuring all ten major sub-regions described previously (Johnston et

al., 2005). More specifically, SED1-nulls feature a well-defined, functional caput as demonstrated by region-specific endogenous β -galactosidase activity, and an initial segment with cell and stereocilia heights that are similar to wildtype. Furthermore, as juveniles, the SED1-null achieves major developmental hallmarks, including proper subcellular localization of components that form the blood-epididymal barrier, and apical localization of a vesicle-membrane fusion protein indicating a secretory epithelium. Together, these data suggest that the SED1-null epididymis is properly patterned and differentiated.

Chapter 4: A Novel Role for SED1 in Maintaining the Integrity of the Epididymal Epithelium

Some written material and figures in Chapter 4 have been published (Raymond and Shur, 2009).

All data and figures in Chapter 4 are the work of Adam S. Raymond.

Chapter 4: A Novel Role for SED1 in Maintaining the Integrity of the Epididymal Epithelium

4.1 Introduction and experimental rationale

SED1 serves as an adhesive protein in a number of systems. For example, SED1 plays a critical role during mammary gland branching morphogenesis (Atabai et al., 2005; Ensslin and Shur, 2007). SED1 produced by the luminal epithelia cells of the developing ductal tree facilitates adhesion to the adjacent myoepithelium and activates intracellular signaling cascades through α_v integrins (Ensslin and Shur, 2007). Similarly, thioglycolate-responsive macrophages secrete SED1 that serves as a molecular “bridge,” facilitating macrophage attachment to, and engulfment of apoptotic lymphocytes (Hanayama et al., 2002; Hanayama et al., 2004). Finally, a porcine homologue of SED1, p47, was isolated from sperm plasma membranes based on its affinity for zona pellucida glycoproteins (Ensslin et al., 1998). Subsequent studies showed that SED1 is secreted from the initial segment of the mouse epididymis, where it coats sperm within the lumen and plays a critical role in sperm adhesion to the zona pellucida (Ensslin and Shur, 2003). In this regard, SED1-null sperm have a reduced capacity to bind eggs in vitro, and SED1-null males have reduced fertility in vivo (Ensslin and Shur, 2003).

Further analysis of the SED1-null male reproductive tract identified an unexpected phenotype in the epididymis: increased incidence of epithelial breakdown and spermatic granulomas. Sperm granulomas contain dense aggregates of immune cells and sperm resulting from an autoimmune response against sperm-associated antigens exposed

following damage to the epididymal epithelium. They can result from both biochemical and surgical insults to the epididymis, and can be large enough to totally occlude the epididymal lumen (Hess et al., 2000; Flickinger et al., 1995). The loss of epithelial integrity and the presence of spermatic granulomas in the absence of other pathologies in testis and efferent ducts prompted us to investigate a tissue-intrinsic role for SED1 in the epididymis. Considering the well-defined role for SED1 in mediating intercellular adhesions in other systems, it is plausible that these pathologies reflect a loss in SED1-dependent adhesion in the epididymis. Here we report that improved fixation protocols reveal that SED1 is found in the basolateral domains of epididymal epithelial cells in vivo, and similarly, SED1 is secreted both apically and basally from polarized epididymal cells in vitro. The basolateral distribution of SED1 suggests that it may play a novel role in epididymal cell adhesion. Consistent with this, in vitro assays show that SED1 supports epididymal cell adhesion via RGD binding to α_v integrin receptors on epididymal epithelial cells. Finally, epididymal cells from SED1-null males show reduced adhesion in vitro, a phenotype that can be rescued with exogenous SED1. These results suggest that SED1 facilitates epididymal cell adhesion, and that its loss leads to breakdown of the epididymal epithelium and consequent development of sperm granulomas.

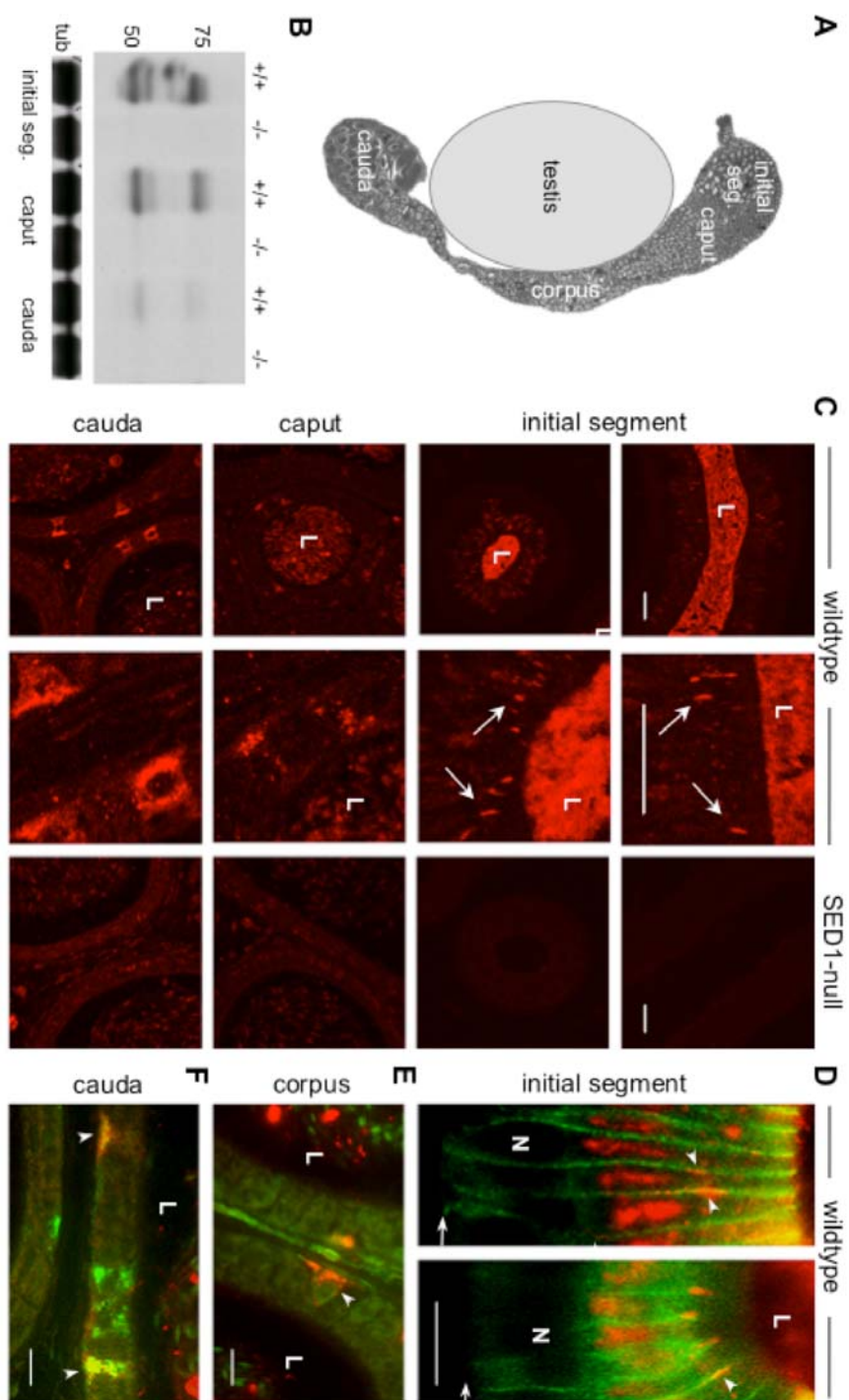
4.2 Results

4.2.1 SED1 is expressed in basal and basolateral domains of epididymal epithelia in vivo

We first characterized SED1 expression throughout the epididymal tubule by immunoblotting and immunofluorescence. Epididymides from wildtype and SED1-null males were isolated, sub-dissected into initial segment, caput, and cauda regions, and prepared for western blotting as described in Materials and Methods (Fig. 4-1A). Probing these preparations with anti-SED1 antibody yields two predominant bands (Fig. 4-1B) characteristic of the short and long isoforms of SED1 (Oshima et al., 1999). SED1 is most highly expressed in the initial segment; expression remains high in the caput, but is reduced in the cauda. SED1-null tissue shows background immunoreactivity.

Previous studies of SED1 expression in the epididymis have relied upon traditional submersion-based fixation. When tissue was perfused with 4% paraformaldehyde to preserve histology that is compromised by submersion fixation we identified novel, unexpected localizations for SED1 in epididymal epithelia. Similar results, using two different anti-SED1 antibodies, were seen in all five males prepared by perfusion fixation. The bulk of SED1 expression is found in the principal cells of the initial segment, where it localizes to the perinuclear Golgi region, as well as punctate foci in the apical compartment suggestive of secretory vesicles. However, following perfusion fixation, SED1 is also found in linear plaques that appear to be between adjacent principal cells in the initial segment (Fig. 4-1C). Double-label indirect

Figure 4-1: SED1 localizes to both apical and basolateral domains of epididymal epithelial cells in vivo. (A) Composite photomicrograph of an epididymal sagittal-section positioned adjacent to a size-appropriate schematic of the testis. The initial segment, caput, corpus, and cauda regions are identified. (B) Immunoblotting for SED1 in three epididymal regions; samples are loaded with equal protein. Immunoblotting of wildtype (+/+) tissue results in two bands consistent with the small and large isoforms of SED1. SED1-null (-/-) tissue produces background immunoreactivity. β -tubulin (tub) serves as a loading control. (C) In the initial segment, SED1 is found in punctate and often filamentous arrays along basolateral borders between adjacent epithelial cells (tissue perfused in 4% PFA). SED1 is also found in vesicles associated with the basal domain of non-principal cells, known as clear cells, in the caput, corpus, and cauda segments (tissue submersion-fixed in Bouins). SED1-null (-/-) tissue shows only background immunoreactivity. (D) Double-label immunofluorescence with E-cadherin (green) illustrates that many of the SED1 plaques (red) seen in the initial segment lie on the cell border (arrowheads). Two examples are shown. The base of the epithelium is designated by small arrows. (E,F) SED1-positive (red) clear cells of the caput and corpus regions fail to stain for the lysosomal marker, LAMP-1 (green), although clear cells in more distal regions, i.e., caput, are LAMP-1 positive, suggesting the protein is not destined for degradation in the proximal segments (caput, corpus) as it appears to be in the distal cauda. Images in panel C represent a merged stack of confocal Z-sections taken through the tissue, whereas those in panels D-F are merged epifluorescence photomicrographs. L = lumen, N = nucleus, bars = 20 μ m (C); 10 μ m (D-F)



immunofluorescence with E-cadherin illustrates that many of the SED1 plaques are located on the lateral membrane (two examples shown, Fig. 4-1D, arrowheads). Higher resolution analysis, including immunolabeling at the ultrastructural level, is required for a more complete appreciation of these novel SED1 plaques.

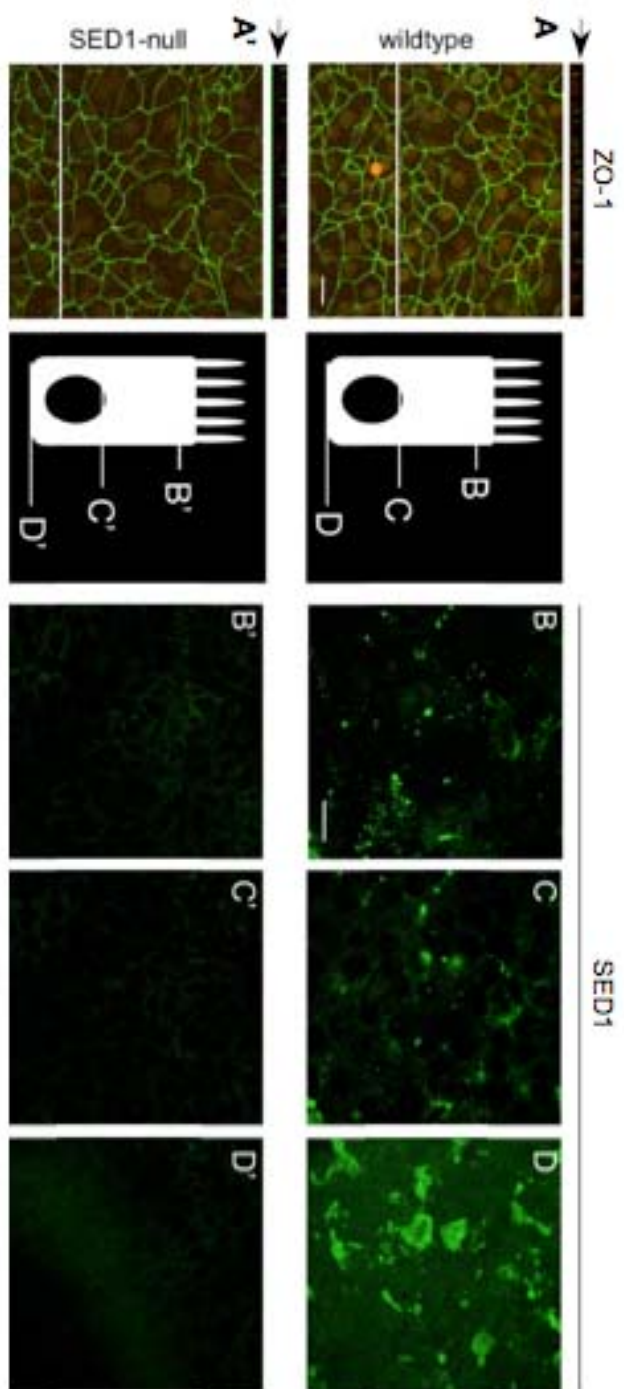
SED1 is also found in vesicles within the apical and basal compartments of clear cells throughout the lower caput, the distal corpus and proximal cauda segments, as previously reported (Fig. 4-1C). The function of clear cells varies according to their location in the epididymis, with more proximal ones thought to regulate acidification, whereas those in the distal segments function in endocytosis, recycling, and/or protein degradation (Robaire and Hinton, 2002). Not surprisingly, the SED1 found in the most distal clear cells (i.e., cauda) appears in the lysosomal pathway, as judged by co-localization with the lysosomal marker, LAMP-1 (Fig. 4-1F). However, the majority of SED1-positive clear cells occur in the distal corpus, and these cells appear negative for the LAMP-1 lysosomal marker, suggesting that SED1 in these cells is destined for recycling, either apically or basally (Fig. 4-1E). Since, at the current resolution, SED1 is not readily detectable on clear cell borders, its fate in these cells remains to be determined. Nevertheless, SED1 is present in cellular domains that appear to be unrelated to its known apical secretion from principal cells of the initial segment. In particular, the SED1 plaques seen between adjacent principal cells of the initial segment is suggestive of a function in cell-cell and/or cell-matrix adhesions.

4.2.2 SED1 is deposited basally by polarized epithelial cells in vitro

In light of the known apical secretion of SED1 from a variety of epithelial cells, including principal cells of the epididymal initial segment, we felt it important to confirm the basolateral secretion of SED1 in epididymal cells polarized in vitro. Primary epididymal cells were isolated and cultured using a previously described protocol with modifications (Carballada and Saling, 1997). Mechanical and enzymatic dissociation of the initial segment/caput generates a mixed population of epithelial, smooth muscle, and fibroblast-like cells resident in the epididymis. We therefore collected an enriched epithelial cell population by pre-plating this heterogeneous population on fibronectin substrates for two hours, followed by aspiration and re-plating of the non-adherent cells. Immunostaining confirms the removal of desmin-positive smooth muscle cells and the enrichment of cytokeratin-positive epithelial cells (data not shown).

Primary epididymal epithelial cells were isolated as above from wildtype and SED1-null males and cultured on transwell permeable filters coated with a thin layer of Matrigel. Cells of both genotypes proliferate to a confluent monolayer within four days. Cell polarization was analyzed by immunolocalization of ZO-1, a zonal occludin protein that localizes to apical tight junctions in confluent epididymal epithelia (Cyr et al., 1999; Levy and Robaire, 1999b). In wildtype and SED1-null monolayers alike, ZO-1 is expressed in the traditional cobblestone pattern consistent with tight junction formation in confluent, polarized epithelia (Fig. 4-2A,4-2A') (Byers et al., 1992).

Figure 4-2: Polarized primary epididymal epithelial cells secrete SED1 both apically and basally. (A, A') Immunofluorescence of the apical zonal occludin protein ZO-1 (green) and basal nuclei (red) in primary epididymal epithelial cells grown on Matrigel-coated transwell filters. X-Y projections and companion z-plane cross-sections (black arrow; white line indicates cross section location) generated by confocal z-stack imaging show wildtype (+/+) and SED1-null (-/-) primary cells polarize and form apical tight junctions in culture. The cell diagram illustrates the approximate depth of confocal scans taken of polarized cultures immunostained with SED1 antisera. (B) In polarized cultures of wildtype (+/+) cells, SED1 appears as punctate bodies in the apical domain of the cell consistent with its known apical secretion. (C) Little SED1 protein is found at the level of the nuclei, however (D) immunoreactivity returns in the sub-nuclear basal domain. Examination reveals this signal is found in the same z-plane as the filter suggesting cells deposit SED1 onto the underlying substrate. (B', C', D') SED1-null cultures assayed in parallel have no immunoreactivity. all bars = 20 μ m.



SED1 localization in these polarized epithelia was analyzed by z-section confocal microscopy of immunolabeled cultures. SED1 localizes to punctate foci in the apical domain of wildtype cells in agreement with its known apical secretion (Fig. 4-2B). Importantly, SED1 immunoreactivity is also found in the basal domain and deposited onto the transwell filter beneath the adherent cells (Fig. 4-2D) confirming the protein is secreted basally or basolaterally. SED1-null cells exhibit background immunoreactivity (Fig. 4-2B'-D').

4.2.3 rSED1 increases the initial adhesion of primary epididymal epithelial cells

To directly test if SED1 can mediate epididymal epithelial cell adhesion, a quantitative cell adhesion assay was developed. Primary epididymal cells were isolated and enriched for epithelial cells as described above from wildtype CD1 males. Cells were cultured on rSED1 for four days to increase the population and to maintain expression of any relevant SED1 receptors. Following culture, cells were gently dissociated with a mild enzymatic digestion and allowed to recover for two hours in medium containing 5% FBS. Pilot experiments optimized the relevant assay conditions, including substrate concentration, length of assay, number of washes prior to fixation, and colorimetric reading of the adherent cells (data not shown). All assays described below were conducted in 96-well microtiter plates at 32°C for 30 minutes and washed twice with PBS prior to fixation with glutaraldehyde. Adherent cells were stained with Crystal Violet; the dye was solubilized with acid and absorbance was measured at 595 nm.

Epididymal cells exhibit a dose-dependent adhesion to rSED1 substrates, whereas control wells lacking substrate contain no adherent cells (Fig. 4-3A,B). As expected, the adherent cells are predominately epithelial as judged by cytokeratin immunoreactivity (Fig. 4-3C). Maximum adhesion is found at 250 ng/well rSED1, and qualitative assays with up to 500 ng of traditional epithelial substrates, including Matrigel and laminin, result in similar levels of adhesion (data not shown).

4.2.4 Epithelial cell adhesion to rSED1 is RGD-dependent

We first considered whether the RGD motif contained within the second EGF domain is important for epithelial cell adhesion. Isolated primary epithelial cells were treated with either RGD peptide or RAD control peptide, and applied to wells coated with SED1 or laminin substrates. While pre-incubation with 100 μ M RGD peptide has no effect on cell adhesion to laminin, adhesion to rSED1 substrates is reduced by 92% compared to cells incubated with control peptide (Fig. 4-4). At this concentration, the control RAD peptide causes minor non-specific inhibition of cell adhesion to both rSED1 and laminin substrates, presumably the result of mild changes in the media pH caused by peptide addition. In any event, the RGD motif of SED1 appears to be indispensable for epididymal epithelial cell adhesion, which is consistent with findings in other systems, including mammary epithelium (Ensslin and Shur, 2007).

Figure 4-3: Exogenous SED1 supports epididymal epithelial cell adhesion in a dose-dependent manner. (A) Increasing levels of SED1 lead to a concomitant increase in cell adhesion, reaching maximal values at 250 ng/well. Cells do not adhere to uncoated “mock” wells. (B) Representative photomicrographs of crystal violet-stained adherent cells on SED1 substrates. (C) Cytokeratin immunoreactivity confirms the adherent cells are predominately epithelial. red = cytokeratin, green = nuclei (SYTO24). error bars = sd

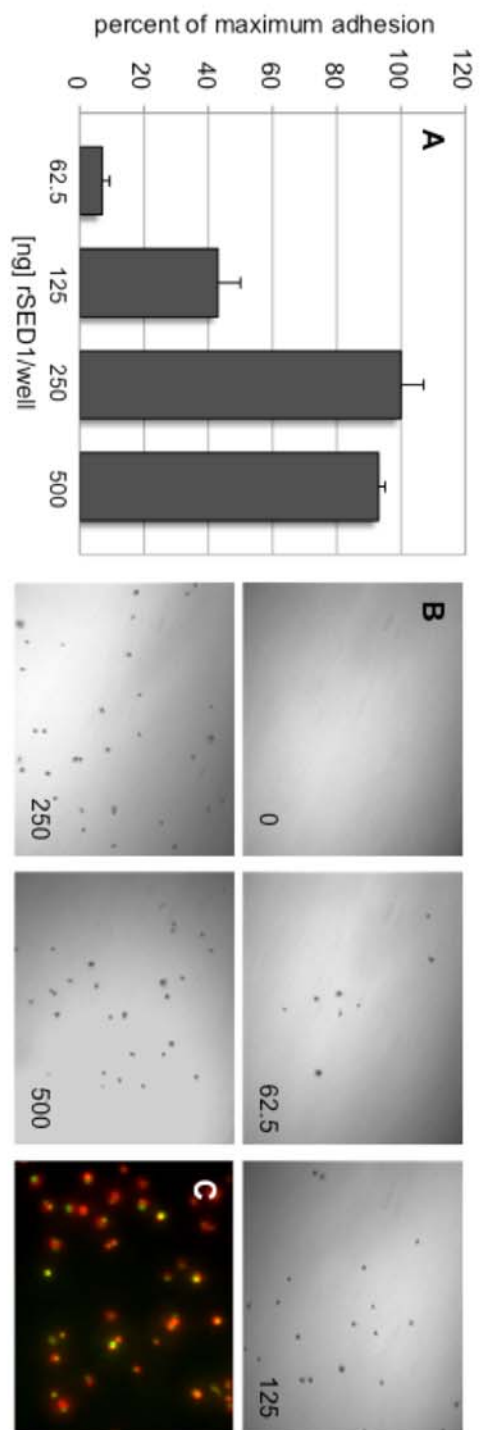
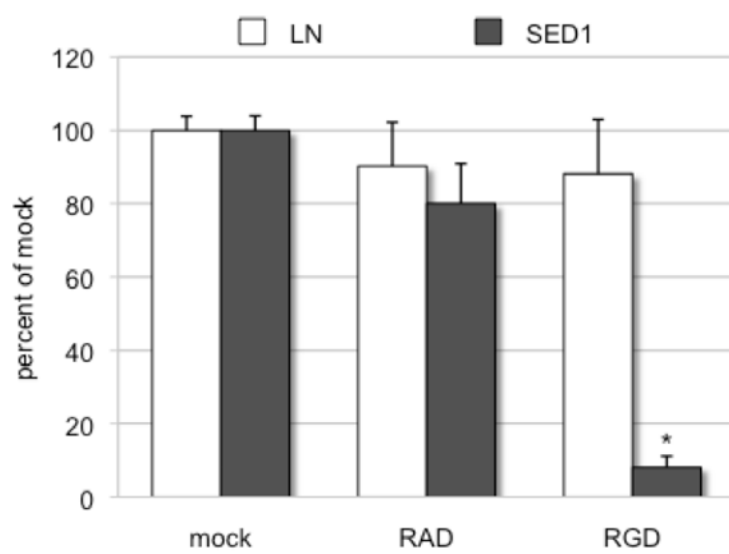


Figure 4-4: The addition of RGD peptides is sufficient to block the initial adhesion of epididymal epithelial cells to SED1. Cells preincubated with media supplemented with 100 μ M RGD or control (RAD) peptides were added to 30-minute adhesion assays on substrates coated with 500 ng/well SED1 or laminin. Data is expressed as a percentage of untreated (mock) cell adhesion to each substrate. RGD reduces adhesion to SED1 by 92% while having no effect on adhesion to laminin. RAD has a mild non-specific effect on cell adhesion to both substrates. error bars = sem, * = $p < 0.0001$



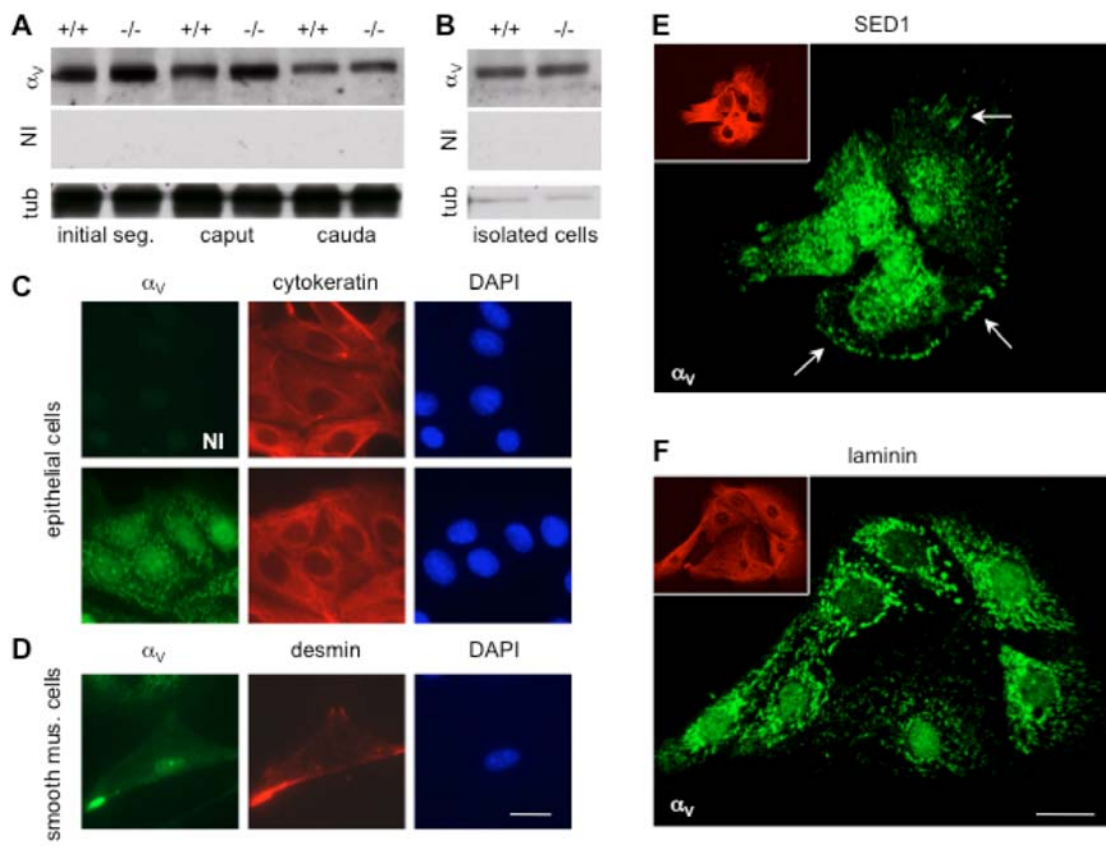
4.2.5 Epididymal epithelial cells express α_v integrins

The $\alpha_v\beta_{3/5}$ integrins have been previously identified as receptors for the RGD motif in SED1 (Andersen et al., 1997; Ensslin and Shur, 2007; Felding-Habermann and Cheresh, 1993; Hanayama et al., 2002; Ruoslahti, 1996; Taylor et al., 1997); however, it is not known if these receptors are expressed in epididymal cells. Immunoblotting with anti- α_v antiserum identifies a single band at 125 kDa in all three epididymal regions of both wildtype and SED1-null tissue (Fig. 4-5A); the predicted molecular weight for α_v under non-reducing conditions (Hirsch et al., 1994; Suzuki et al., 1987). Expression is approximately similar in the initial segment and caput, but slightly reduced in the cauda.

In addition to principal cells, these tissue homogenates contain a mix of other cell types resident in the epididymis, including capillary endothelial cells that are predicted to express α_v integrins (Eliceiri and Cheresh, 2000). Therefore, enriched epithelial cells (isolated as above) were probed with α_v antiserum, which detects a similar 125 kDa band indicating that α_v is expressed in epithelial cells (Fig. 4-5B). The large reduction in tubulin levels between tissue and single cell homogenates, without a significant difference in α_v levels, reflects the removal of tubulin-rich mouse sperm that are devoid of α_v (Ensslin and Shur, 2003).

The presence and distribution of α_v integrins in cultures of primary epididymal cells, containing both epithelial and non-epithelial cell types, were analyzed by immunocytochemistry. Cytokeratin-positive cells from both wildtype and SED1-null genotypes express α_v (Fig. 4-5C), while desmin-positive smooth muscle cells yield only background immunoreactivity, similar to non-immune controls (Fig. 4-5D).

Figure 4-5: The α_V integrin subunit is expressed in epididymal epithelial cells and localizes to focal plaques in cells adherent to SED1. (A) Immunoblotting for α_V in the three epididymal regions; samples are loaded with equal protein. Immunoblotting of wildtype (+/+) and SED1-null (-/-) tissue under non-reducing conditions results in a single prominent band at 125 kDa, the reported molecular weight for α_V under non-reduced conditions. Wildtype and SED1-null tissue express α_V at similar levels. (B) Similarly, lysates of epithelial-enriched primary epididymal cells immunoprobed for α_V exhibit a single 125 kDa band. β -tubulin serves as a loading control. (C) Immunostaining of cells cultured on SED1 reveals cytokeratin-positive epididymal epithelial cells (red) that express α_V integrins (green) in punctate bundles arranged along the basal surface. (D) Desmin-positive (red) smooth muscle cells exhibit little or no α_V immunoreactivity. Non-immune (NI) stained cells produce background immunoreactivity. All images are from parallel experiments imaged under identical conditions. (E) Confocal micrographs reveal that cytokeratin-positive (inserts) epithelial cells cultured on SED1 localize α_V to focal plaques along the lamellipodia (arrows). (F) Epithelial cells cultured on laminin also express α_V , however the immunoreactivity is not distributed in focal plaques as on SED1 substrates, but remains perinuclear. all bars = 20 μm .



Furthermore, confocal analysis reveals that α_V integrin is organized into distinct foci or focal plaques when cells are cultured on rSED1 substrates (Fig. 4-5E). These foci are arranged along the peripheral aspects of the cell lamellipodia and reside along the basal surface as judged by z-section imaging (arrows). Importantly, these α_V -plaques are notably absent from α_V -positive epithelial cells cultured on laminin, indicating that this distribution is dependent on the presence of SED1 substrates (Fig. 4-5F). These data confirm that α_V integrins are expressed in epididymal epithelial cells and suggest that SED1 serves as a ligand for these receptors.

4.2.6 α_V integrins are required for epididymal epithelial cell adhesion to SED1

To directly test the role of α_V integrins in epithelial cell adhesion to SED1, a small molecule inhibitor, L-954, was obtained from Merck, Inc. that is specific for both $\alpha_V\beta_3$ and $\alpha_V\beta_5$ heterodimers, similar to that previously characterized (Kumar et al., 2001; Murphy et al., 2005). The addition of 0.1-1000 nM L-954 results in a dose-dependent reduction in cell adhesion to rSED1, while having no effect on cell adhesion to laminin (Fig. 4-6). L-954 inhibits SED1-dependent adhesion at concentrations as low as 1 nM, with nearly 100% inhibition at 1000 nM.

As a further test of α_V integrin function in SED1-dependent epididymal cell adhesion, we examined the effects of an α_V function blocking antibody (RMV-7) (Takahashi et al., 1990). The addition of 50 $\mu\text{g/ml}$ IgG results in a small (18%) reduction in adhesion compared to mock assays, whereas 100 $\mu\text{g/ml}$ reduces initial adhesion by 57% (Fig. 6-7). Non-immune IgG has no effect. The degree of inhibition in our studies

Figure 4-6: A small molecule inhibitor of $\alpha_v\beta_{3/5}$ integrin heterodimers (L-954) selectively blocks epididymal cell adhesion to SED1. Increasing concentrations of L-954 were added to 30-minute adhesion assays, eliciting a dose-dependent decrease in adhesion to SED1 substrates (500 ng/well). The inhibitor has little effect on cell adhesion to laminin-coated substrates (500 ng/well). Data is expressed as a percentage of untreated (mock) cell adhesion to each substrate. As little as 1 nM of inhibitor is sufficient to reduce adhesion to SED1 by 19%, while 1000 nM inhibits adhesion by 93%. error bars = sem, * = $p < 0.0001$.

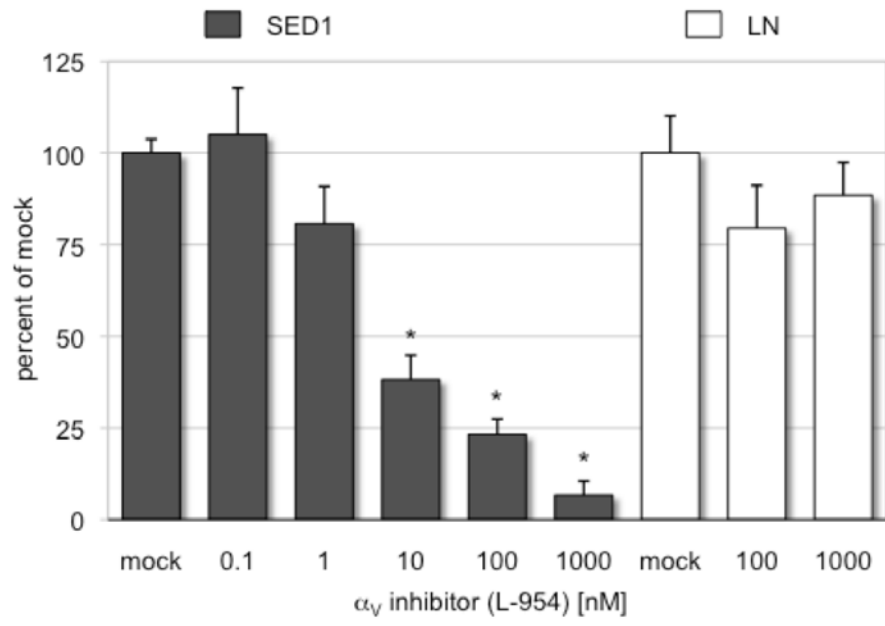
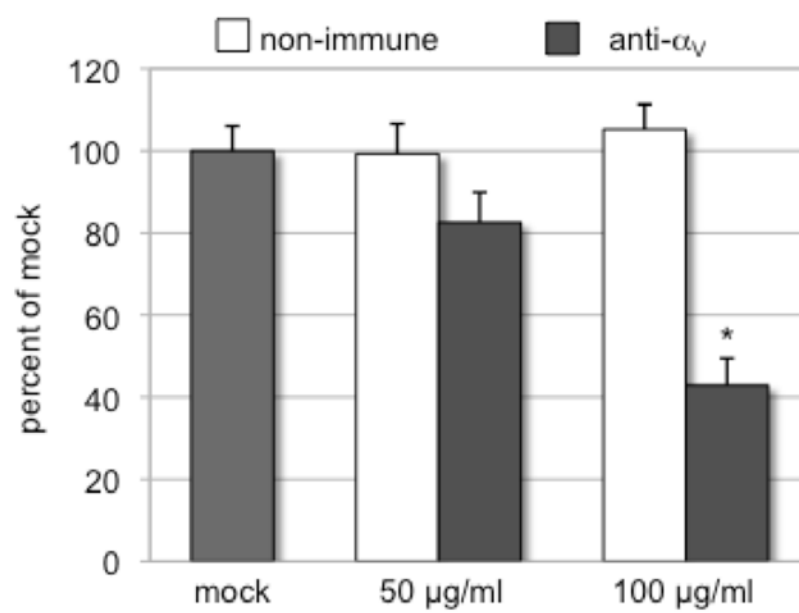


Figure 4-7: Function-blocking antibodies against α_v integrin block epididymal cell adhesion to SED1. The addition of α_v -blocking IgG (RMV-7) (50 $\mu\text{g/ml}$ or 100 $\mu\text{g/ml}$) results in a dose-dependent reduction in epithelial cell adhesion to SED1 of 18% and 57%, respectively. Control IgG has no effect. Data is expressed as a percentage of untreated (mock) cell adhesion. error bars = sem, * = $p < 0.0001$.



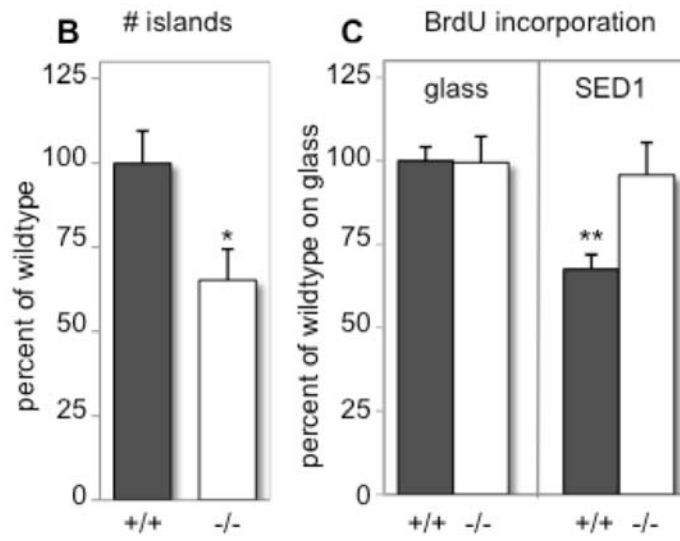
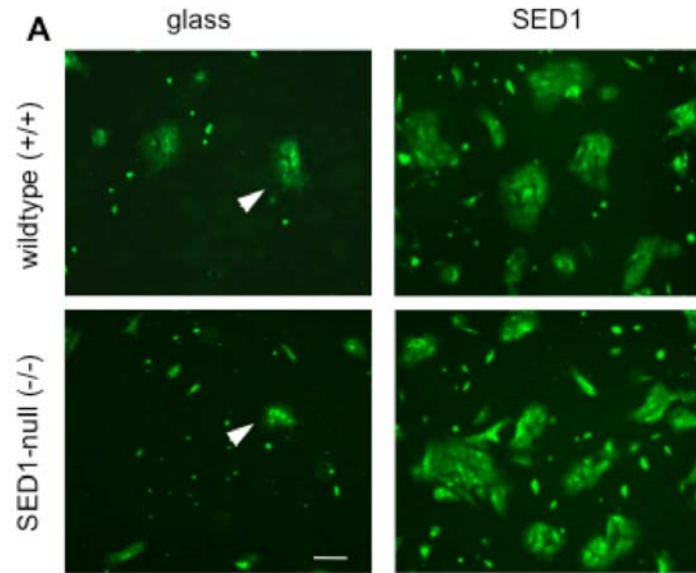
(i.e., 57%) is similar to that reported by others using the same RMV-7 IgG (Takahashi et al., 1990). Together, these data confirm that SED1 serves as a ligand for $\alpha_v\beta_{3/5}$ integrins expressed on epididymal epithelial cells.

4.2.7 SED1-null epithelial cells show reduced adhesion in vitro

Although wildtype and SED1-null cells behave similarly on transwell filters coated with Matrigel, they show striking differences when cultured on glass substrates lacking exogenous matrix. When similar numbers of wildtype and SED1-null epithelial cells are cultured on glass chamberslides, both wildtype and SED1-null cells grow as epithelial clusters, or islands; however, SED1-null cultures contain 35% fewer islands than wildtype cultures (Fig. 4-8A,B). Importantly, when cells of either genotype are provided with rSED1 substrates, many small epithelial islands quickly formed with no detectable difference between genotypes. Thus, SED1-null cells have an intrinsic deficiency in their behavior on traditional tissue culture surfaces that is negated when cells are grown on exogenous SED1.

Although these results are consistent with a role for SED1 in epididymal adhesion, we examined the possibility that the reduction in epithelial islands in SED1-null cultures reflects a primary defect in cell proliferation, rather than a defect in initial cell adhesion. This is particularly relevant here, since we have previously described the activation of MAPK-dependent proliferation cascades following SED1 binding to α_v integrins on mammary epithelial cells (Ensslin and Shur, 2007), and integrin receptors are known to influence a variety of intracellular signaling pathways

Figure 4-8: Loss of SED1 leads to deficient cellular adhesion in vitro. Primary epithelial-enriched epididymal cells were isolated and cultured for 4 days on uncoated glass or SED1 substrates. Attached cells were pulsed with BrdU for 4 hours, fixed, and immunostained for BrdU. Epididymal “islands” (arrowheads) containing ≥ 4 nuclei were counted. (A) Epifluorescent imaging of SYTO24 counterstain illustrates a reduction in the number of SED1-null (-/-) epithelial islands relative to wildtype (+/+). This phenotype is rescued when cells are cultured on SED1 substrates; under these conditions cells of both genotypes produce abundant islands. (B) Quantification shows that SED1-null (-/-) cells generate 35% fewer islands than wildtype (+/+) cells when cultured on glass substrates. (C) BrdU-positive nuclei associated with epithelial islands were counted and expressed as a percent of total nuclei associated with islands. Data from multiple experiments was averaged and the wildtype (+/+) rate of proliferation was normalized to 100%. Although SED1-null (-/-) cells generate fewer islands than wildtype, the rate of proliferation for the two genotypes is identical on glass substrates. Furthermore, the presence of SED1 substrates does not lead to increased proliferation relative to cells cultured on glass. bar = 100 μm , * = $p=0.01$, ** = $p<0.001$.



(Felding-Habermann and Cheresch, 1993; Hynes, 1992). To investigate the possibility that differences in epithelial cell growth reflect a SED1-dependent proliferation cascade, the rate of epididymal epithelial cell proliferation in wildtype and SED1-null cultures was determined by BrdU incorporation. Despite differences in the total number of epithelial islands, wildtype and SED1-null cultures show virtually identical rates of cell proliferation when grown on glass substrates (Fig. 4-8C). Furthermore, the presence of rSED1 substrates, which results in greatly increased numbers of epithelial islands, does not produce a concomitant increase in cell proliferation (Fig. 4-8C), and in fact, leads to a slightly reduced level of proliferation in wildtype cells, the basis of which remains unexplored. In any event, these data indicate that SED1 can support epididymal cell adhesion, and that the loss of SED1 results in compromised cellular adhesion.

4.3 Discussion

In light of SED1's role in cell adhesion in other systems, we designed a series of experiments to test the possibility that SED1 also facilitates cell adhesion in the epididymis (Andersen et al., 1997; Andersen et al., 2000; Ensslin et al., 1998; Ensslin and Shur, 2007; Hanayama et al., 2002; Taylor et al., 1997). Using more appropriate fixation conditions, we determined that SED1 is found along lateral cell-cell borders of the initial segment in addition to its previously reported apical localization (Ensslin and Shur, 2003). SED1 also localizes to the basal domain of clear cells in the caput and corpus, although it is not readily apparent if these cells synthesize SED1 and/or endocytose luminal SED1 for recycling and/or transcytosis, as reported for the epididymal epithelium

(Cooper et al., 1988). Unlike that seen in more proximal regions, SED1 appears targeted for degradation in the distal clear cells of the cauda. In any event, wildtype primary cells grown to confluence and polarized on permeable substrates secrete SED1 both apically and basally. It is not clear why the basal distribution of SED1 seen in cultures of polarized epithelial cells is non-uniform, or patchy, but this may reflect the presence of principal cells from both the initial segment as well as the caput epididymis that does not secrete SED1. The mechanism whereby SED1 is targeted for either apical or basolateral secretion is poorly understood but likely involves vesicle-dependent trafficking, since cleavage of the N-terminal signal sequence produces a vesicle-enclosed soluble protein. Furthermore, a basal localization of SED1 has also been reported for mammary epithelial cells (Ensslin and Shur, 2007), and a SED1 homologue known as Del-1 is a component of the extracellular matrix (Hidai et al., 2007).

The basolateral distribution of SED1 in epididymal epithelial cells is consistent with a role in cell adhesion. This was confirmed by the ability of rSED1 to support the adhesion of primary epididymal epithelial cells in a dose-dependent manner. Furthermore, the addition of RGD peptides to primary cell adhesion assays significantly reduces adhesion to rSED1, while having no effect on adhesion to laminin substrates. Since integrin heterodimers containing α_v subunits have been reported to serve as receptors for the RGD sequence in SED1, among other adhesive glycoproteins, we determined that epididymal epithelial cells expresses α_v integrin. Interestingly, epididymal cells organize α_v receptors into focal plaques when cultured on SED1, but they do not do so on laminin substrates suggesting a physiological response to the

underlying substrate. Furthermore, α_v integrins on epididymal epithelia may only recognize, or bind, the RGD motif in the context of the SED1 polypeptide backbone, since epididymal cells do not adhere to vitronectin, an RGD-containing substrate known to bind α_v integrins (data not shown) (Felding-Habermann and Cheresch, 1993). In any event, the involvement of α_v integrins in mediating SED1-dependent adhesion was confirmed through the use of specific low molecular weight inhibitors as well as by α_v function-blocking antibodies.

Consistent with SED1 function as an adhesive component in the epididymis, SED1-null cells were shown to display an intrinsic defect in cell adhesion. When wildtype and SED1-null primary epithelial cells were isolated and applied to uncoated glass substrates, wildtype cultures had characteristically larger numbers of epithelial islands than seen in SED1-null cultures. Control experiments eliminated the possibility that these differences reflect genotype-specific differences in cell proliferation. These results are in good agreement with *in vivo* BrdU assays indicating that wildtype and SED1-null initial segment epididymides proliferate at similar rates (data not shown). Perhaps more importantly, cultures of both genotypes grown on rSED1 substrates contain an abundance of epithelial islands while maintaining similar rates of proliferation to wildtype cells grown on glass. Therefore, the reduced number of cells in SED1-null cultures reflects reduced cell adhesion at plating, which we believe is a consequence of their inability to synthesize and secrete SED1 substrates as do wildtype cells.

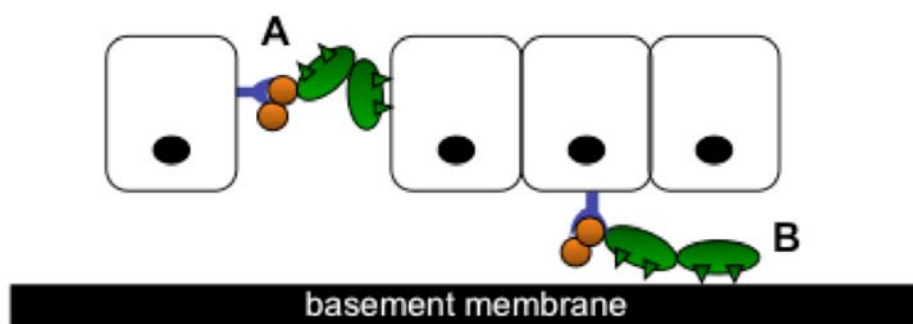
These data allow us to develop a simple working model for SED1-dependent epithelial cell adhesion in the epididymis. It is proposed that SED1 localized to

basolateral domains facilitates cell adhesion via binding of its N-terminal RGD motif to cell surface α_V integrin receptors, whereas the C-terminal F5/8C-discoidin domains bind to phospholipid bilayers on adjacent epithelial cells, as shown by others (Andersen et al., 1997; Andersen et al., 2000) (Fig. 4-9A). Alternatively, SED1 may mediate cell adhesion to the underlying basal lamina, as suggested for the SED1 homologue, Del-1 (Hidai et al., 2007), by the binding of F5/8C-discoidin domains to negatively charged components of the extracellular matrix (Fig. 4-9B). Distinguishing between these possibilities would be greatly facilitated by localization of $\alpha_V\beta_{3/5}$ integrins *in vivo*, however multiple attempts using various commercially available α_V antibodies and different fixation conditions failed to yield a reliable signal for α_V in epididymal sections.

Although SED1 expression is highest in the initial segment, the majority of SED1-dependent phenotypes manifest in the distal corpus and cauda, similar to other systems reporting spermatic granulomas (Flickinger et al., 1995; Hess et al., 2000). Thus, SED1 may impact epithelial integrity either locally and/or long-range. Since SED1 is found both within the epididymal lumen as well as in apical and basal domains of clear cells that are prevalent in the corpus, it is possible that SED1 is synthesized and/or transcytosed by these cells and deposited in the basement membrane where it serves as an adhesive ligand. Alternatively, SED1 may serve an adhesive function in the initial segment that is required, indirectly, for the integrity of the distal epididymis. Such is the case for the ER-null epididymis, in which a defect in the expression and localization of sodium exchangers in the efferent ducts is coincident with the appearance of sperm granulomas in the distal epididymis (Hess et al., 2000). Furthermore, binding of SED1 or

Figure 4-9: Working model of SED1-dependent epididymal epithelial cell adhesion.

The EFG domains (orange circles) and F5/8C-discoidin domains (green ovals) of SED1 are depicted bound to epididymal epithelial cells. The second EGF domain of SED1 contains a RGD motif and is proposed to serve as ligand for $\alpha_V\beta_3$ or $\alpha_V\beta_5$ integrins (blue receptor) expressed by the epithelial cells. Two models of adhesion are presented: A) cell-cell adhesion and B) cell-basement membrane adhesion. The F5/8C-discoidin domains are predicted to function by binding either (A) anionic phospholipids on the cell surface or (B) negatively charged residues within the basement membrane.



Del-1 to $\alpha_v\beta_{3/5}$ integrins is known to activate intracellular signaling cascades in other systems (Ensslin and Shur, 2007; Penta et al., 1999; Wu et al., 2005), such that the loss of this interaction may affect important epithelial cell functions such as protein secretion, ultimately impacting the overall fortitude and function of the epididymis.

The realization that the loss of SED1 leads to an epididymal phenotype raises the possibility that SED1 does not participate in sperm adhesion to the egg coat as previously reported (Ensslin and Shur, 2003), but rather suggests that the defective sperm-egg binding may be a secondary consequence of defective epididymal integrity. A number of observations indicate that this is not a likely possibility. First, a variety of reagents that specifically block SED1 function, such as blocking antibodies, recombinant SED1, and truncated SED1 proteins, are able to competitively inhibit the binding of wildtype sperm to eggs. Second, the penetrance of the fertility phenotype reported previously, as well as the penetrance of the epididymal pathologies reported here, show distinctly different strain-specific expression. In this regard, the original null mutation was generated on the mosaic B6/129 background, which produced a variable, but highly penetrant (~89%) fertility phenotype, whereas epididymal lesions did not occur until late adulthood (data not shown). In contrast, backcrossing the SED1-null mutation onto the B6 congenic background produced a weak fertility phenotype, possibly due to maintaining them by homozygous matings, although B6 SED1-null males show a clearly penetrant (~50%), but variable, epididymal phenotype as early as seven weeks of age. Thus, the sub-fertility of the B6/129 SED1-null males is not likely the result of defects in epididymal integrity.

Even though many questions remain unanswered, the data presented here clearly show that SED1 plays an important role in the maintenance of the epididymis, in addition to its role in facilitating sperm-egg adhesion. These results further illustrate the complex relationship between seemingly disconnected regions of the epididymis, and may have important implications for the development of new fertility and contraceptive technologies as the epididymis becomes an increasingly important target for reproductive interventions.

Chapter 5: Loss of SED1 Results in Altered Luminal Physiology in the Epididymis

Some written material and figures in Chapter 5 will be published in the future (Raymond et al., 2009a).

All data and figures in Chapter 5 are the work of Adam S. Raymond with the exception of Figure 5-5(A) that is the work of Brooke Elder.

Chapter 5: Loss of SED1 Results in Altered Luminal Physiology in the Epididymis

5.1 Introduction and experimental rationale

Originally identified as an epididymally-secreted protein that coats sperm, SED1 was found to be critical for the ability of sperm to bind the zona pellucida (Ensslin and Shur, 2003). Additionally, we report in Chapter 3 that the loss of SED1 leads to breakdown of the epididymal epithelium, with the consequent development of spermatocytic granulomas. Results presented in Chapter 4 indicate that SED1 facilitates intercellular adhesion between epididymal cells by binding to $\alpha_v\beta_{3/5}$ integrin receptors. In this scenario, loss of SED1 leads to epithelial breakdown, exposure of sperm associated antigens, and development of spermatocytic granulomas. Although the data suggest that the epithelial pathology results from a loss of SED1-dependent adhesion, the downstream consequences of defective SED1-dependent adhesions, and any associated integrin-based signaling cascades, remain undefined.

We therefore undertook a more detailed analysis of the SED1-null epididymis and show here that the loss of SED1 leads to an inability of the epididymal epithelium to properly acidify the luminal fluid, which is known to be absolutely critical for sperm maturation and for their ability to fertilize eggs. The failure to acidify is not a secondary consequence of abnormal epididymal development or differentiation, nor is it the result of defects in the upstream tissues of testis or efferent ducts, as is the case in other systems (Hess et al., 2000; Zhou et al., 2001). Rather, the failure to acidify the luminal fluid is accompanied by alterations in cell morphology, intracellular vesicles, and subcellular

distribution of transporters involved in luminal acidification, among other abnormalities, all of which contribute to the defective regulation of the luminal fluid pH.

5.2 Results

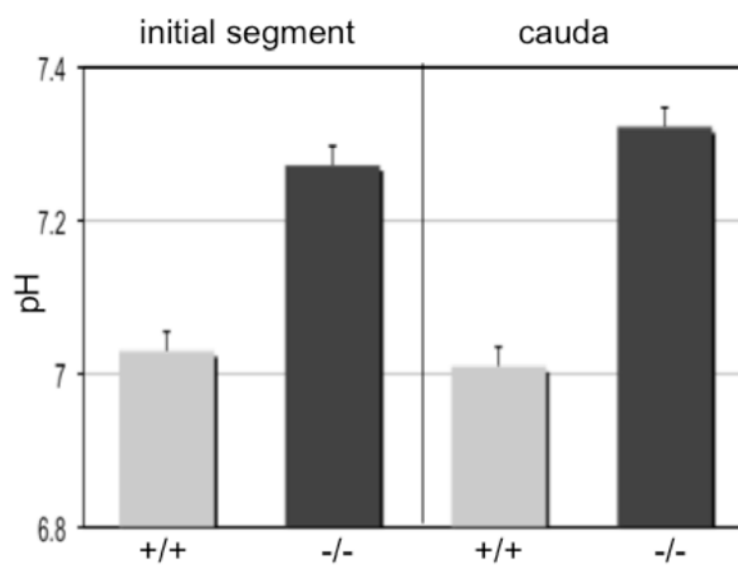
5.2.1 Loss of SED1 results in an increase in luminal pH

We have reported that the SED1-null epididymis exhibits an increased occurrence of spermatic granulomas. In some models that contain spermatic granulomas, including the ER knockout, upstream tissues possess an underlying defect in the maintenance of luminal fluid dynamics (Hess et al., 2000; Zhou et al., 2001). Additionally, infertile *c-ros* knockout males do not exhibit spermatic lesions, but nonetheless harbor a physiological phenotype, including elevated luminal pH (Yeung et al., 2004b). We therefore investigated the effect a loss of SED1 may have on the luminal fluid by first determining the pH in wildtype and SED1-null animals.

Wildtype and SED1-null animals were sacrificed in pairs, and each epididymis was sub-dissected into the caput and cauda. Luminal contents from the distal cut surface were gently massaged onto litmus paper and compared to a series of buffered standards to determine the pH. Luminal fluid harvested from both the distal end of the initial segment and cauda regions of SED1-null epididymides are ~0.3 pH units higher than wildtype ($p \leq 0.006$) (Fig. 5-1). This increase in pH is similar to the difference detected when comparing wildtype and *c-ros* knockout animals, and indicates that the SED1-null epididymis fails to properly acidify the epididymal lumen (Yeung et al., 2004b).

Figure 5-1: The SED1-null epididymis fails to acidify the luminal fluid.

Epididymides were isolated, subdissected, and luminal contents were extruded onto litmus paper in ex vivo pH assays. Fluid isolated at the distal end of the initial segment measured 7.03 ± 0.03 for wildtype and 7.27 ± 0.02 for SED1-null ($p = 0.006$), a difference that persists in the cauda: 7.01 ± 0.02 and 7.32 ± 0.01 for wildtype and SED1-null ($p < 0.001$), respectively.



Importantly, the difference can be measured as early as the caput indicating that the defect most likely occurs in the proximal region of the epididymis.

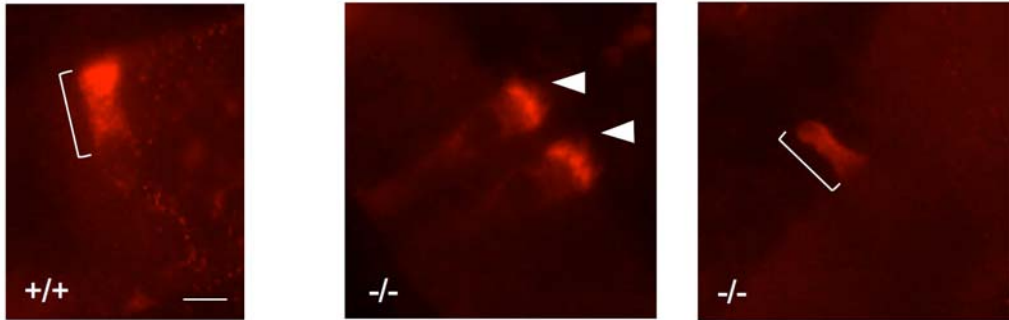
5.2.2 SED1-null epididymides exhibit morphological correlates of defective fluid regulation

Although development and differentiation of the SED1-null epididymis appears grossly normal, the epithelium is characterized by a number of subtle morphological features that have been reported in other systems to be associated with defective regulation of the luminal pH. Clear cells throughout the epididymis express VAPase, a protein complex that transports protons across cell membranes (Brown et al., 1992). Under normal conditions, VAPase recycles between endosomes and the apical membrane where it delivers protons to the luminal fluid; however, VAPase remains at the apical membrane under alkaline pH and high bicarbonate levels. It is therefore interesting that the distribution of VAPase in clear cells of the SED1-null initial segment, where they are called narrow cells, and in the cauda is more apically localized than in wildtype (Fig. 5-2A,B). These observations are consistent with the occurrence of acidified luminal fluid in the SED1-null epididymis, and suggest a potential compensatory mechanism.

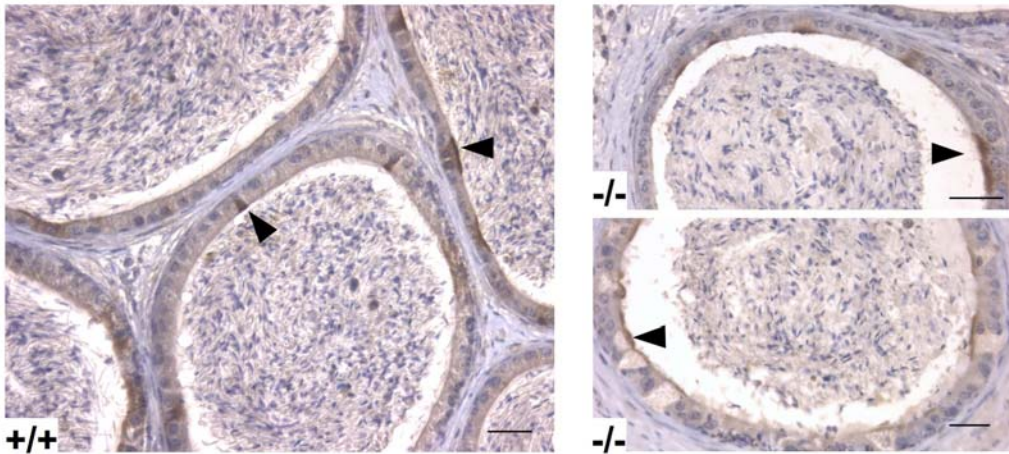
Additionally, transmission electron microscopy reveals that some aspects of the subcellular architecture are affected in the absence of SED1. Within the principal cells of the SED1-null initial segment, the mitochondria are often swollen and damaged, a phenotype that can reflect hypo-osmotic conditions (Fig. 5-2C) (McGill et al., 1973). As

Figure 5-2: The SED1-null epididymis exhibits characteristics consistent with an elevated pH and hypo-osmotic luminal fluid. A) PFA-perfused, and B) Bouin's-fixed tissue were immunostained with VATPase, labeling narrow cells in the initial segment (A) and clear cells in the cauda (B). VATPase is consistently distributed throughout the apical domain of wildtype cells (A, +/- bracket; B, arrowheads), while being concentrated at the adluminal surface of SED1-null cells (A, (-/- arrowheads), a localization that is consistent with alkaline luminal fluid. Furthermore, SED1-null narrow cells often extend VATPase enriched apical processes into the lumen (A, -/- bracket), whereas wildtype cells maintain flat or rounded apical domains. C) Transmission electron micrographs of wildtype and SED1-null principal epithelial cells. Mutant tissue contains a high frequency of swollen and damaged mitochondria (arrowheads) that is indicative of increased sensitivity to hypo-osmotic milieu when processed by submersion fixation. bars = 15 μm (A); 25 μm (B); 1.7 μm (C)

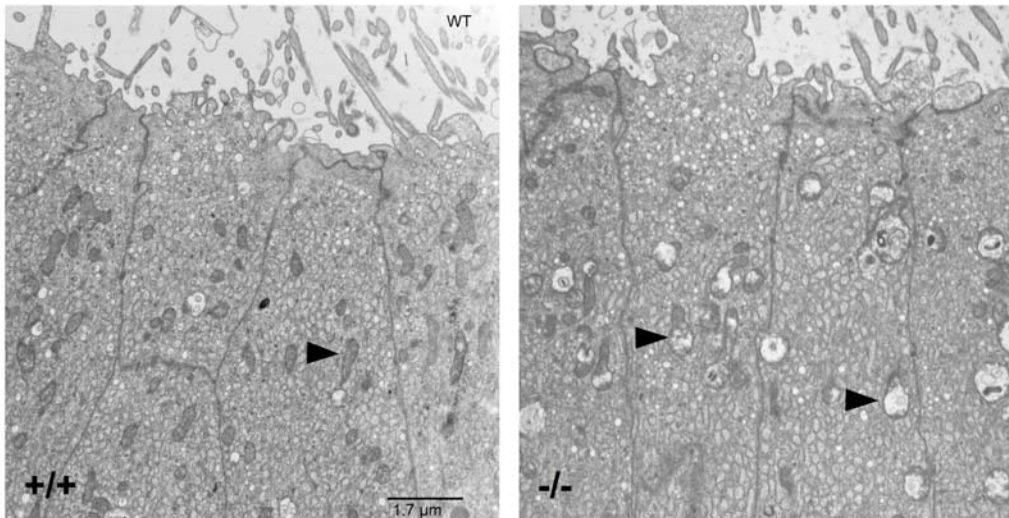
A VATPase, initial segment



B VATPase, cauda



C TEM, initial segment

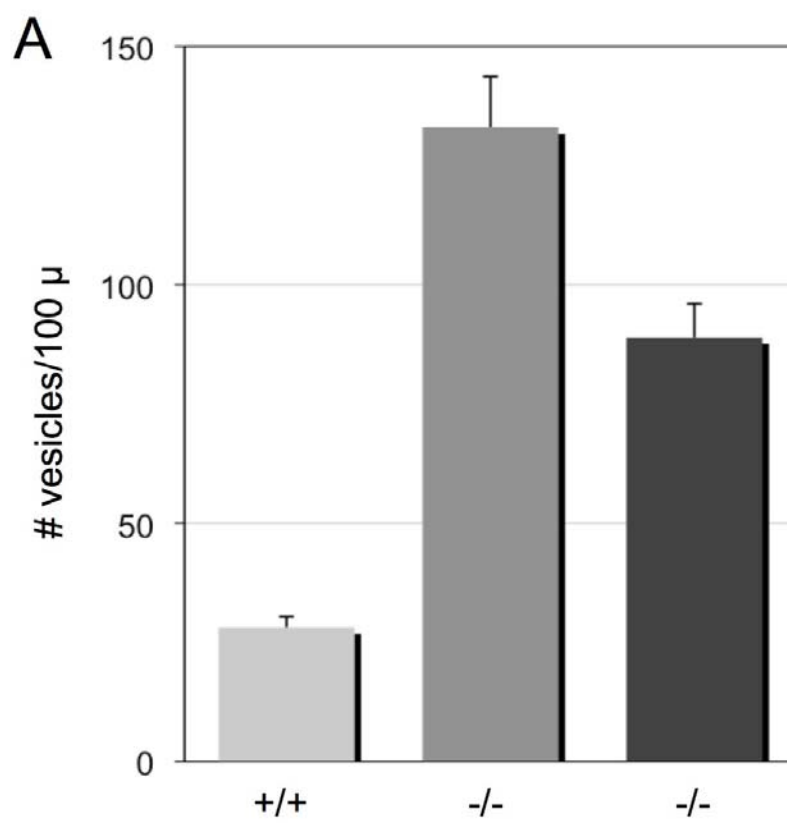


reported by others, this phenotype may be, in-part, an artifact of submersion fixation of the tissue; however, wildtype and knockout material prepared in parallel indicate that the SED1-null is more sensitive to these conditions than normal tissue. Since luminal pH is coupled with fluid transport, it is not surprising that the SED1-null shows features characteristic of a hypo-osmotic luminal environment.

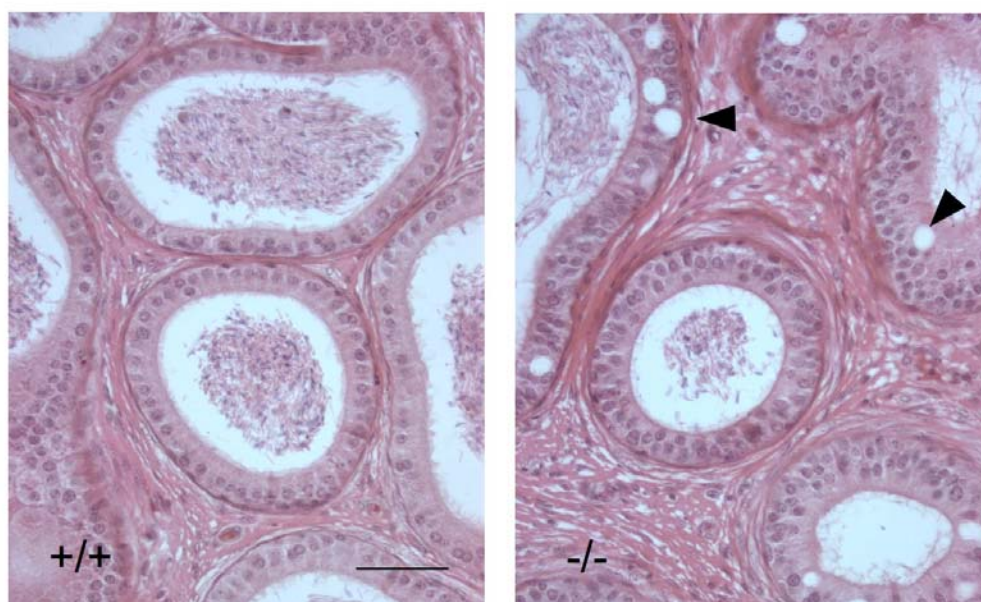
These observations drew our attention to other hallmarks of defective osmolarity and fluid regulation. Semi-thin sections were prepared, stained with toluidine blue, and used to examine vesicles present in different regions of the epididymis that express SED1. Quantification of vesicles in the highly endocytic caput III region indicates that the SED1-null has more vesicles than the equivalent region in wildtype, suggesting increased, compensatory endocytosis resulting from poor fluid reabsorption (SED1-null devoid of granuloma: 133.1 ± 8.7 vesicles/100 μm tubule circumference; SED1-null with distal granuloma: 88.9 ± 6.5 vesicles/100 μm ; wildtype: 28.1 ± 3.1 vesicles/100 μm ; $p < 0.0001$) (Fig. 5-3A) (Abou-Haèila and Fain-Maurel, 1984). Furthermore, this suggestion is supported by the appearance of highly vacuolated epithelium in SED1-null epididymides, a characteristic of abnormal luminal fluid adsorption (Fig. 5-3B) (Itoh et al., 1999).

Finally, in this regard, the clear cells of the proximal segments of the SED1-null epididymis show an unusual pathology not previously seen in other epididymal models. In the initial segment and caput II regions of wildtype animals, the narrow cells in the initial segment and prominent cells in caput II extend cap-like protrusions containing large clear vacuoles into the lumen that presumably contains machinery to facilitate

Figure 5-3: The SED1-null epididymis possesses characteristics consistent with compensatory endocytosis. A) Semi-thin sections containing caput region III were prepared and stained with toluidine blue. Vesicles were quantified in wildtype (+/+, light gray; 276 vesicles in 15 tubule sections), SED1-null without apparent spermatic granulomas (-/-, dark gray; 932 vesicles in 11 tubules), and SED1-null tissue containing a caudal granuloma (-/-, black; 666 vesicles in 15 tubules). Total vesicle counts were normalized to 100 μm of adluminal membrane length. SED1-null tissue exhibits greatly increased intracellular vesicles irrelevant of the presence of spermatic granulomas ($p < 0.0001$). B) Sections of SED1-null epithelium stained with hematoxylin and eosin show an increase frequency of large vacuoles (arrowheads), a phenotype characteristic of abnormal fluid regulation and which is thought to precede granuloma formation in other systems. bar = 50 μm



B



acidification (Abou-Haèila and Fain-Maurel, 1984; Hinton and Palladino, 1995). However, the apical domains of virtually all narrow cells, and most prominent cells, in the SED1-null have a rough, shredded morphology, devoid of vesicles (Fig. 5-4). Similar results are seen when these cells are immunostained for intracellular markers, such as chloride channels (Fig. 5-4). The basis of this defective apical morphology remains unknown, but suggests that the cell's endocytic, and/or VATPase recycling machinery can not be regenerated as well as in wildtype.

5.2.3 Many proteins that regulate the composition of the luminal fluid are expressed and localized normally in the SED1-null epididymis

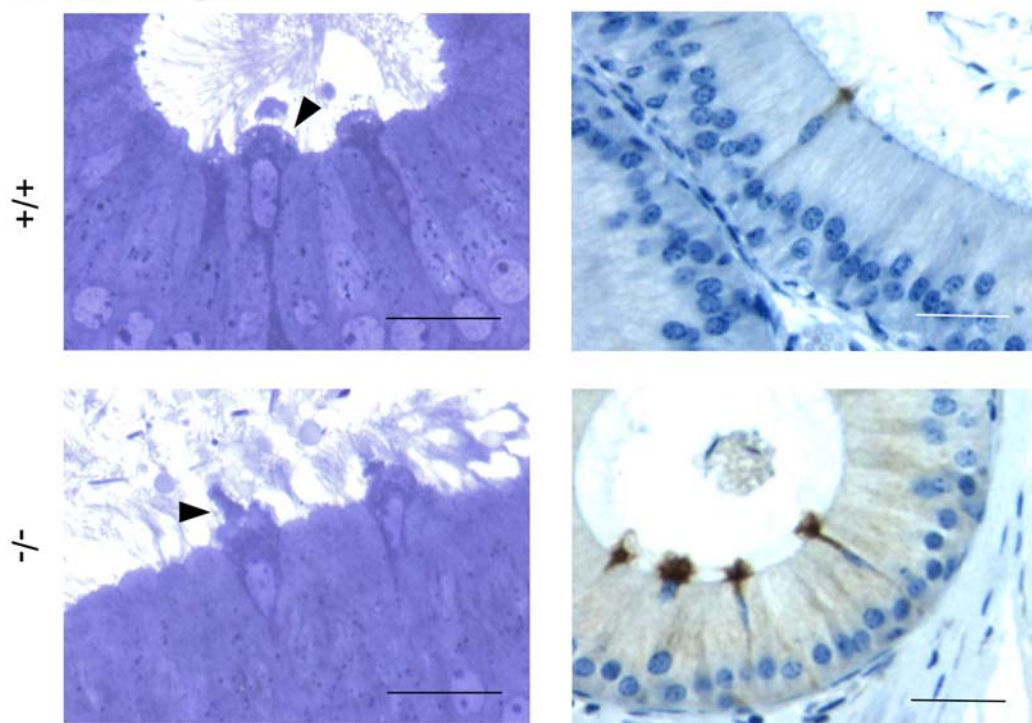
The observations reported above are consistent with inappropriate regulation of fluid dynamics in the SED1-null epididymis, and therefore, we considered possible mechanisms whereby loss of SED1 may affect this physiology. Analogous to the proximal convoluted tubule of the kidney, fluid reabsorption and pH regulation in the proximal epididymis require proper expression, localization, and function of a broad spectrum of ion transporters, membrane pumps and channels, and enzymes that facilitate acid-base chemistry. Epididymal mutants, including the ER knockout and the *c-ros* knockout, share similar defects in the expression and localization of sodium/hydrogen exchangers at the apical plasma membrane of epithelial cells (Yeung et al., 2004b; Zhou et al., 2001). We therefore considered the possibility that loss of SED1 may affect the proper targeting and/or turnover of fluid regulatory proteins at the apical and basolateral

Figure 5-4: SED1-null narrow and prominent cells exhibit altered morphology.

Toluidine blue stained semi-thin sections and paraffin-embedded sections immunolabeled with C1 antibody (anti-CLC3/5) illustrate abnormalities in SED1-null cells. (A) Narrow cells of the initial segment typically feature a smooth apical cap (arrowheads) that protrudes into the lumen (+/+); however, in the SED1-null these cells have a rough, sheared morphology (-/-). (B) Likewise, prominent (clear) cells in caput II extend a large, vesicle-filled protrusion into the lumen (+/+, arrowhead). In SED1-deficient animals, the prominent cells are often devoid of their apical protrusions, which appear to be released into the lumen. Occasionally, prominent cells are seen being extruded from the mutant epithelium (insert), a phenotype not seen in wildtype. When assessed by immunostaining in paraffin-embedded tissue (CLC3/5 shows example), the apical protrusions of SED1-null cells appear fragmented. all bars = 25 μ m

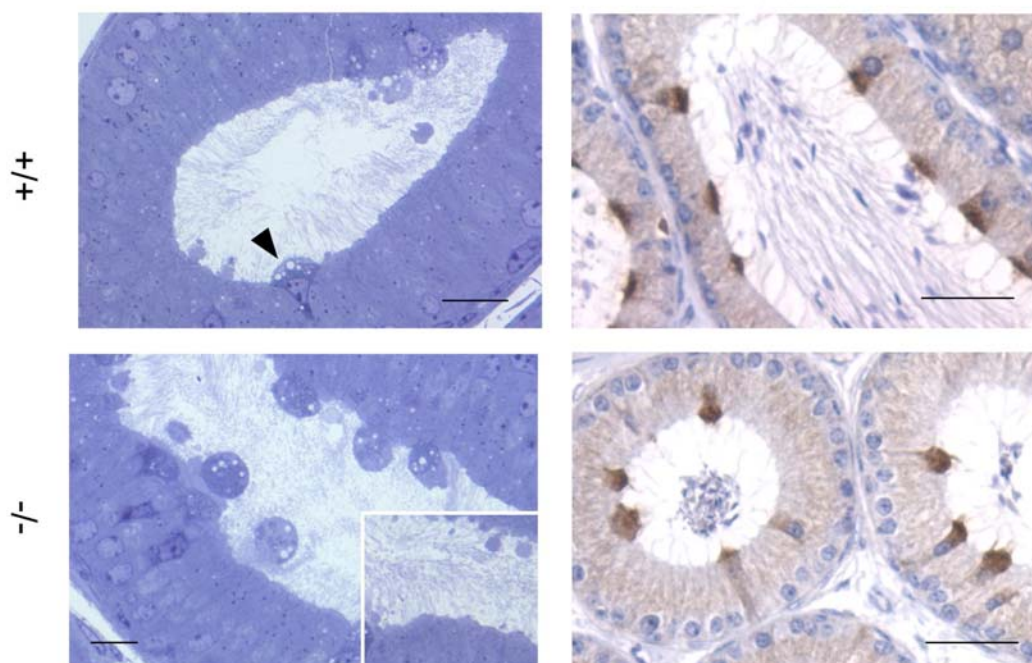
A initial segment

CIC3/5



B caput II

CIC3/5



membranes, since SED1 is thought to influence intracellular vesicle formation and/or secretion (Oshima et al., 2002).

We identified a subset of these proteins with known expression in the mouse or rat epididymis, and characterized their expression and localization throughout wildtype and SED1-null epididymides (Table 5-1). Proteins examined by western blot analysis and immunocytochemistry of epididymal tissue include: NHE2, NHE3 sodium/hydrogen exchangers; NBC1 sodium/bicarbonate cotransporter; CLC3 and CLC5 chloride channels; AE2 anion exchanger; EAAC1 glutamate transporter; Aquaporin-9 (AQP-9) water channel; VATPase proton pump; CAII, CAXIV, CAIV carbonic anhydrases; Cx43 gap junction component; ZO-1 tight junction component. The immunocytochemical localization of these proteins was found to be similar in wildtype and SED1-null tissue (Table 5-2, Fig. 5-5). Furthermore, the level of protein expression as judged by western blot analysis is also similar between genotypes, although some proteins, such as CAXIV, were occasionally reduced in SED1-null samples. However, these differences were not consistently seen.

5.2.4 SED1 is associated with mouse epididymosomes

Among a number of tissues, SED1 is also expressed by dendritic cells and adipocytes where it associates with non-classical microvesicles known as exosomes (Aoki et al., 2007; They et al., 1999). Exosomes function, in-part, as paracrine factors transducing long-range signals to distant cells (Guermónprez et al., 2002). In this regard, principal epithelial cells of the epididymis shed microvesicles known as

Table 5-1: Proteins known to effect regulation of luminal composition and their reported expression and localization in the epididymis.

Protein	Function	Species	Western	Initial Segment		Caput		Corpus		Cauda		Reference
				Principal	Narrow	Principal	Clear	Principal	Clear	Principal	Clear	
NHE2	Na ⁺ /H ⁺ exchanger	rat	NA	*	*	✓	*	✓	*	✓	*	Chew et al., 2000
NHE3	Na ⁺ /H ⁺ exchanger	mouse	120 kDa	✓ (W)	NA	✓ (W)	NA	*	NA	*	NA	Yeung et al., 2004b
		rat	80 kDa	✓	*	✓	*	NA	NA	✓	*	Baganis et al., 2001 & Puskin et al., 2000
NBC1	Na ⁺ /HCO ₃ ⁻ cotransporter	mouse	88 kDa	weak (W)	NA	* (W)	NA	weak (W)	NA	✓ (W)	NA	Yeung et al., 2004b
		rat	160 kDa	✓	✓	weak	weak	weak	weak	weak	weak	Jensen et al., 1999a
Cl ⁻ CLC3/5	Cl ⁻ channel	rat	85 kDa	✓	*	✓	✓	weak	weak	✓	✓	Isnard-Bagnis et al., 2003
		rat	85 kDa	*	*	*	✓	weak	weak	*	✓	Isnard-Bagnis et al., 2003
AE2	anion exchanger	rat/mouse	180 kDa	✓	NA	weak	NA	*	NA	✓	NA	Jensen et al., 1999b
EAAC	glutamate transporter	mouse	NA	✓	NA	✓	NA	weak	*	✓	*	Wagenfeld et al., 2002
AQP-9	water channel	rat	NA	✓	*	weak	*	weak	*	✓	✓	Badran and Hermo et al., 2002
VATPase	proton pump	rat	NA	*	✓	*	✓	✓	*	✓	*	Breton et al., 1999
CAII	carbonic anhydrase	rat	29 kDa	✓	✓+	✓	*	✓	*	✓	*	Hermo et al., 2005
CAIV	carbonic anhydrase	rat	39 kDa	*	*	some	*	✓	*	some	*	Kaunisto et al., 1995
CAXIV	carbonic anhydrase	rat	NA	✓	*	✓	*	✓	*	✓	*	Hermo et al., 2005
Cx43	gap junction component	rat	42 kDa	✓	NA	✓	NA	✓	NA	✓	NA	Cyr et al., 2007
ZO-1	tight junction component	mouse	NA	✓	NA	✓	NA	weak	NA	weak	NA	Levy and Robaire., 1999

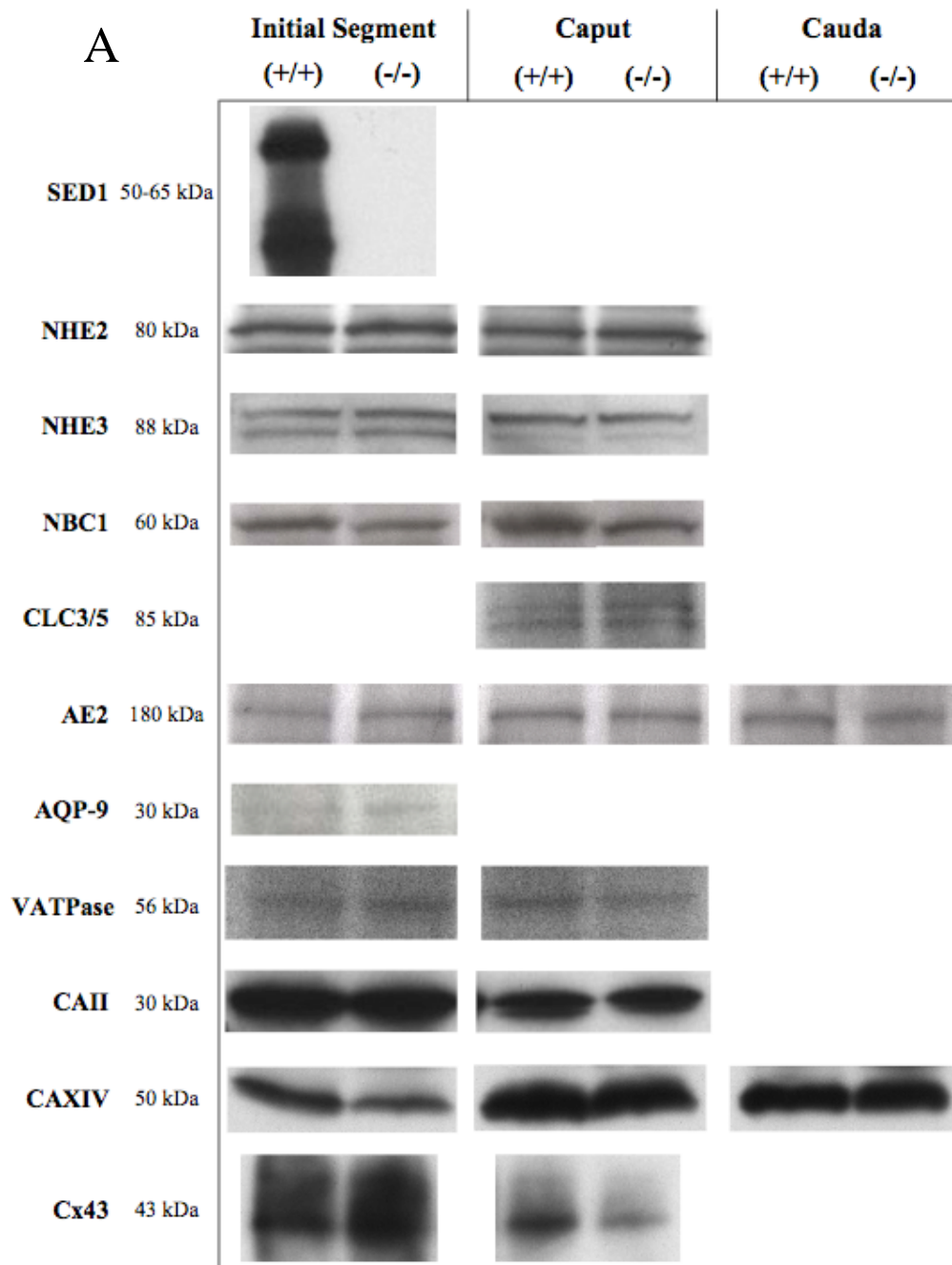
✓ detection of immunoreactivity
 * absence of immunoreactivity
 NA "not addressed"
 (W) localization was determined by region-specific western blotting

Table 5-2: Proteins known to effect regulation of luminal composition and their observed expression and localization in the epididymis.

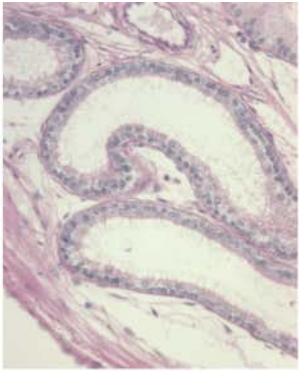
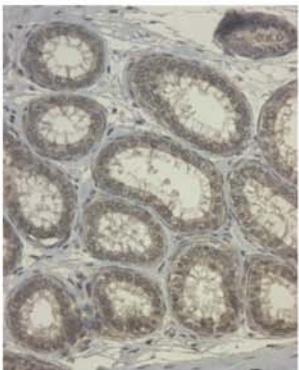
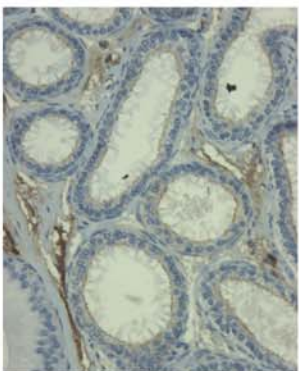
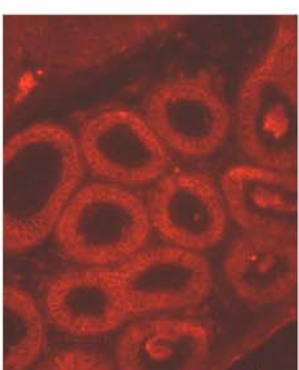
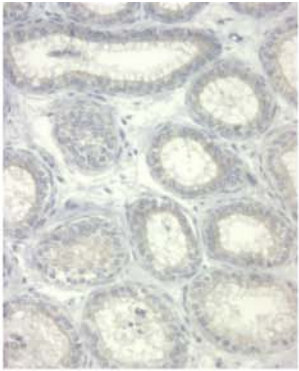
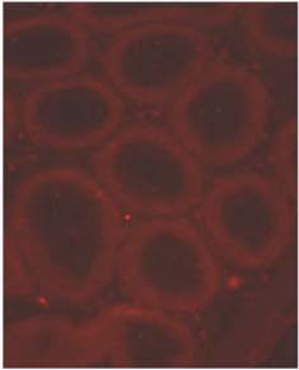
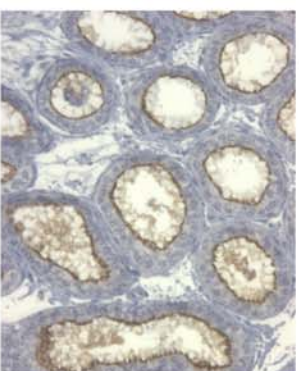
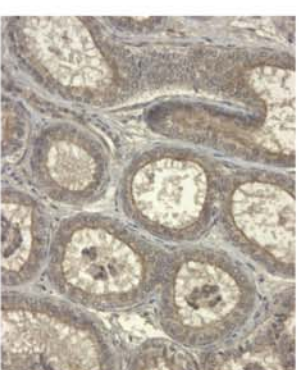
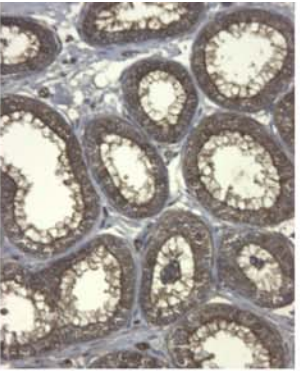
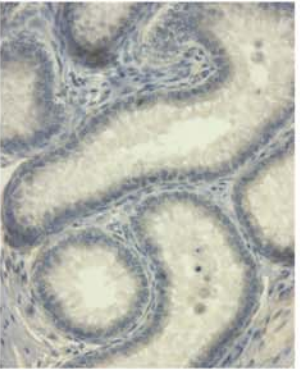
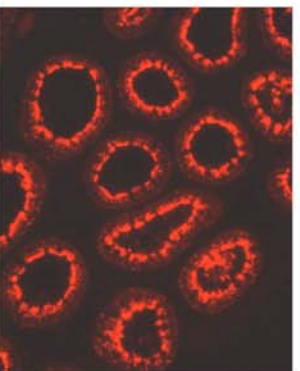
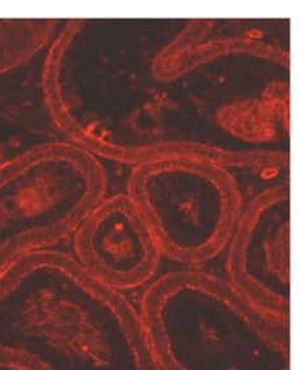
Protein	Function	Western *	Localization	Efferent Ducts		Initial Segment		Caput		Corpus		Cauda	
				Principal	Narrow	Principal	Narrow	Principal	Clear	Principal	Clear	Principal	Clear
SEDI	adhesion Na ⁺ /H ⁺ exchanger	✓	intracellular	*	no signal	✓	no signal	II, III, IV	NA	*	no signal	*	prox. only
NHE2	Na ⁺ /H ⁺ exchanger	✓	no signal	no signal	no signal	no signal	no signal	no signal	no signal	no signal	no signal	no signal	no signal
NHE3	Na ⁺ /H ⁺ exchanger	✓	apical membrane	✓	*	*	NA	*	*	*	*	✓	*
NBC1	Na ⁺ /HCO ₃ - cotransporter	✓	basolateral	strong	weak	NA	NA	II (weak), III (moderate)	NA	*	*	NA	NA
Cl CLC3/5	Cl- channel	✓	apical cytoplasmic	weak	*	✓	*	*	II, III, IV, V	*	✓	*	✓
AE2	anion exchanger	✓	no signal	no signal	no signal	no signal	no signal	no signal	no signal	no signal	no signal	no signal	no signal
EAAC	glutamate transporter	*	microvilli	*	*	*	NA	II (strong), III (weak)	NA	*	*	strong	NA
AQP-9	water channel	✓	microvilli	✓	✓	NA	NA	II, IV, V (weak)	*	✓	NA	✓	*
VATPase	proton pump	✓	apical cytoplasmic	NA	*	✓	✓	II, III, IV, V	II (strong)	*	*	*	✓
CAII	carbonic anhydrase	✓	intracellular	✓	✓	✓	✓	II (weak)	II (strong)	some	NA	✓	strong
CAIV	carbonic anhydrase	*	apical membrane	*	*	*	NA	V (some)	NA	✓	NA	prox. (strong), distal (weak)	NA
CAXIV	carbonic anhydrase	✓	no signal	no signal	no signal	no signal	no signal	no signal	no signal	no signal	no signal	no signal	no signal
Cx43	gap junction component	✓	intracellular, basal & lateral border plaques	✓	✓	NA	NA	II, III (weak), V	NA	weak	NA	weak	NA
ZO-1	tight junction component	*	apical borders	✓	NA	✓	NA	NA	II, III, IV, V	✓	NA	✓	NA

✓ detection of immunoreactivity
 * absence of immunoreactivity
 NA "not addressed"
 * molecular weight determined by western blot of initial segment tissue
 no signal no immunolocalization was determined

Figure 5-5: Many proteins that regulate the composition of the luminal fluid are expressed and localized normally in the SED1-null epididymis. Immunoblot (A) and immunocytochemical analyses (B-J) of proteins that regulate the luminal fluid are presented throughout the epididymal tubule. Expression levels are similar in wildtype (+/+) and SED1-null (-/-) tissue as judged by immunoblot, and show similar localizations in both genotypes (wildtype tissue shown). Some antibodies were only able to produce immunoblot or immunolocalization signals. PAS staining and SED1-immunoreactivity are illustrated for reference purposes. bars = μ .

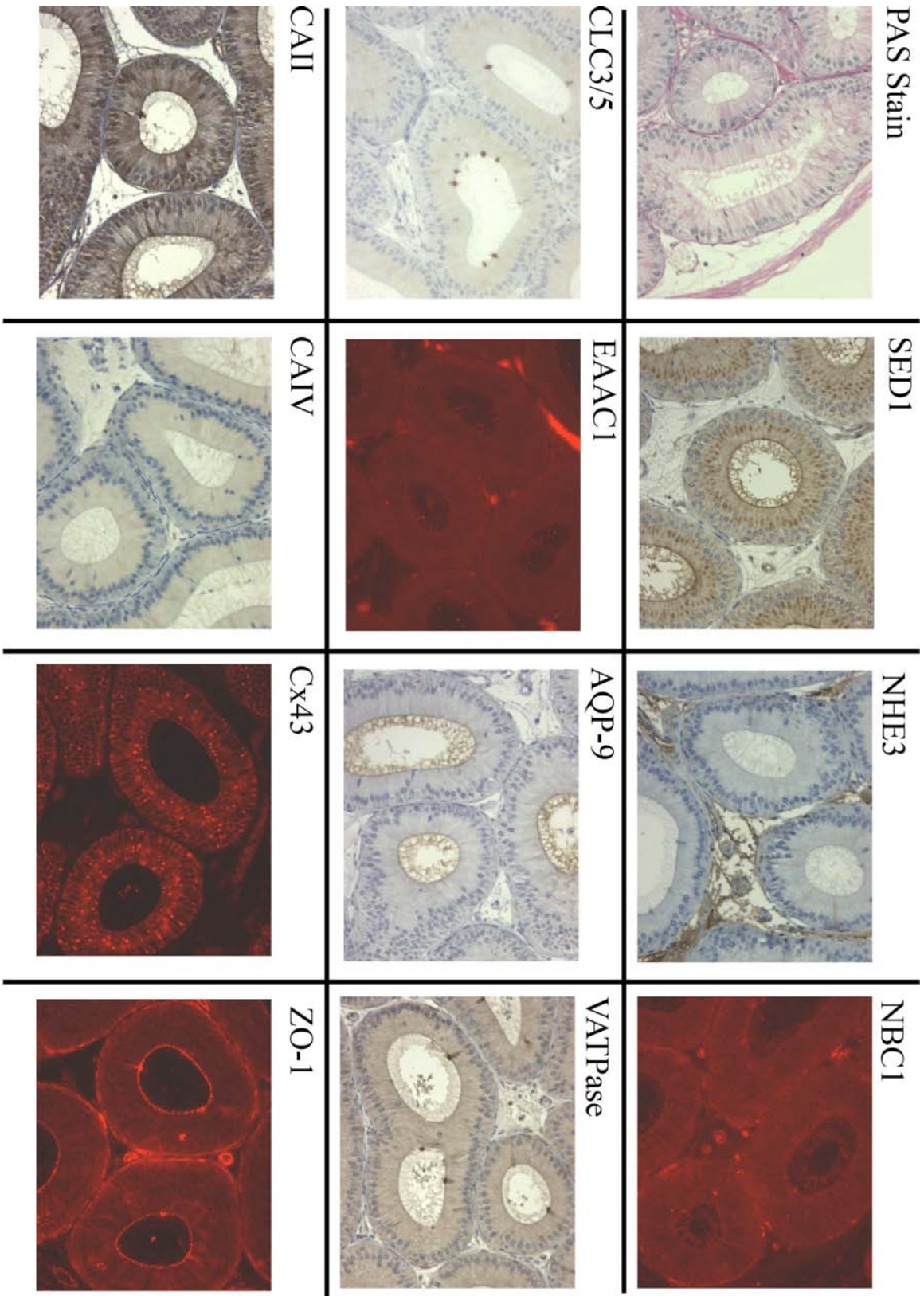


B Efferent Ducts

 <p>PAS Stain</p>	 <p>SED1</p>	 <p>NHE3</p>	 <p>NBC1</p>
 <p>CLC3/5</p>	 <p>EAAC1</p>	 <p>AQP-9</p>	 <p>VATPase</p>
 <p>CAII</p>	 <p>CAIV</p>	 <p>CX43</p>	 <p>ZO-1</p>

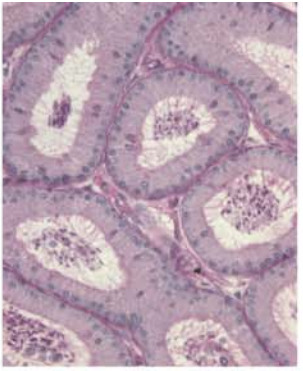
EFFERENT DUCTS

C Initial Segment

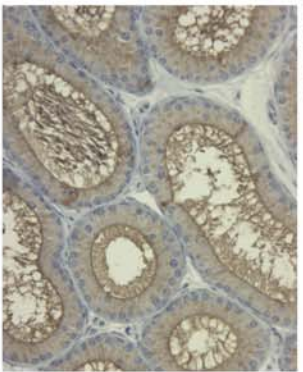


INITIAL SEGMENT

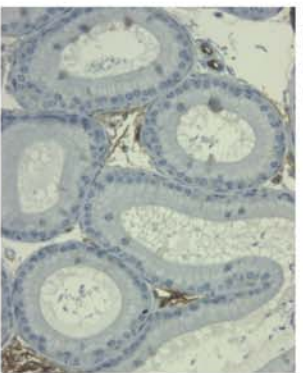
PAS Stain



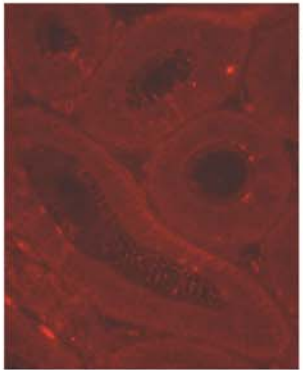
SED1



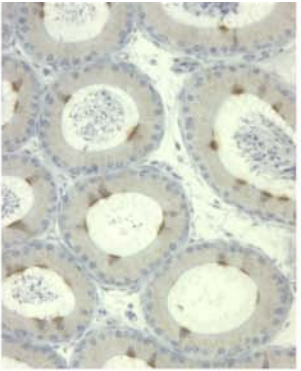
NHE3



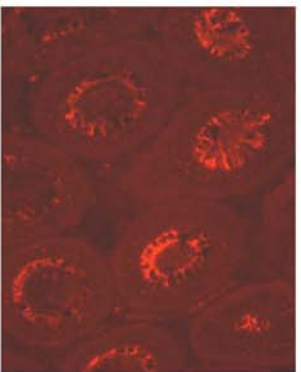
NBC1



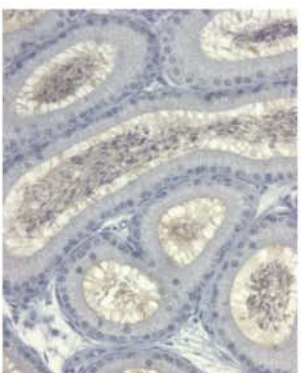
CLC3/5



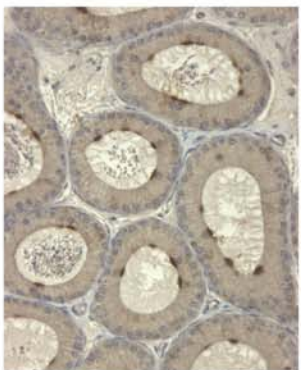
EAAC1



AQP-9



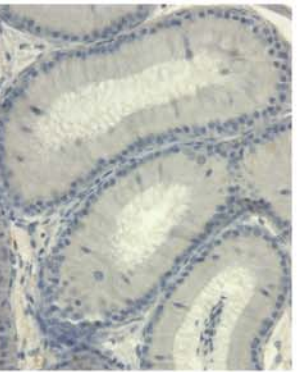
VATPase



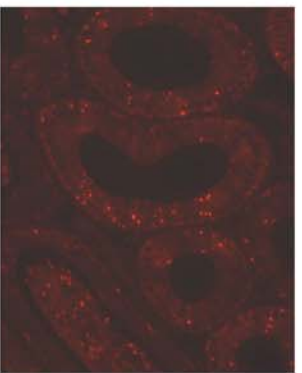
CAII



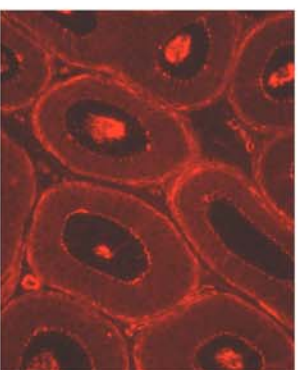
CAIV



Cx43

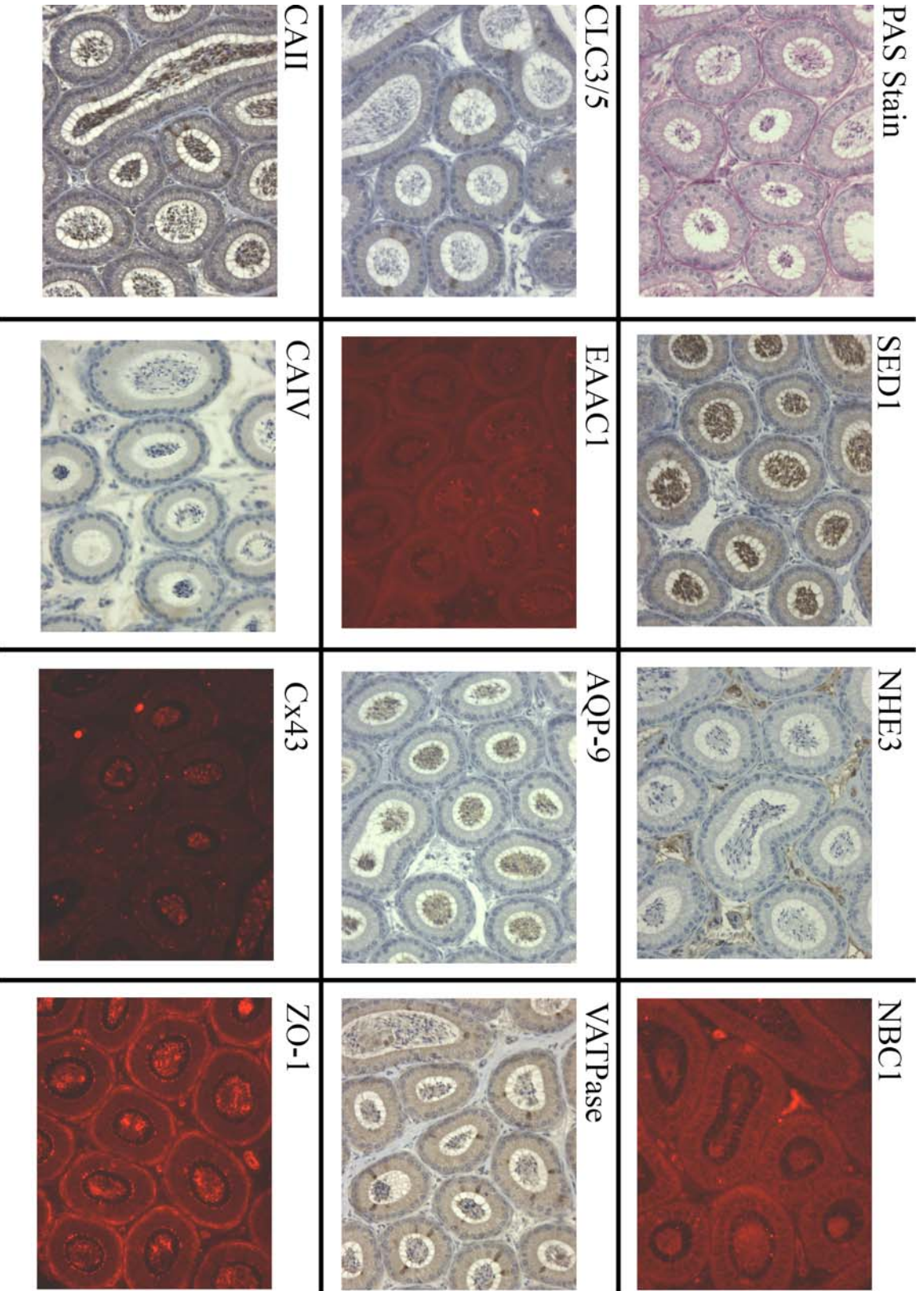


ZO-1

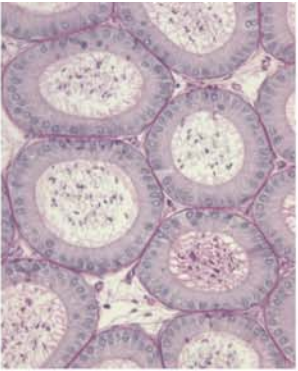
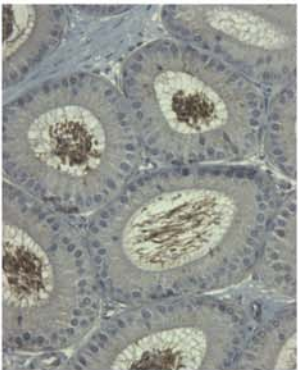
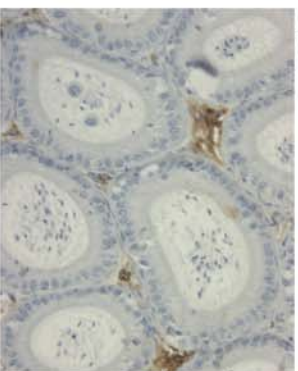
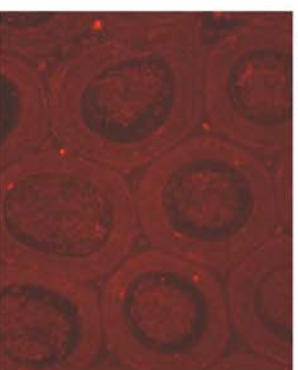
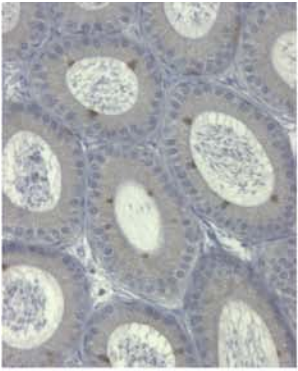
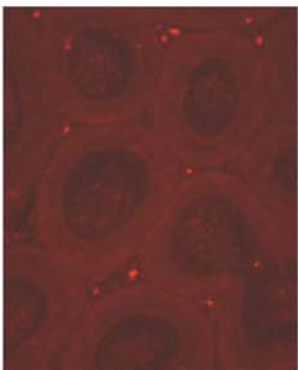
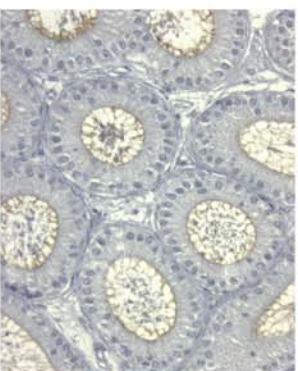
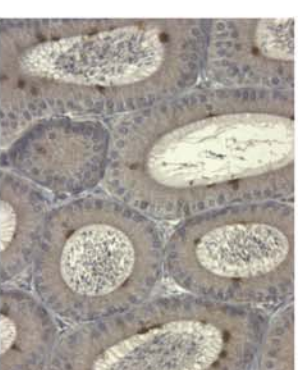
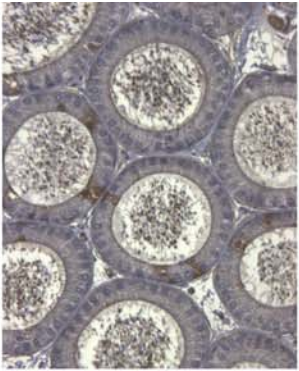
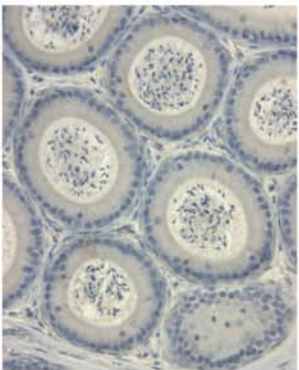
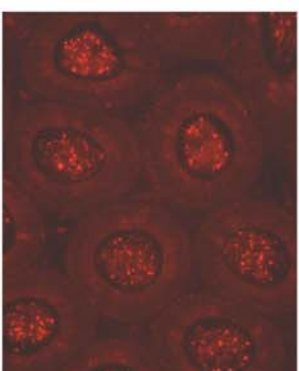
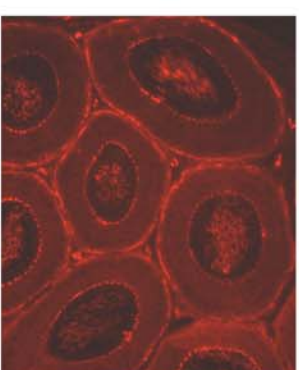


D Caput II

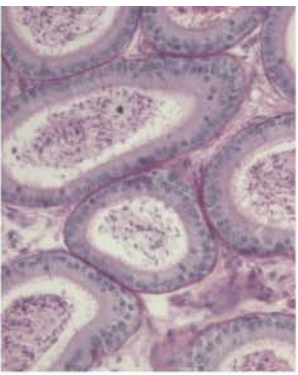
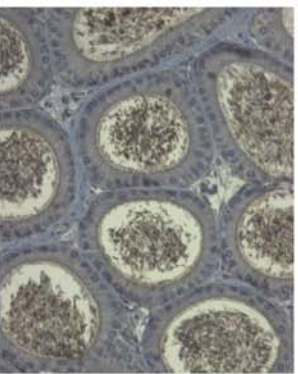
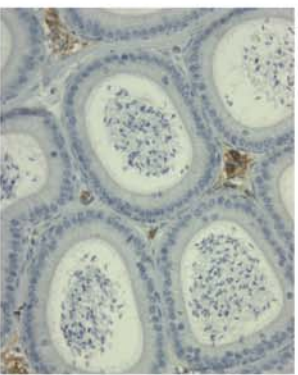
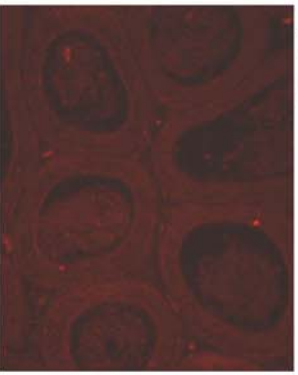
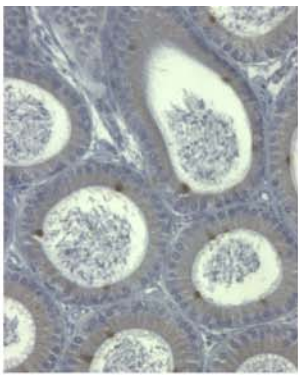
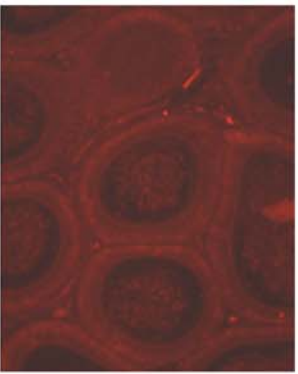
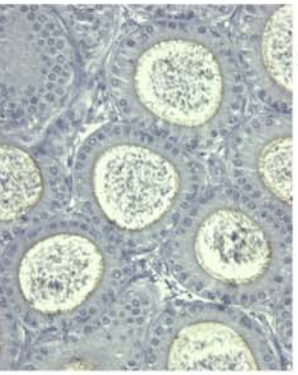
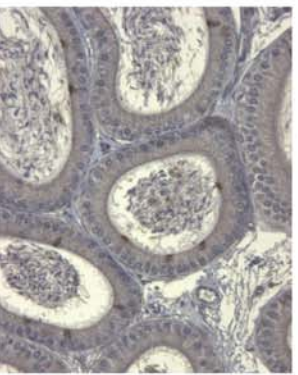
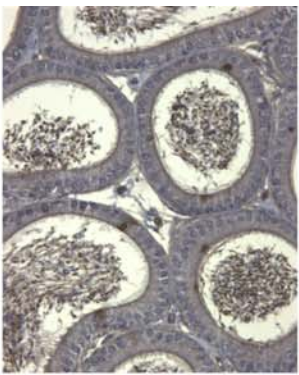
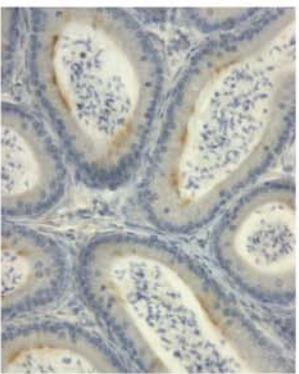
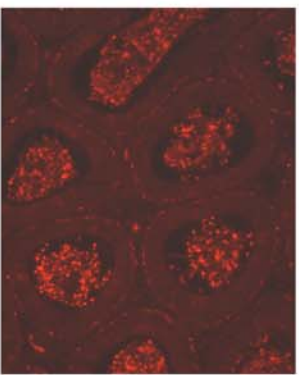
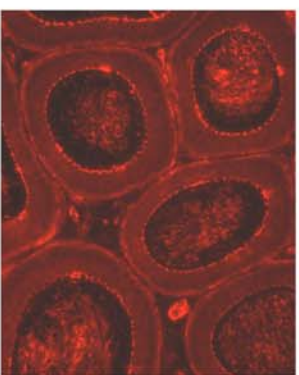
E Caput III



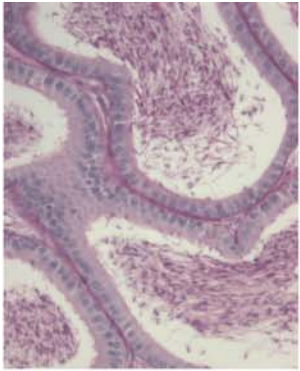
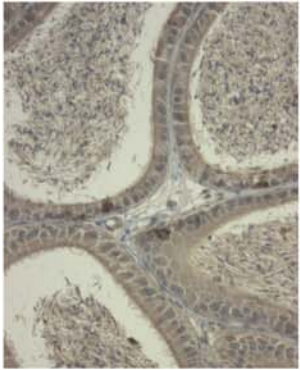
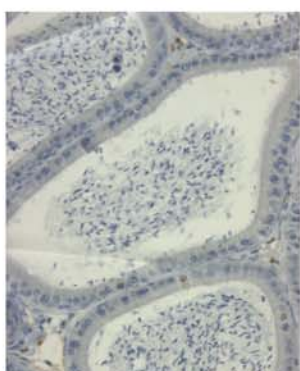
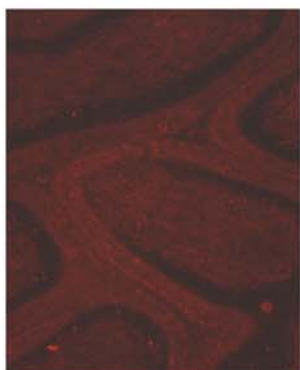
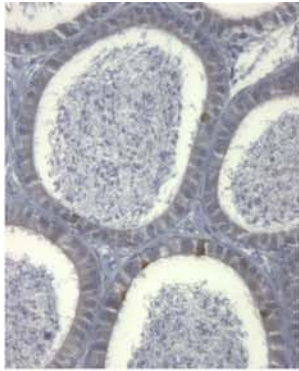
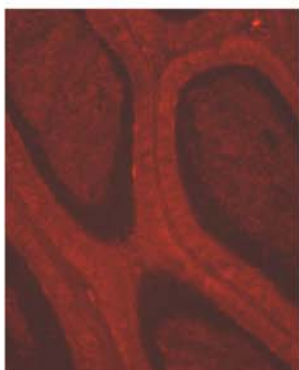
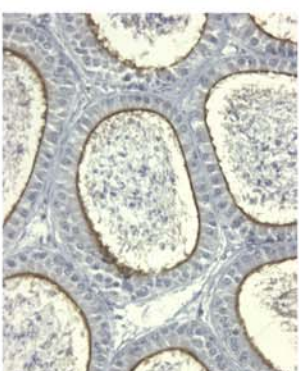
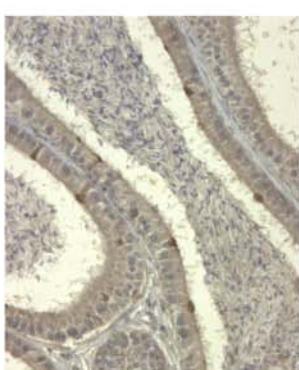
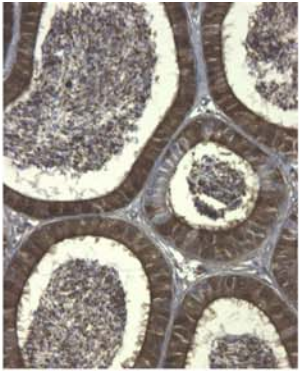
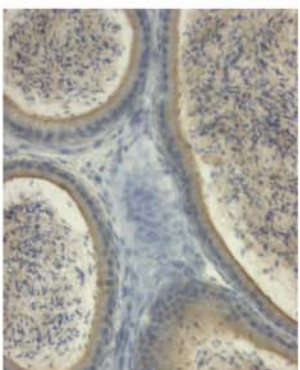
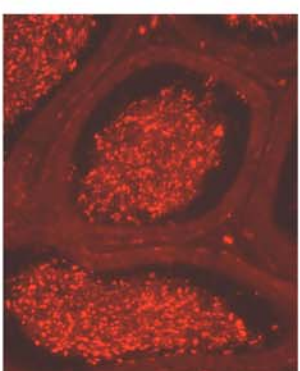
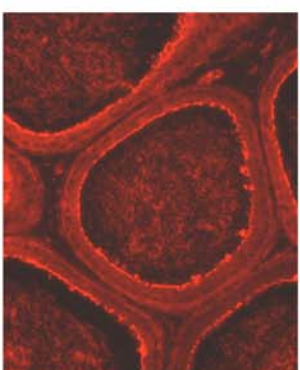
F Caput IV

 <p>PAS Stain</p>	 <p>SED1</p>	 <p>NHE3</p>	 <p>NBC1</p>
 <p>CLC3/5</p>	 <p>EAAC1</p>	 <p>AQP-9</p>	 <p>VATPase</p>
 <p>CAII</p>	 <p>CAIV</p>	 <p>Cx43</p>	 <p>ZO-1</p>

G Caput V

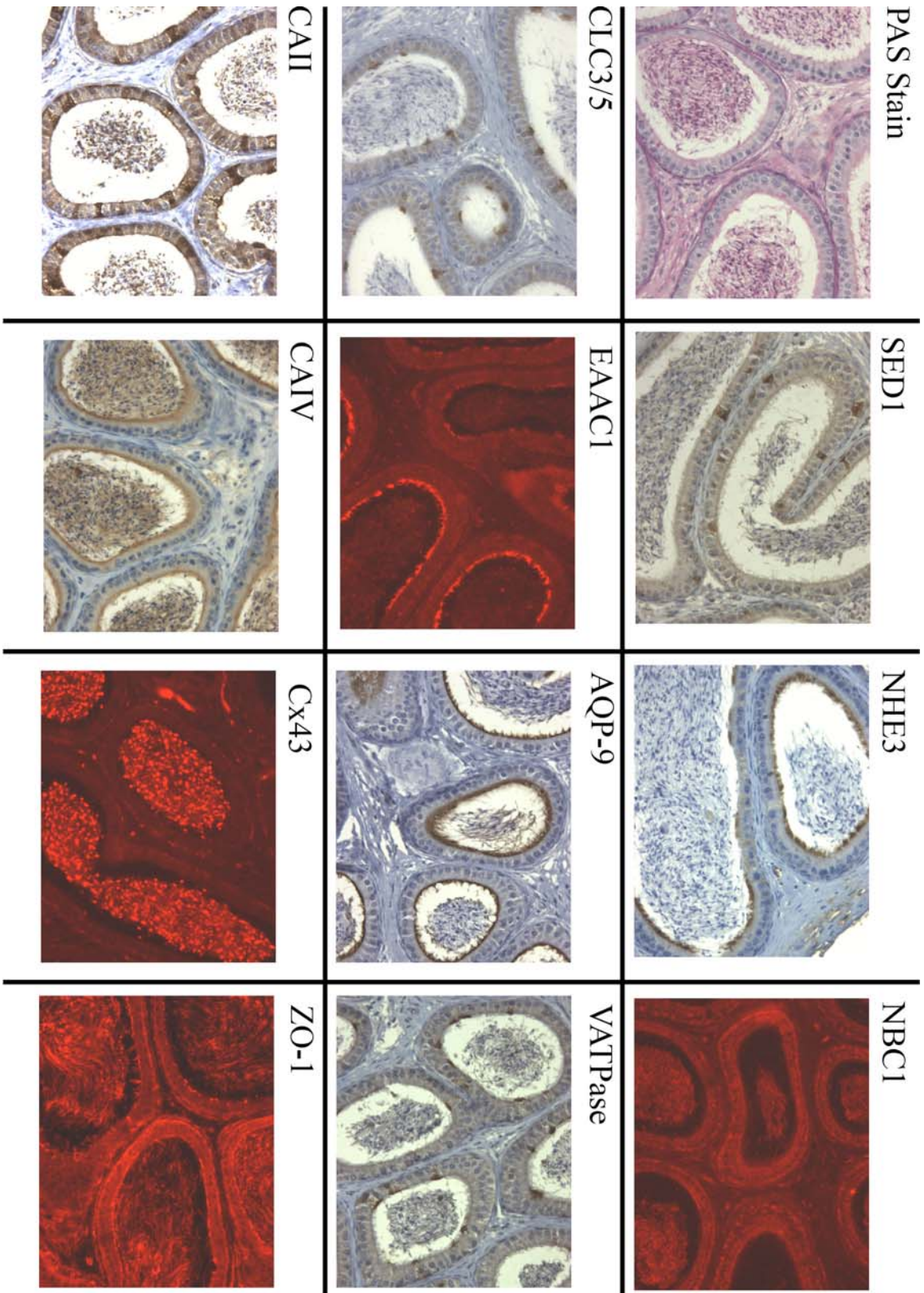
 <p>PAS Stain</p>	 <p>SEDI</p>	 <p>NHE3</p>	 <p>NBC1</p>
 <p>CLC3/5</p>	 <p>EAAC1</p>	 <p>AQP-9</p>	 <p>VATPase</p>
 <p>CAII</p>	 <p>CAIV</p>	 <p>Cx43</p>	 <p>ZO-1</p>

H Corpus

 <p>PAS Stain</p>	 <p>SED1</p>	 <p>NHE3</p>	 <p>NBC1</p>
 <p>CLC3/5</p>	 <p>EAAC1</p>	 <p>AQP-9</p>	 <p>VATPase</p>
 <p>CAII</p>	 <p>CAIV</p>	 <p>Cx43</p>	 <p>ZO-1</p>

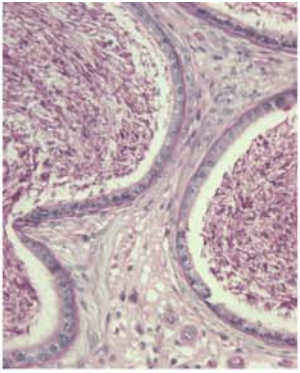
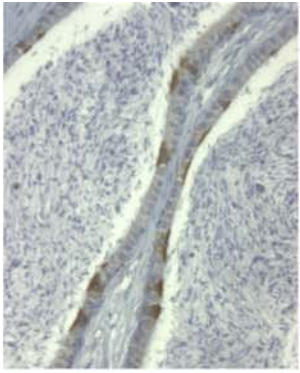
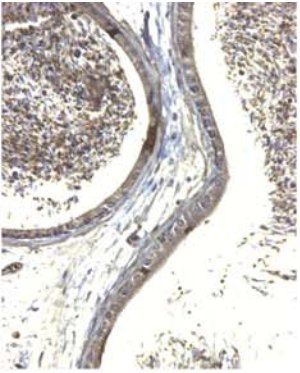
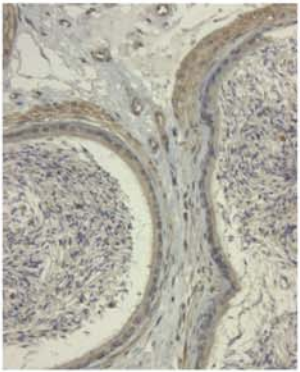
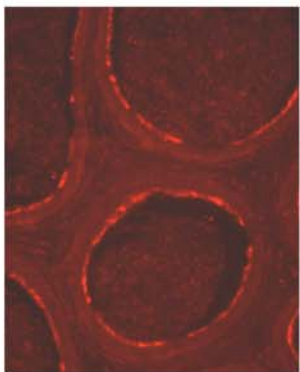
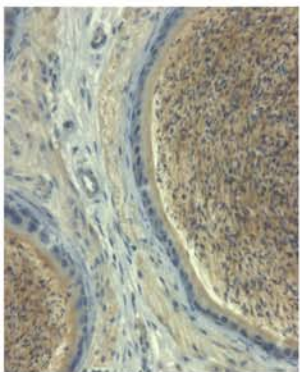
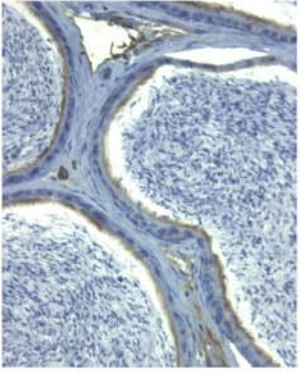
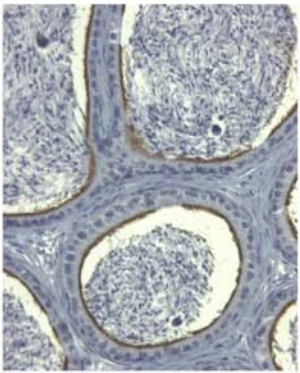
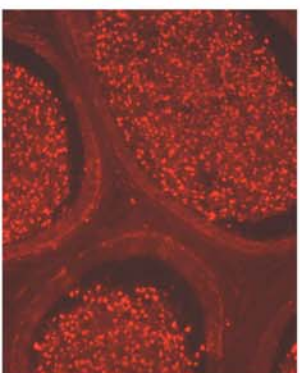
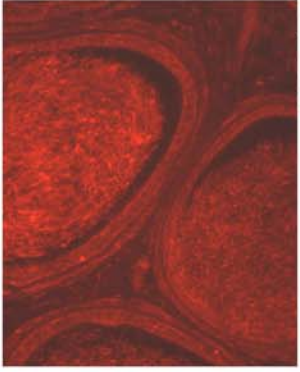
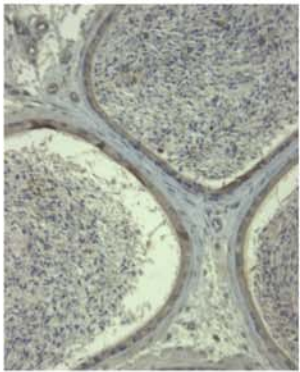
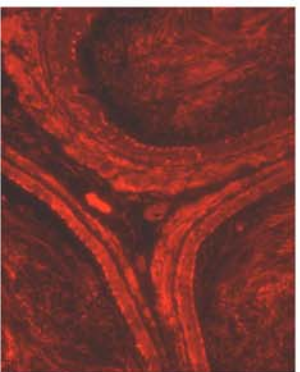
CORPUS

I Corpus-Cauda transition



CORPUS/CAUDA transition

J Cauda

 <p>PAS Stain</p>	 <p>CLC3/5</p>	 <p>CAII</p>
 <p>SEDI</p>	 <p>EAAC1</p>	 <p>CAIV</p>
 <p>NHE3</p>	 <p>AQP-9</p>	 <p>Cx43</p>
 <p>NBC1</p>	 <p>VATPase</p>	 <p>ZO-1</p>

CAUDA

epididymosomes, which are thought to play a critical role in the transfer of membrane-associated proteins and lipids on and/or off of sperm during transient contact within the lumen (Gatti et al., 2005; Hermo and Jacks, 2002; Rejraji et al., 2006; Thimon et al., 2008). Proteomic analysis confirms that epididymosomes also contain carbonic anhydrase and VAMPase that may also contribute to modification of the luminal fluid (Gatti et al., 2005; Thimon et al., 2008). Expression of SED1 increases the frequency and activity of exosomes in certain cell types, possibly by influencing the ability of host cells to produce and/or secrete microvesicles (Morelli et al., 2004; Oshima et al., 2002). We therefore determined if SED1 is associated with mouse epididymosomes. Luminal fluid was isolated from the caput and cauda regions, and ultracentrifugation results in an insoluble, transparent-yellow membrane fraction similar to that described by others (Gatti et al., 2005). Proteins associated with the vesicle fraction were separated by SDS-PAGE and immunoblotted for SED1. Consistent with a proteomic analysis reporting SED1 is a component of ram epididymosomes, the vesicle fractions of both caput and cauda regions are immunoreactive for SED1 suggesting it is also associated with mouse epididymosomes (data not shown) (Gatti et al., 2005).

To confirm that SED1 is associated with vesicles and not simply fragmented membranes created during the isolation protocol, fluid was collected from wildtype and SED1-null caput regions and loaded onto a continuous 15-45% sucrose gradient. Fractions were collected, and migration of unknown proteins and SED1 were monitored by silver stain and western blot. The sucrose gradient resolves a broad size (mass) spectrum of vesicles, ranging from small vesicles to organelles such as endosomes.

Silver staining reveals that the overall protein profile changes along the gradient (data not shown), and immunoblotting indicates SED1 is concentrated in gradient fractions known to contain small vesicles, and to a lesser extent with larger membranes, including plasma membrane fragments and endosomes (Fig. 5-6) (Clift-O'Grady et al., 1998). This experiment was repeated using a continuous 5-25% glycerol gradient, which offers a platform for higher resolution of the small vesicle population. Immunoblotting reveals a peak of SED1 activity across several fractions in the center of the gradient (Fig. 5-6), which are of similar size to 30-60 nm PC12 synaptic vesicles (Clift-O'Grady et al., 1998; Clift-O'Grady et al., 1990). In agreement with these data, mouse epididymosomes have been estimated to range in size from 20-200 nm (Rejraji et al., 2006). The distribution of SED1 across both sucrose and glycerol gradients was highly reproducible, and only background immunoreactivity was detected in SED1-null preparations.

We next investigated the presence of 30-60 nm epididymosomes in SED1-deficient fluid. Using wildtype material, Cx43 was identified as a component of epididymosomes that migrated coincident with SED1, making it a useful reagent for tracking 30-60 nm vesicles in SED1-deficient fluid. Luminal fluid was collected from wildtype and SED1-null epididymides, and resolved on glycerol gradients in parallel. Immunoblotting wildtype and SED1-null gradient fractions for Cx43 reveals that both genotypes feature similar 30-60 nm vesicle populations (Fig 5-6). It is not clear if small variations in the profile of Cx43 between wildtype and SED1-null blots are the result of minor variation in the preparations, or physiological relevant differences. Nonetheless, the loss of SED1 does not prevent production or secretion of all 30-60 nm vesicles. At

Figure 5-6: SED1 is associated with 30-60 nm epididymosomes. Mouse epididymosomes were purified from luminal fluid by sucrose and glycerol velocity gradients, and fractions immunoprobed for SED1 or Cx43. When resolved by sucrose gradient centrifugation, SED1 is found in fractions that contain small secretory-like vesicles (#11+) as well as larger endosome-like vesicles (#5-7). Soluble material remains at the gradient top (#17-18). Likewise, when the same material is resolved on glycerol gradients, SED1 partitions to fractions containing 30-60 nm vesicles (#7-11). Non-specific immunoreactivity is present in soluble material at the top of both wildtype and SED1-null gradients. Cx43 is found coincident with SED1 in wildtype material, and equivalent fractions containing SED1-deficient material also labels with Cx43, suggesting SED1-null luminal fluid contains 30-60 nm epididymosomes.

this time however, it is not apparent how epididymosomes contribute to phenotypes displayed by the SED1-null, and a more comprehensive proteomic approach is required to investigate the complete composition and function of wildtype and SED1-null epididymosomes.

5.3 Discussion

We have reported in Chapter 3-5 that SED1 is highly expressed in the initial segment of the epididymis, where it localizes to linear arrays on the lateral borders of principal epithelial cells. Data presented in Chapter 4 indicate that extracellular SED1 increases epididymal cell attachment by serving as a ligand for α_v integrins expressed by these same cells, and SED1-null cells are deficient in adhesion suggesting this interaction may be protective against sperm granulomas in SED1-null mice. Surprisingly, granulomas occur most frequently in the distal cauda of the epididymis disconnected from the region of highest SED1 localization, which may indicate that simple adhesion is not sufficient to explain this pathology.

In the efferent ducts and the initial segment of the epididymis, more than 50% of the testicular fluid is reabsorbed and a process of luminal acidification begins (Levine and Marsh, 1971). Sub-fertile genetic models including the ER knockout and *c-ros* knockout suggest these processes are indispensable in sperm maturation and epididymal integrity, however secondary consequences in these animals, including spermatic granulomas and abnormal sperm response to osmolytes suggest the pathways disrupted in these animals may also have long-range effects (Hess et al., 2000; Yeung et al., 2004a;

Zhou et al., 2001). In this report, we have continued our analysis of SED1 function in the epididymis by investigating possible SED1-dependent functions in the proximal epididymis that may have long-range effects on distal tissue, such as protection against spermatocytic granulomas.

SED1 is most prominently expressed in principal cells of the initial segment, as well as the clear cells and the basal cells of the cauda. Although these are very different cell types with unique functions, all three are known to contribute in some capacity to regulation of the luminal milieu: initial segment principal epithelia and basal cells use diverse pathways to regulate fluid reabsorption, while the same principal cells and clear cells acidify the lumen through mechanisms involving proton secretion (Robaire and Hinton, 2002). Therefore, we considered the possibility that the luminal fluid of the SED1 knockout was altered in the absence of SED1. Ex vivo analysis of luminal pH reveals SED1-null fluid is alkaline relative to wildtype, suggesting that these animals fail to properly acidify the epididymal lumen. Importantly, the absolute difference in pH between wildtype and SED1-null is similar to that reported using the same assay to assess luminal pH in the *c-ros* knockout animals, which are deficient in pH and luminal osmolyte regulation (Yeung et al., 2004a; Yeung et al., 2004b).

During this analysis, we also identified a number of characteristics of SED1-null tissue that are consistent with dysregulation of the epididymal fluid. Narrow cells exhibit sheared luminal projections, the caput contains greatly increased endocytic vesicles, clear cells tend to localize V-ATPase more apically than wildtype, the epithelium is highly vacuolated, and submersion-fixed tissue contains a high incidence of dilated

mitochondria. Due to the high frequency of sperm granulomas, it is difficult to know for certain if all of these characteristics are the result of the underlying SED1-deficiency, or excess fluid created by a lesion-obstructed tubule. It is important to note, however, that *ex vivo* pH measurements were consistently below wildtype regardless of the presence or absence of a lesion. Similarly, the increased incidence of endocytic vesicles occurred independent of granulomas, and it has been reported that the vacuolated epithelium precedes granuloma formation (Itoh et al., 1999). Nonetheless, similar observations to these have been reported by others in the context of dysfunctional fluid transport and alkaline luminal pH, and collectively support our assertion that the SED1-null epididymis is defective in fluid regulation.

We next considered how SED1 might be involved in processes or pathways that regulate luminal fluid dynamics. SED1 is a bi-motif protein that orchestrates a number of extracellular interactions. In a number of well-defined instances, including phagocyte engulfment of apoptotic cells, cell-cell adhesion, and anti-apoptotic pathways during vasculogenesis, the RGD-motif-containing EGF-2 domain serves as a ligand for integrins, while in some cases the C-terminal domains also bind exposed phosphatidyl serine-rich membranes, or carbohydrates (Ensslin and Shur, 2007; Hanayama et al., 2004; Silvestre et al., 2005). However, intracellular functions of SED1 remain more ambiguous. SED1 is known to be secreted as a component of exosome-like microvesicles from a variety of cell types, and when transfected with SED1 constructs, some cell lines increase microvesicle secretion (Oshima et al., 2002). Although the precise mechanisms are unclear, data suggest that SED1 localizes to the apical membrane

of these cells in a C-terminal domain-dependent manner, where it may facilitate vesicle secretion.

In other epididymal models, including the ER and *c-ros* knockouts, phenotypes are in-part facilitated by loss of proper expression and/or localization of critical transmembrane proteins. Therefore, we considered the possibility that SED1 may influence the trafficking, localization, or recycling of cytoplasmic and transmembrane proteins that drive fluid reabsorption and acidification. Semi-quantitative western blots indicate that wildtype and SED1-nulls initial segment tissue contain equivalent levels of numerous ion exchangers, membrane pumps, water channels, and enzymes important in fluid modification, and immunohistochemistry confirms that these proteins localize similarly to predictable domains in both genotypes.

Alternatively, the epididymal epithelium is also known to secrete epididymosome microvesicles into the lumen through a process of membrane shedding known as apocrine secretion (Gatti et al., 2005; Hermo and Jacks, 2002; Rejraji et al., 2006). SED1 is known to be associated with epididymosomes in at least one other species, and we confirmed it is also a component of mouse derived-microvesicles (Gatti et al., 2005). Data from this emerging field suggests that secretion of epididymosomes and their interaction with sperm may be essential to sperm maturation and perhaps the luminal milieu as well. SED1-positive epididymosomes populate a vesicle fraction of 30-60 nm, which also contain Cx43-positive vesicles. Parallel experiments confirm that luminal fluid lacking SED1 also contains Cx43-positive 30-60 nm vesicles, suggesting that loss of the SED1 does not completely inhibit the secretion of membrane-bound microvesicles.

Nevertheless, additional experiments are required to investigate the role SED1 may play in effecting the composition and/or function of these vesicles.

Chapter 6: Conclusions and Future Directions

All data and the figure in Chapter 6 are the work of Adam S. Raymond.

6.1 Conclusions

6.1.1 Overview

A large number of epididymally-secreted proteins have been characterized for their role in sperm maturation. One of these is SED1, also known as MFG-E8, lactadherin, among other names (Andersen et al., 1997; Couto et al., 1996; Ensslin et al., 1998; Larocca et al., 1991; Ogura et al., 1996; Stubbs et al., 1990). The loss of SED1 from the epididymal epithelium, where it is normally secreted and associates with the sperm membrane, produced unexpected epididymal phenotypes. Most notable among these are detached epithelia and spermatic granulomas, which result from the exposure of sperm-associated antigens and a consequent immune response. The underlying dysfunction appears to be intrinsic to the epididymis as the associated upstream regions of the reproductive tract, including the efferent ducts and testis, are morphologically normal and devoid of notable pathologies. Surprisingly, the SED1-null epididymis also develops and differentiates normally. In this regard, SED1-null epididymides contain all ten anatomical sub-regions. The initial segment differentiates into a tall columnar epithelium exhibiting similar height and containing stereocilia of similar length, to wildtype. Immunolocalization of Syntaxin-3 and ZO-1 suggest the SED1-null forms a polarized secretory epithelium and a functional blood-epididymal barrier. Together these data are suggestive of a tissue-intrinsic role in the epididymis, and its loss in otherwise normal tissue results in adult-onset granuloma formation.

6.1.2 Maintenance of the epididymal epithelium

The adhesive nature of SED1 and the loss of the epithelial adhesion in the SED1-null spermatid granulomas immediately suggest a role for SED1 in epididymal adhesion. Using perfusion-based fixative procedures, SED1 is found localized in the basolateral domains of epididymal epithelial cells *in vivo*, and similarly, SED1 is secreted both apically and basally from polarized epididymal cells *in vitro*. The basolateral distribution of SED1 suggests that it may play a role in epididymal cell adhesion. Quantitative *in vitro* assays demonstrate that SED1 supports epididymal cell adhesion via RGD binding to α_V integrin receptors on epididymal epithelial cells. In support of these results, epididymal cells from SED1 -null males show reduced adhesion *in vitro*, a phenotype that can be rescued with exogenous SED1. These results suggest that SED1 may facilitate epididymal cell adhesion, and that its loss leads to breakdown of the epididymal epithelium and consequent development of spermatid granulomas.

6.1.3 SED1 function in regulation of luminal fluid of the epididymis

The location of the SED1- α_V interaction, however, is presumably restricted to the initial segment, while sperm granulomas occur most frequently in the distal cauda. Other epididymal models feature molecular and cellular dysfunctions that are also dissociated from the location of epididymal lesions, so we therefore investigated SED1-dependent mechanisms that may serve a long-range function (Hess et al., 2000; Zhou et al., 2001). Similar to the *c-ros* knockout, the SED1-null is defective in luminal acidification, suggesting a possible role for the protein in regulation of the luminal fluid in the

epididymis (Yeung et al., 2004b). In fact, the SED1-null epididymis also exhibits a number of morphological characteristics of a hypo-osmotic environment including apical distribution of VATPase, fragile mitochondria, and compensatory endocytosis. SED1 is known to affect vesicle secretion, and we hypothesized that loss of the protein in SED1-deficient animals may effect the targeting of various other factors important in regulation of luminal fluid (Oshima et al., 2002). Surprisingly, a panel of known acid/base transporters and enzymes are expressed and localized normally in the SED1-null.

It was also determined that SED1 is secreted from the caput epididymis in association with microvesicles known as epididymosomes, of approximately 30-60 nm. These vesicles are thought play a critical function in sperm maturation, and they are known to also carry acid/base transporters, including VATPase and carbonic anhydrase whose functions are not clear in this context (Gatti et al., 2005; Thimon et al., 2008). Our data confirm that SED1-nulls secrete 30-60 nm vesicles as do wildtype; however, it is possible that loss of SED1 affects the composition and/or function of these microvesicles in the epididymal lumen,

6.1.4 Conclusions

The findings presented here suggest that SED1 is secreted from the initial segment and some regions of the caput epididymis, where it serves as a ligand for epithelial adhesion and as a factor in sperm maturation. Although provocative in many respects, the data do not indicate an obvious SED1-dependent pathway that would lead to spermatoc granulosas or an alkaline luminal pH in SED1-deficient animals. One

possible model is that SED1 binding to α_v integrins during epididymal cell adhesion elicits integrin-dependent regulatory pathways. A similar interaction featuring the SED1 homologue Del1 has been found to activate transcription factors and subsequent protein synthesis in a model for vascular recovery following ischemia (Ho et al., 2004). Alternatively, the C-terminal domains of SED1 may affect the transport or targeting of intracellular vesicles to various intracellular domains, or even facilitate the secretion of epididymal microvesicles. At this time, however, the specific proteins trafficked with SED1 and their function in modification of luminal fluid, and/or protection against sperm granulomas remains illusive.

6.2 Future directions

Among other interesting avenues, such as an analysis of SED1- α_v -dependent signaling pathways in maintenance of the epididymal epithelium, future directions should include a proteomic profiling of wildtype and SED1-null epididymosomes. Using methods presented in Chapter 5, highly purified SED1-positive vesicles can be isolated for mass spectroscopy analysis. First, whole epididymal fluid is separated on a 5-25% continuous glycerol gradient. Next, SED1-positive fractions from the center of the gradient (fractions #7-11) are collected, combined, and supplemented with sucrose to 45%. The material is applied to the bottom of a 45%, 30%, 5% (sucrose) discontinuous density equilibrium gradient. Each fraction is collected and precipitated free from sucrose. Resuspended samples are resolved by SDS-PAGE and immunoprobed for SED1; stripped and reprobed for Cx43 (Fig. 6-1A). Probing for SED1 reveals a classical

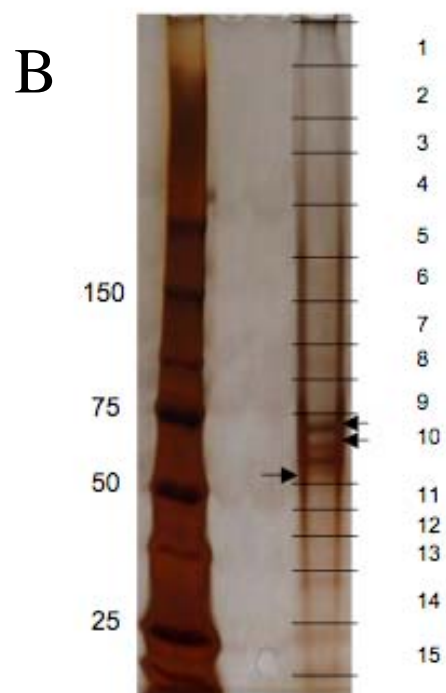
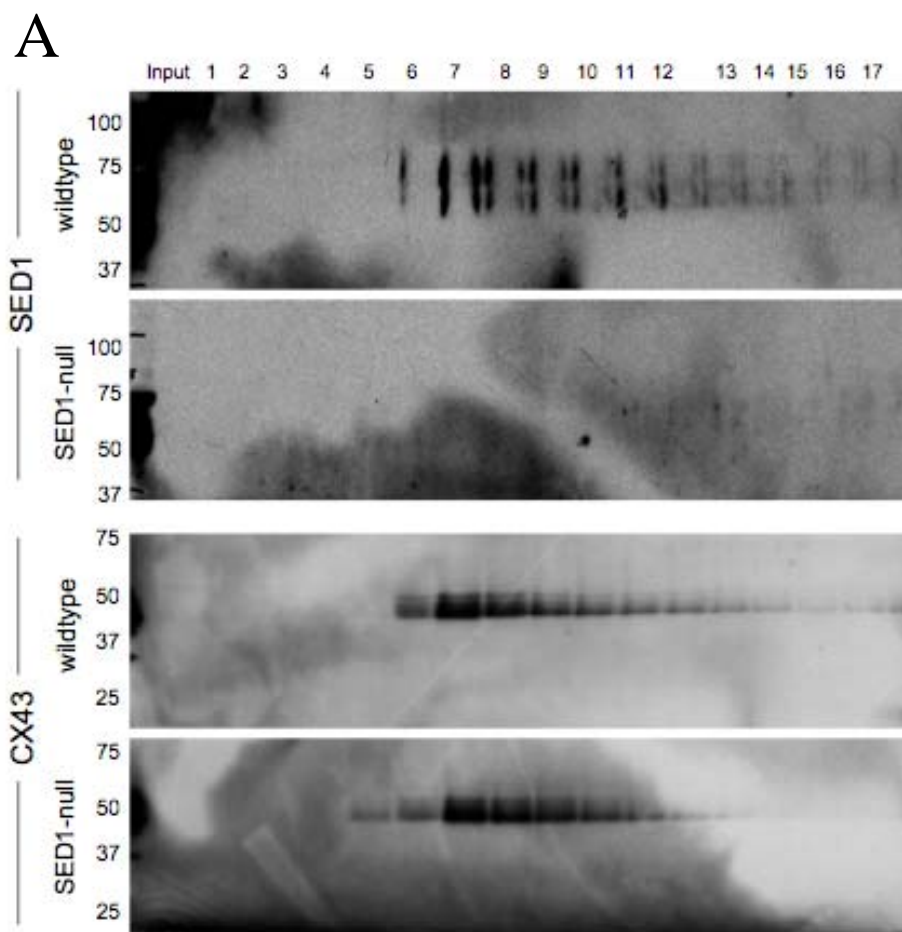
tear-drop distribution along the gradient, concentrating near 25% sucrose (fractions 7-9) and trailing off in higher percentage fractions. Not surprisingly, the distribution of Cx43 is nearly identical, and can be used to track 30-60 nm vesicles isolated from SED-deficient fluid.

Subsequently, fractions from multiple sucrose gradients were analyzed for SED1 reactivity, and three fractions containing the peak of SED1 reactivity were combined, precipitated, resolved by SDS-PAGE, and stained with silver. Several bands were evident, and the Emory University Microsequencing Core identified the presence of SED1 from the region between 50-65 kDa. This result confirms the feasibility of identifying other protein components of 30-60 nm epididymosomes by mass spectroscopic analysis of other regions of the gel (Fig. 6-B.).

6.3 Use of SED1 in reproductive interventions

SED1 plays multiple roles during sperm maturation and fertilization, and therefore opens the possibility of using SED1 antagonists as potential contraceptive agents. The timing and delivery of this therapeutic should be carefully considered, however, as one might expect that antagonists administered to men would target not only the surface of sperm, but also the ligand source for α_v integrins and other potential epididymal-intrinsic functions of SED1, thereby inducing granuloma formation. Granulomas are a common side-affect of vasectomy and although they are not harmful, they are often inconsistent with reversible contraception. Alternatively, since SED1 is added to mature sperm post-meiotically, it may be possible to enhance the fertilizing

Figure 6-1: SED1-positive epididymosomes can be purified and analyzed by mass spectroscopy. A) Wildtype and SED1-null luminal fluid was collected and resolved on a 5-25% glycerol gradient (not shown). SED1-positive fractions #7-11 were collected, pooled, and applied to a 45%, 30%, 5% (sucrose) discontinuous density equilibrium gradient in which 30-60 nm vesicles focus, free from soluble contaminants. SED1-positive vesicles are enriched in fractions #7-9, which are also Cx43 positive. As expected, SED1-null material is devoid of SED1 immunoreactivity, but exhibits a similar profile of Cx43-positive fractions. In subsequent experiments, fractions #7-9 from multiple gradients were pool, precipitated, and resolved by SDS-PAGE. B) Silver-stained gel, divided into arbitrary segments, shows several bands in region 10 (50-56 kDa range). SED1 was identified by mass spectroscopy among the proteins extracted from 3 bands (arrows) in this region.



potential of sperm with low fertilizing efficacy by the application of SED1 during intercourse. Additional investigations into the mechanisms of SED1-dependent binding may offer new insights that can be used to develop recombinant or synthetic compounds with even higher efficacy of action. Furthermore, if loss of SED1 does lead to altered composition and/or function of epididymosomes, additional avenue for influencing male fertility may open.

Chapter 7: References

Chapter 7: References

Abe, K., Takano, H. and Ito, T. (1983). Ultrastructure of the mouse epididymal duct with special reference to the regional differences of the principal cells. *Archivum histologicum Japonicum. Nippon soshikigaku kiroku* **46**, 51-68.

Abou-Haèila, A. and Fain-Maurel, M. A. (1984). Regional differences of the proximal part of mouse epididymis: morphological and histochemical characterization. *The Anatomical record* **209**, 197-208.

Acott, T. S. and Carr, D. W. (1984). Inhibition of bovine spermatozoa by caudal epididymal fluid: II. Interaction of pH and a quiescence factor. *Biol Reprod* **30**, 926-35.

Ait-Oufella, H., Kinugawa, K., Zoll, J., Simon, T., Boddaert, J., Heeneman, S., Blanc-Brude, O., Barateau, V., Potteaux, S., Merval, R. et al. (2007). Lactadherin deficiency leads to apoptotic cell accumulation and accelerated atherosclerosis in mice. *Circulation* **115**, 2168-77.

Akakura, S., Singh, S., Spataro, M., Akakura, R., Kim, J. I., Albert, M. L. and Birge, R. B. (2004). The opsonin MFG-E8 is a ligand for the alphavbeta5 integrin and triggers DOCK180-dependent Rac1 activation for the phagocytosis of apoptotic cells. *Exp Cell Res* **292**, 403-16.

Andersen, M. H., Berglund, L., Rasmussen, J. T. and Petersen, T. E. (1997). Bovine PAS-6/7 binds alpha v beta 5 integrins and anionic phospholipids through two domains. *Biochemistry* **36**, 5441-6.

Andersen, M. H., Graversen, H., Fedosov, S. N., Petersen, T. E. and Rasmussen, J. T. (2000). Functional analyses of two cellular binding domains of bovine lactadherin. *Biochemistry* **39**, 6200-6.

Aoka, Y., Johnson, F. L., Penta, K., Hirata Ki, K., Hidai, C., Schatzman, R., Varner, J. A. and Quertermous, T. (2002). The embryonic angiogenic factor Dell accelerates tumor growth by enhancing vascular formation. *Microvasc Res* **64**, 148-61.

Aoki, M., Kanamori, M., Ohmori, K., Takaishi, M., Huh, N. H., Nogami, S. and Kimura, T. (2005). Expression of developmentally regulated endothelial cell locus 1 was induced by tumor-derived factors including VEGF. *Biochem Biophys Res Commun* **333**, 990-5.

Aoki, N., Jin-no, S., Nakagawa, Y., Asai, N., Arakawa, E., Tamura, N., Tamura, T. and Matsuda, T. (2007). Identification and characterization of microvesicles secreted by 3T3-L1 adipocytes: redox- and hormone-dependent induction of milk fat globule-epidermal growth factor 8-associated microvesicles. *Endocrinology* **148**, 3850-62.

Asano, K., Miwa, M., Miwa, K., Hanayama, R., Nagase, H., Nagata, S. and Tanaka, M. (2004). Masking of phosphatidylserine inhibits apoptotic cell engulfment and induces autoantibody production in mice. *J Exp Med* **200**, 459-67.

Atabai, K., Fernandez, R., Huang, X., Ueki, I., Kline, A., Li, Y., Sadatmansoori, S., Smith-Steinhart, C., Zhu, W., Pytela, R. et al. (2005). Mfge8 is critical for mammary gland remodeling during involution. *Molecular biology of the cell* **16**, 5528-37.

Avram, C. E. and Cooper, T. G. (2004). Development of the caput epididymidis studied by expressed proteins (a glutamate transporter, a lipocalin and beta-galactosidase) in the c-ros knockout and wild-type mice with prepubertally ligated efferent ducts. *Cell Tissue Res* **317**, 23-34.

Badran, H. H. and Hermo, L. S. (2002). Expression and regulation of aquaporins 1, 8, and 9 in the testis, efferent ducts, and epididymis of adult rats and during postnatal development. *J Androl* **23**, 358-73.

Bagnis, C., Marsolais, M., Biemesderfer, D., Laprade, R. and Breton, S. (2001). Na⁺/H⁺-exchange activity and immunolocalization of NHE3 in rat epididymis. *Am J Physiol Renal Physiol* **280**, F426-36.

Balzar, M., Briaire-de Bruijn, I. H., Rees-Bakker, H. A., Prins, F. A., Helfrich, W., de Leij, L., Riethmuller, G., Alberti, S., Warnaar, S. O., Fleuren, G. J. et al. (2001). Epidermal growth factor-like repeats mediate lateral and reciprocal interactions of Ep-CAM molecules in homophilic adhesions. *Mol Cell Biol* **21**, 2570-80.

Boddaert, J., Kinugawa, K., Lambert, J. C., Boukhtouche, F., Zoll, J., Merval, R., Blanc-Brude, O., Mann, D., Berr, C., Vilar, J. et al. (2007). Evidence of a role for lactadherin in Alzheimer's disease. *Am J Pathol* **170**, 921-9.

Breton, S., Smith, P. J., Lui, B. and Brown, D. (1996). Acidification of the male reproductive tract by a proton pumping (H⁺)-ATPase. *Nature medicine* **2**, 470-2.

Breton, S., Tyszkowski, R., Sabolic, I. and Brown, D. (1999). Postnatal development of H⁺ ATPase (proton-pump)-rich cells in rat epididymis. *Histochem Cell Biol* **111**, 97-105.

Brown, D., Lui, B., Gluck, S. and Sabolic, I. (1992). A plasma membrane proton ATPase in specialized cells of rat epididymis. *Am J Physiol* **263**, C913-6.

Bu, H. F., Zuo, X. L., Wang, X., Ensslin, M. A., Koti, V., Hsueh, W., Raymond, A. S., Shur, B. D. and Tan, X. D. (2007). Milk fat globule-EGF factor 8/lactadherin plays a crucial role in maintenance and repair of murine intestinal epithelium. *The Journal of clinical investigation* **117**, 3673-83.

Burgess, B. L., Abrams, T. A., Nagata, S. and Hall, M. O. (2006). MFG-E8 in the retina and retinal pigment epithelium of rat and mouse. *Mol Vis* **12**, 1437-47.

Byers, S. W., Citi, S., Anderson, J. M. and Hoxter, B. (1992). Polarized functions and permeability properties of rat epididymal epithelial cells in vitro. *Journal of reproduction and fertility* **95**, 385-96.

Carballada, R. and Saling, P. M. (1997). Regulation of mouse epididymal epithelium in vitro by androgens, temperature and fibroblasts. *Journal of reproduction and fertility* **110**, 171-81.

Carr, D. W., Usselman, M. C. and Acott, T. S. (1985). Effects of pH, lactate, and viscoelastic drag on sperm motility: a species comparison. *Biol Reprod* **33**, 588-95.

Cheung, K. H., Leung, G. P., Leung, M. C., Shum, W. W., Zhou, W. L. and Wong, P. Y. (2005). Cell-cell interaction underlies formation of fluid in the male reproductive tract of the rat. *J Gen Physiol* **125**, 443-54.

Chew, S. B., Leung, G. P., Leung, P. Y., Tse, C. M. and Wong, P. Y. (2000). Polarized distribution of NHE1 and NHE2 in the rat epididymis. *Biol Reprod* **62**, 755-8.

Choi, E. Y., Chavakis, E., Czabanka, M. A., Langer, H. F., Fraemohs, L., Economopoulou, M., Kundu, R. K., Orlandi, A., Zheng, Y. Y., Prieto, D. A. et al. (2008). Del-1, an endogenous leukocyte-endothelial adhesion inhibitor, limits inflammatory cell recruitment. *Science* **322**, 1101-4.

Clift-O'Grady, L., Desnos, C., Lichtenstein, Y., Faundez, V., Horng, J. T. and Kelly, R. B. (1998). Reconstitution of synaptic vesicle biogenesis from PC12 cell membranes. *Methods* **16**, 150-9.

Clift-O'Grady, L., Linstedt, A. D., Lowe, A. W., Grote, E. and Kelly, R. B. (1990). Biogenesis of synaptic vesicle-like structures in a pheochromocytoma cell line PC-12. *J Cell Biol* **110**, 1693-703.

Cooper, T. G., Yeung, C. H. and Bergmann, M. (1988). Transcytosis in the epididymis studied by local arterial perfusion. *Cell and tissue research* **253**, 631-7.

Couto, J. R., Taylor, M. R., Godwin, S. G., Ceriani, R. L. and Peterson, J. A. (1996). Cloning and sequence analysis of human breast epithelial antigen BA46 reveals an RGD cell adhesion sequence presented on an epidermal growth factor-like domain. *DNA and cell biology* **15**, 281-6.

Cyr, D. G., Hermo, L., Egenberger, N., Mertineit, C., Trasler, J. M. and Laird, D. W. (1999). Cellular immunolocalization of occludin during embryonic and postnatal development of the mouse testis and epididymis. *Endocrinology* **140**, 3815-25.

Cyr, D. G., Hermo, L. and Laird, D. W. (1996). Immunocytochemical localization and regulation of connexin43 in the adult rat epididymis. *Endocrinology* **137**, 1474-84.

Denzer, K., Kleijmeer, M. J., Heijnen, H. F., Stoorvogel, W. and Geuze, H. J. (2000). Exosome: from internal vesicle of the multivesicular body to intercellular signaling device. *J Cell Sci* **113 Pt 19**, 3365-74.

Eliceiri, B. P. and Cheresh, D. A. (2000). Role of alpha v integrins during angiogenesis. *Cancer journal (Sudbury, Mass.)* **6**, S245-9.

Ensslin, M., Vogel, T., Calvete, J. J., Thole, H. H., Schmidtke, J., Matsuda, T. and Tøpfer-Petersen, E. (1998). Molecular cloning and characterization of P47, a novel boar sperm-associated zona pellucida-binding protein homologous to a family of mammalian secretory proteins. *Biology of reproduction* **58**, 1057-64.

Ensslin, M. A. and Shur, B. D. (2003). Identification of mouse sperm SED1, a bimotif EGF repeat and discoidin-domain protein involved in sperm-egg binding. *Cell* **114**, 405-17.

Ensslin, M. A. and Shur, B. D. (2007). The EGF repeat and discoidin domain protein, SED1/MFG-E8, is required for mammary gland branching morphogenesis. *Proceedings of the National Academy of Sciences of the United States of America* **104**, 2715-20.

Fadok, V. A. (1999). Clearance: the last and often forgotten stage of apoptosis. *J Mammary Gland Biol Neoplasia* **4**, 203-11.

Felding-Habermann, B. and Cheresh, D. A. (1993). Vitronectin and its receptors. *Current opinion in cell biology* **5**, 864-8.

Fens, M. H., Mastrobattista, E., de Graaff, A. M., Fleisch, F. M., Ultee, A., Rasmussen, J. T., Molema, G., Storm, G. and Schiffelers, R. M. (2008). Angiogenic

endothelium shows lactadherin-dependent phagocytosis of aged erythrocytes and apoptotic cells. *Blood* **111**, 4542-50.

Flickinger, C. J. (1981). Regional differences in synthesis, intracellular transport, and secretion of protein in the mouse epididymis. *Biology of reproduction* **25**, 871-83.

Flickinger, C. J., Howards, S. S. and Herr, J. C. (1995). Effects of vasectomy on the epididymis. *Microscopy research and technique* **30**, 82-100.

Fuentes-Prior, P., Fujikawa, K. and Pratt, K. P. (2002). New insights into binding interfaces of coagulation factors V and VIII and their homologues lessons from high resolution crystal structures. *Current protein & peptide science* **3**, 313-39.

Gatti, J. L., Metayer, S., Belghazi, M., Dacheux, F. and Dacheux, J. L. (2005). Identification, proteomic profiling, and origin of ram epididymal fluid exosome-like vesicles. *Biol Reprod* **72**, 1452-65.

Glover, T. D. and Nicander, L. (1971). Some aspects of structure and function in the mammalian epididymis. *J Reprod Fertil Suppl* **13**, Suppl 13:39-50.

Guermonez, P., Valladeau, J., Zitvogel, L., Thery, C. and Amigorena, S. (2002). Antigen presentation and T cell stimulation by dendritic cells. *Annu Rev Immunol* **20**, 621-67.

Hanayama, R., Tanaka, M., Miwa, K., Shinohara, A., Iwamatsu, A. and Nagata, S. (2002). Identification of a factor that links apoptotic cells to phagocytes. *Nature* **417**, 182-7.

Hanayama, R., Tanaka, M., Miyasaka, K., Aozasa, K., Koike, M., Uchiyama, Y. and Nagata, S. (2004). Autoimmune disease and impaired uptake of apoptotic cells in MFG-E8-deficient mice. *Science (New York, N.Y.)* **304**, 1147-50.

Hermo, L., Chong, D. L., Moffatt, P., Sly, W. S., Waheed, A. and Smith, C. E. (2005). Region- and cell-specific differences in the distribution of carbonic anhydrases II, III, XII, and XIV in the adult rat epididymis. *J Histochem Cytochem* **53**, 699-713.

Hermo, L. and Jacks, D. (2002). Nature's ingenuity: bypassing the classical secretory route via apocrine secretion. *Mol Reprod Dev* **63**, 394-410.

Hess, R. A., Bunick, D., Lubahn, D. B., Zhou, Q. and Bouma, J. (2000). Morphologic changes in efferent ductules and epididymis in estrogen receptor-alpha knockout mice. *Journal of andrology* **21**, 107-21.

Hidai, C., Kawana, M., Habu, K., Kazama, H., Kawase, Y., Iwata, T., Suzuki, H., Quertermous, T. and Kokubun, S. (2005). Overexpression of the Dell1 gene causes dendritic branching in the mouse mesentery. *Anat Rec A Discov Mol Cell Evol Biol* **287**, 1165-75.

Hidai, C., Kawana, M., Kitano, H. and Kokubun, S. (2007). Discoidin domain of Dell1 protein contributes to its deposition in the extracellular matrix. *Cell and tissue research* **330**, 83-95.

Hidai, C., Zupancic, T., Penta, K., Mikhail, A., Kawana, M., Quertermous, E. E., Aoka, Y., Fukagawa, M., Matsui, Y., Platika, D. et al. (1998). Cloning and characterization of developmental endothelial locus-1: an embryonic endothelial cell protein that binds the alphavbeta3 integrin receptor. *Genes Dev* **12**, 21-33.

Hinton, B. T. and Palladino, M. A. (1995). Epididymal epithelium: its contribution to the formation of a luminal fluid microenvironment. *Microscopy research and technique* **30**, 67-81.

Hirsch, E., Gullberg, D., Balzac, F., Altruda, F., Silengo, L. and Tarone, G. (1994). Alpha v integrin subunit is predominantly located in nervous tissue and skeletal muscle during mouse development. *Developmental dynamics : an official publication of the American Association of Anatomists* **201**, 108-20.

Ho, H. K., Jang, J. J., Kaji, S., Spektor, G., Fong, A., Yang, P., Hu, B. S., Schatzman, R., Quertermous, T. and Cooke, J. P. (2004). Developmental endothelial locus-1 (Del-1), a novel angiogenic protein: its role in ischemia. *Circulation* **109**, 1314-9.

Hoffhines, A. J., Jen, C. H., Leary, J. A. and Moore, K. L. (2008). Tyrosylprotein sulfotransferase-2 expression is required for sulfation of Rnase9 and Mfge8 in vivo. *J Biol Chem*.

Humphries, M. J. (1998). Cell-Substrate Adhesion Assays: John Wiley & Sons, Inc.

Hynes, R. O. (1992). Integrins: versatility, modulation, and signaling in cell adhesion. *Cell* **69**, 11-25.

Isnard-Bagnis, C., Da Silva, N., Beaulieu, V., Yu, A. S., Brown, D. and Breton, S. (2003). Detection of CIC-3 and CIC-5 in epididymal epithelium: immunofluorescence and RT-PCR after LCM. *Am J Physiol Cell Physiol* **284**, C220-32.

Itoh, M., Miyamoto, K., Satriotomo, I. and Takeuchi, Y. (1999). Spermatid granulomata are experimentally induced in epididymides of mice receiving high-dose testosterone implants. I. A light-microscopical study. *J Androl* **20**, 551-8.

Jensen, L. J., Schmitt, B. M., Berger, U. V., Nsumu, N. N., Boron, W. F., Hediger, M. A., Brown, D. and Breton, S. (1999a). Localization of sodium bicarbonate cotransporter (NBC) protein and messenger ribonucleic acid in rat epididymis. *Biol Reprod* **60**, 573-9.

Jensen, L. J., Stuart-Tilley, A. K., Peters, L. L., Lux, S. E., Alper, S. L. and Breton, S. (1999b). Immunolocalization of AE2 anion exchanger in rat and mouse epididymis. *Biol Reprod* **61**, 973-80.

Johnston, D. S., Jelinsky, S. A., Bang, H. J., DiCandeloro, P., Wilson, E., Kopf, G. S. and Turner, T. T. (2005). The mouse epididymal transcriptome: transcriptional profiling of segmental gene expression in the epididymis. *Biol Reprod* **73**, 404-13.

Kaunisto, K., Parkkila, S., Parkkila, A. K., Waheed, A., Sly, W. S. and Rajaniemi, H. (1995). Expression of carbonic anhydrase isoenzymes IV and II in rat epididymal duct. *Biol Reprod* **52**, 1350-7.

Kumar, C. C., Malkowski, M., Yin, Z., Tanghetti, E., Yaremko, B., Nechuta, T., Varner, J., Liu, M., Smith, E. M., Neustadt, B. et al. (2001). Inhibition of angiogenesis and tumor growth by SCH221153, a dual alpha(v)beta3 and alpha(v)beta5 integrin receptor antagonist. *Cancer research* **61**, 2232-8.

Kvistgaard, A. S., Pallesen, L. T., Arias, C. F., Lopez, S., Petersen, T. E., Heegaard, C. W. and Rasmussen, J. T. (2004). Inhibitory effects of human and bovine milk constituents on rotavirus infections. *J Dairy Sci* **87**, 4088-96.

Larocca, D., Peterson, J. A., Urrea, R., Kuniyoshi, J., Bistrain, A. M. and Ceriani, R. L. (1991). A Mr 46,000 human milk fat globule protein that is highly expressed in human breast tumors contains factor VIII-like domains. *Cancer research* **51**, 4994-8.

Leonardi-Essmann, F., Emig, M., Kitamura, Y., Spanagel, R. and Gebicke-Haerter, P. J. (2005). Fractalkine-upregulated milk-fat globule EGF factor-8 protein in cultured rat microglia. *J Neuroimmunol* **160**, 92-101.

Levine, N. and Marsh, D. J. (1971). Micropuncture studies of the electrochemical aspects of fluid and electrolyte transport in individual seminiferous tubules, the epididymis and the vas deferens in rats. *The Journal of physiology* **213**, 557-70.

Levy, S. and Robaire, B. (1999a). Segment-specific changes with age in the expression of junctional proteins and the permeability of the blood-epididymis barrier in rats. *Biol Reprod* **60**, 1392-401.

Levy, S. and Robaire, B. (1999b). Segment-specific changes with age in the expression of junctional proteins and the permeability of the blood-epididymis barrier in rats. *Biology of reproduction* **60**, 1392-401.

Lin, L., Huai, Q., Huang, M., Furie, B. and Furie, B. C. (2007). Crystal structure of the bovine lactadherin C2 domain, a membrane binding motif, shows similarity to the C2 domains of factor V and factor VIII. *Journal of molecular biology* **371**, 717-24.

Liu, Y., Chiriva-Internati, M., You, C., Luo, R., You, H., Prasad, C. K., Grizzi, F., Cobos, E., Klimberg, V. S., Kay, H. et al. (2005). Use and specificity of breast cancer antigen/milk protein BA46 for generating anti-self-cytotoxic T lymphocytes by recombinant adeno-associated virus-based gene loading of dendritic cells. *Cancer Gene Ther* **12**, 304-12.

Macedo-Ribeiro, S., Bode, W., Huber, R., Quinn-Allen, M. A., Kim, S. W., Ortel, T. L., Bourenkov, G. P., Bartunik, H. D., Stubbs, M. T., Kane, W. H. et al. (1999). Crystal structures of the membrane-binding C2 domain of human coagulation factor V. *Nature* **402**, 434-9.

McGill, M., Hsu, T. C. and Brinkley, B. R. (1973). Electron-dense structures in mitochondria induced by short-term ethidium bromide treatment. *J Cell Biol* **59**, 260-5.

Miksa, M., Amin, D., Wu, R., Ravikumar, T. S. and Wang, P. (2007). Fractalkine-induced MFG-E8 leads to enhanced apoptotic cell clearance by macrophages. *Mol Med* **13**, 553-60.

Miksa, M., Wu, R., Dong, W., Das, P., Yang, D. and Wang, P. (2006). Dendritic cell-derived exosomes containing milk fat globule epidermal growth factor-factor VIII attenuate proinflammatory responses in sepsis. *Shock* **25**, 586-93.

Miyasaka, K., Hanayama, R., Tanaka, M. and Nagata, S. (2004). Expression of milk fat globule epidermal growth factor 8 in immature dendritic cells for engulfment of apoptotic cells. *Eur J Immunol* **34**, 1414-22.

Monks, J., Geske, F. J., Lehman, L. and Fadok, V. A. (2002). Do inflammatory cells participate in mammary gland involution? *J Mammary Gland Biol Neoplasia* **7**, 163-76.

Monks, J., Rosner, D., Geske, F. J., Lehman, L., Hanson, L., Neville, M. C. and Fadok, V. A. (2005). Epithelial cells as phagocytes: apoptotic epithelial cells are engulfed by mammary alveolar epithelial cells and repress inflammatory mediator release. *Cell Death Differ* **12**, 107-14.

Morelli, A. E., Larregina, A. T., Shufesky, W. J., Sullivan, M. L., Stolz, D. B., Papworth, G. D., Zahorchak, A. F., Logar, A. J., Wang, Z., Watkins, S. C. et al. (2004). Endocytosis, intracellular sorting, and processing of exosomes by dendritic cells. *Blood* **104**, 3257-66.

Murphy, M. G., Cerchio, K., Stoch, S. A., Gottesdiener, K., Wu, M. and Recker, R. (2005). Effect of L-000845704, an alphaVbeta3 integrin antagonist, on markers of bone turnover and bone mineral density in postmenopausal osteoporotic women. *The Journal of clinical endocrinology and metabolism* **90**, 2022-8.

Nandrot, E. F., Anand, M., Almeida, D., Atabai, K., Sheppard, D. and Finnemann, S. C. (2007). Essential role for MFG-E8 as ligand for alphavbeta5 integrin in diurnal retinal phagocytosis. *Proc Natl Acad Sci U S A* **104**, 12005-10.

Nandrot, E. F., Anand, M., Sircar, M. and Finnemann, S. C. (2006). Novel role for alphavbeta5-integrin in retinal adhesion and its diurnal peak. *Am J Physiol Cell Physiol* **290**, C1256-62.

Nandrot, E. F., Kim, Y., Brodie, S. E., Huang, X., Sheppard, D. and Finnemann, S. C. (2004). Loss of synchronized retinal phagocytosis and age-related blindness in mice lacking alphavbeta5 integrin. *J Exp Med* **200**, 1539-45.

Neutzner, M., Lopez, T., Feng, X., Bergmann-Leitner, E. S., Leitner, W. W. and Udey, M. C. (2007). MFG-E8/lactadherin promotes tumor growth in an angiogenesis-dependent transgenic mouse model of multistage carcinogenesis. *Cancer Res* **67**, 6777-85.

Newburg, D. S., Peterson, J. A., Ruiz-Palacios, G. M., Matson, D. O., Morrow, A. L., Shults, J., Guerrero, M. L., Chaturvedi, P., Newburg, S. O., Scallan, C. D. et al. (1998). Role of human-milk lactadherin in protection against symptomatic rotavirus infection. *Lancet* **351**, 1160-4.

Ogura, K., Nara, K., Watanabe, Y., Kohno, K., Tai, T. and Sanai, Y. (1996). Cloning and expression of cDNA for O-acetylation of GD3 ganglioside. *Biochemical and biophysical research communications* **225**, 932-8.

Orgebin-Crist, M. C. (1969). Studies on the function of the epididymis. *Biology of reproduction* **1**, Suppl 1:155-75.

Oshima, K., Aoki, N., Kato, T., Kitajima, K. and Matsuda, T. (2002). Secretion of a peripheral membrane protein, MFG-E8, as a complex with membrane vesicles. *European journal of biochemistry / FEBS* **269**, 1209-18.

Oshima, K., Aoki, N., Negi, M., Kishi, M., Kitajima, K. and Matsuda, T. (1999). Lactation-dependent expression of an mRNA splice variant with an exon for a multiply O-glycosylated domain of mouse milk fat globule glycoprotein MFG-E8. *Biochemical and biophysical research communications* **254**, 522-8.

Pastor-Soler, N., Beaulieu, V., Litvin, T. N., Da Silva, N., Chen, Y., Brown, D., Buck, J., Levin, L. R. and Breton, S. (2003). Bicarbonate-regulated adenylyl

cyclase (sAC) is a sensor that regulates pH-dependent V-ATPase recycling. *J Biol Chem* **278**, 49523-9.

Pastor-Soler, N., Pietrement, C. and Breton, S. (2005). Role of acid/base transporters in the male reproductive tract and potential consequences of their malfunction. *Physiology (Bethesda)* **20**, 417-28.

Pavlok, A. (1974). Development of the penetration activity of mouse epididymal spermatozoa in vivo and in vitro. *J Reprod Fertil* **36**, 203-5.

Penta, K., Varner, J. A., Liaw, L., Hidai, C., Schatzman, R. and Quertermous, T. (1999). Dell induces integrin signaling and angiogenesis by ligation of alphaVbeta3. *The Journal of biological chemistry* **274**, 11101-9.

Pratt, K. P., Shen, B. W., Takeshima, K., Davie, E. W., Fujikawa, K. and Stoddard, B. L. (1999). Structure of the C2 domain of human factor VIII at 1.5 Å resolution. *Nature* **402**, 439-42.

Pushkin, A., Clark, I., Kwon, T. H., Nielsen, S. and Kurtz, I. (2000). Immunolocalization of NBC3 and NHE3 in the rat epididymis: colocalization of NBC3 and the vacuolar H⁺-ATPase. *J Androl* **21**, 708-20.

Raymond, A. S., Ensslin, M. A., Elder, B. and Shur, B. D. (2009a). Loss of SED1/MFG-E8 results in altered luminal physiology in the epididymis. **Submitted**.

Raymond, A. S., Ensslin, M. A. and Shur, B. D. (2009b). SED1/MFG-E8: a bi-motif protein that orchestrates diverse cellular interactions. *Journal Cellular Biochemistry* **Accepted**.

Raymond, A. S. and Shur, B. D. (2009). A novel role for SED1/MFG-E8 in maintaining the integrity of the epididymal epithelium. *Journal of Cell Science* **Accepted**.

Reitherman, R. W., Rosen, S. D., Frasier, W. A. and Barondes, S. H. (1975). Cell surface species-specific high affinity receptors for discoidin: developmental regulation in Dictyostelium discoideum. *Proc Natl Acad Sci U S A* **72**, 3541-5.

Rejraji, H., Sion, B., Prensier, G., Carreras, M., Motta, C., Frenoux, J. M., Vericel, E., Grizard, G., Vernet, P. and Drevet, J. R. (2006). Lipid remodeling of murine epididymosomes and spermatozoa during epididymal maturation. *Biol Reprod* **74**, 1104-13.

Rezaee, M., Penta, K. and Quertermous, T. (2002). Dell mediates VSMC adhesion, migration, and proliferation through interaction with integrin alpha(v)beta(3). *Am J Physiol Heart Circ Physiol* **282**, H1924-32.

Robaire, B. and Hinton, B. T. (2002). *The Epididymis From Molecules to Clinical Practice*. New York: Kluwer Academic/Plenum Publishers.

Ruoslahti, E. (1996). RGD and other recognition sequences for integrins. *Annual review of cell and developmental biology* **12**, 697-715.

Salazar, G., Love, R., Werner, E., Doucette, M. M., Cheng, S., Levey, A. and Faundez, V. (2004). The zinc transporter ZnT3 interacts with AP-3 and it is preferentially targeted to a distinct synaptic vesicle subpopulation. *Mol Biol Cell* **15**, 575-87.

Segura, E., Amigorena, S. and Thery, C. (2005). Mature dendritic cells secrete exosomes with strong ability to induce antigen-specific effector immune responses. *Blood Cells Mol Dis* **35**, 89-93.

Setchell, B. P., Maddocks, S. and Brooks, D. E. (1994). *Anatomy, Vascularization, Innervation, and Fluids of the Male Reproductive Tract*. New York: Raven Press, Ltd.

Shahriar, F., Ngeleka, M., Gordon, J. R. and Simko, E. (2006). Identification by mass spectroscopy of F4ac-fimbrial-binding proteins in porcine milk and characterization of lactadherin as an inhibitor of F4ac-positive *Escherichia coli* attachment to intestinal villi in vitro. *Dev Comp Immunol* **30**, 723-34.

Shao, C., Novakovic, V. A., Head, J. F., Seaton, B. A. and Gilbert, G. E. (2008). Crystal structure of lactadherin C2 domain at 1.7Å resolution with mutational and computational analyses of its membrane-binding motif. *The Journal of biological chemistry* **283**, 7230-41.

Shi, J. and Gilbert, G. E. (2003). Lactadherin inhibits enzyme complexes of blood coagulation by competing for phospholipid-binding sites. *Blood* **101**, 2628-36.

Shi, J., Heegaard, C. W., Rasmussen, J. T. and Gilbert, G. E. (2004). Lactadherin binds selectively to membranes containing phosphatidyl-L-serine and increased curvature. *Biochimica et biophysica acta* **1667**, 82-90.

Shi, J., Pipe, S. W., Rasmussen, J. T., Heegaard, C. W. and Gilbert, G. E. (2008). Lactadherin blocks thrombosis and hemostasis in vivo: correlation with platelet phosphatidylserine exposure. *Journal of thrombosis and haemostasis : JTH* **6**, 1167-74.

Shur, B. D., Ensslin, M. A. and Rodeheffer, C. (2004). SED1 function during mammalian sperm-egg adhesion. *Current opinion in cell biology* **16**, 477-85.

Silvestre, J. S., Thery, C., Hamard, G., Boddaert, J., Aguilar, B., Delcayre, A., Houbron, C., Tamarat, R., Blanc-Brude, O., Heeneman, S. et al. (2005). Lactadherin promotes VEGF-dependent neovascularization. *Nat Med* **11**, 499-506.

Sonnenberg-Riethmacher, E., Walter, B., Riethmacher, D., Godecke, S. and Birchmeier, C. (1996). The c-ros tyrosine kinase receptor controls regionalization and differentiation of epithelial cells in the epididymis. *Genes Dev* **10**, 1184-93.

Stubbs, J. D., Lekutis, C., Singer, K. L., Bui, A., Yuzuki, D., Srinivasan, U. and Parry, G. (1990). cDNA cloning of a mouse mammary epithelial cell surface protein reveals the existence of epidermal growth factor-like domains linked to factor VIII-like sequences. *Proceedings of the National Academy of Sciences of the United States of America* **87**, 8417-21.

Sullivan, R., Saez, F., Girouard, J. and Frenette, G. (2005). Role of exosomes in sperm maturation during the transit along the male reproductive tract. *Blood Cells Mol Dis* **35**, 1-10.

Suzuki, S., Argraves, W. S., Arai, H., Languino, L. R., Pierschbacher, M. D. and Ruoslahti, E. (1987). Amino acid sequence of the vitronectin receptor alpha subunit and comparative expression of adhesion receptor mRNAs. *The Journal of biological chemistry* **262**, 14080-5.

Takahashi, K., Nakamura, T., Koyanagi, M., Kato, K., Hashimoto, Y., Yagita, H. and Okumura, K. (1990). A murine very late activation antigen-like

extracellular matrix receptor involved in CD2- and lymphocyte function-associated antigen-1-independent killer-target cell interaction. *Journal of immunology (Baltimore, Md. : 1950)* **145**, 4371-9.

Taylor, M. R., Couto, J. R., Scallan, C. D., Ceriani, R. L. and Peterson, J. A. (1997). Lactadherin (formerly BA46), a membrane-associated glycoprotein expressed in human milk and breast carcinomas, promotes Arg-Gly-Asp (RGD)-dependent cell adhesion. *DNA and cell biology* **16**, 861-9.

Thery, C., Regnault, A., Garin, J., Wolfers, J., Zitvogel, L., Ricciardi-Castagnoli, P., Raposo, G. and Amigorena, S. (1999). Molecular characterization of dendritic cell-derived exosomes. Selective accumulation of the heat shock protein hsc73. *J Cell Biol* **147**, 599-610.

Thimon, V., Frenette, G., Saez, F., Thabet, M. and Sullivan, R. (2008). Protein composition of human epididymosomes collected during surgical vasectomy reversal: a proteomic and genomic approach. *Hum Reprod* **23**, 1698-707.

Venegas, V. and Zhou, Z. (2007). Two alternative mechanisms that regulate the presentation of apoptotic cell engulfment signal in *Caenorhabditis elegans*. *Mol Biol Cell* **18**, 3180-92.

Veron, P., Segura, E., Sugano, G., Amigorena, S. and Thery, C. (2005). Accumulation of MFG-E8/lactadherin on exosomes from immature dendritic cells. *Blood Cells Mol Dis* **35**, 81-8.

Wagenfeld, A., Yeung, C. H., Lehnert, W., Nieschlag, E. and Cooper, T. G. (2002). Lack of glutamate transporter EAAC1 in the epididymis of infertile c-ros receptor tyrosine-kinase deficient mice. *J Androl* **23**, 772-82.

Weng, S., Zemany, L., Standley, K. N., Novack, D. V., La Regina, M., Bernal-Mizrachi, C., Coleman, T. and Semenkovich, C. F. (2003). Beta3 integrin deficiency promotes atherosclerosis and pulmonary inflammation in high-fat-fed, hyperlipidemic mice. *Proc Natl Acad Sci U S A* **100**, 6730-5.

Wu, Y., Singh, S., Georgescu, M. M. and Birge, R. B. (2005). A role for Mer tyrosine kinase in alphavbeta5 integrin-mediated phagocytosis of apoptotic cells. *Journal of cell science* **118**, 539-53.

Yamaguchi, H., Takagi, J., Miyamae, T., Yokota, S., Fujimoto, T., Nakamura, S., Ohshima, S., Naka, T. and Nagata, S. (2008). Milk fat globule EGF factor 8 in the serum of human patients of systemic lupus erythematosus. *J Leukoc Biol* **83**, 1300-7.

Yeung, C. H., Anapolski, M., Setiawan, I., Lang, F. and Cooper, T. G. (2004a). Effects of putative epididymal osmolytes on sperm volume regulation of fertile and infertile c-ros transgenic Mice. *J Androl* **25**, 216-23.

Yeung, C. H., Breton, S., Setiawan, I., Xu, Y., Lang, F. and Cooper, T. G. (2004b). Increased luminal pH in the epididymis of infertile c-ros knockout mice and the expression of sodium-hydrogen exchangers and vacuolar proton pump H⁺-ATPase. *Mol Reprod Dev* **68**, 159-68.

Zeelenberg, I. S., Ostrowski, M., Krumeich, S., Bobrie, A., Jancic, C., Boissonnas, A., Delcayre, A., Le Pecq, J. B., Combadiere, B., Amigorena, S. et al.

(2008). Targeting tumor antigens to secreted membrane vesicles in vivo induces efficient antitumor immune responses. *Cancer Res* **68**, 1228-35.

Zhong, J., Eliceiri, B., Stupack, D., Penta, K., Sakamoto, G., Quertermous, T., Coleman, M., Boudreau, N. and Varner, J. A. (2003). Neovascularization of ischemic tissues by gene delivery of the extracellular matrix protein Del-1. *J Clin Invest* **112**, 30-41.

Zhou, Q., Clarke, L., Nie, R., Carnes, K., Lai, L. W., Lien, Y. H., Verkman, A., Lubahn, D., Fisher, J. S., Katzenellenbogen, B. S. et al. (2001). Estrogen action and male fertility: roles of the sodium/hydrogen exchanger-3 and fluid reabsorption in reproductive tract function. *Proc Natl Acad Sci U S A* **98**, 14132-7.